EFFECTS OF SALINITY ON THE EXPRESSION OF ION-TRANSPORTERS IN THE LARVAL MOSQUITO, *AEDES AEGYPTI*

Amber Nicole Reinsborough

A THESIS SUBMITTED TO THE FACULTY OF GRADUATE STUDIES
IN PARTIAL FULFILLMENT OF THE REQUIREMENTS
FOR THE DEGREE OF MASTER OF SCIENCE

GRADUATE PROGRAM IN BIOLOGY
YORK UNIVERSITY
TORONTO, ONTARIO, CANADA

JUNE 2026

©Amber Nicole Reinsborough, 2026

Abstract

Aedes aegypti inhabit freshwater (FW) and brackish water relying on adjustments to their physiology to maintain salt and water balance. This is likely to involve changes in expression of ion transporters in epithelia of osmoregulatory organs. The aim of this study is to evaluate expression of AeNHA1, AeNHA2, AeCCC3 and AeCA9, ion transporters expressed in epithelia in the osmoregulatory organs: midgut, Malpighian tubules, hindgut and anal papillae of larval *A. aegypti* exposed to freshwater and brackish water. Expression of these transporters was detected in all osmoregulatory organs with exposure to salinated water showing a reduction in *ccc3* expression in the midgut. Abundance of *nha1* decreased in anal papillae but, protein abundance remained consistent with salinated water exposure. Immunohistochemistry revealed that AeNHA1 is localized to the basolateral membrane of epithelia in these organs. This study provides novel foundational knowledge on the expression of ion transporters in osmoregulatory organs larval *A. aegypti*.

Acknowledgments

I would first like to thank my one of a kind supervisor, Dr. Andrew Donini. I am truly so lucky to have not only had the chance to work with you but also learn from you in these past few years. Thank you for always supporting every decision I made and helping provide me with your guidance, advice and reassurance whenever I was in doubt, which is about 99.9% of the time. Thank you for all of the opportunities you gave me, no matter what the case or situation was you always did as much as you could to ensure I had an amazing experience from my master's and got the most out of it. I am extremely grateful for the support and patience you have given me the last few years. Without any hesitation you have always supported whichever direction I wanted to take with my research to make sure I finished on time and could follow what was next for me. Thank you for your unwavering support and motivation throughout my time in the lab. I could not have asked for a better supervisor and I will always have gratitude for everything you have done for me and taught me.

I would also like to thank my supervisory committee. Thank you, Dr. Raymond Kwong, for all of your help and feedback throughout my master's, I appreciate it greatly. Furthermore, I would like to thank both Dr. Scott Kelly and Dr. Rolando Ceddia for taking the time to review and read my thesis and attend my defence.

A big thank you is also owed to Dr. Britney Picinic. Thank you for getting me through this master's and helping teach me most of what I know. You are an amazing mentor and have taught me so many of the skills I have learned from my time in the Donini Lab. Aside from being an incredible mentor, thank you for being a supportive, hilarious, uplifting, helpful and all-around amazing friend. You never failed to make me laugh or have a good day even at some of the lowest of times. I appreciate your consistent support and motivation throughout this experience. One of the most valuable things I gained from my master's was your friendship, so thank you for everything.

Thank you to my family for their support, to my sister's for always listening to me overthink my research a million times over. Finally, thank you to Trey. Thank you for listening to me stress for the last two years and still reminding me to follow what makes me happy without any complaints. I am excited to relieve you of my long talks about mosquito or midge larvae, but I unfortunately will still be searching for larvae every single time we go tide pooling. There is no escaping that. Thank you for all the sacrifice you have made so that we can pursue our goals in this lifetime.

Table of Contents

Abstract ii

Acknowledgments iii

Table of Contents iv

List of Tables vi

List of Figures vii

List of Abbreviations ix

Statement of Contributions xii

1.0. Introduction 1

1.1. *Aedes aegypti* lifecycle, control and relevance 1

1.2. Osmoregulation and salinity tolerance of *Aedes aegypti* 3

1.3. The role of iono- and osmoregulating organs in *Aedes aegypti* larvae 4
1.3.1. Midgut 4
1.3.2. Malpighian tubules 6
1.3.3. Hindgut 8
1.3.4. Anal papillae 8

1.4. Active transporters in ion-regulatory epithelia 11

1.5. Ion-transport models in the ion-regulating organs of *Aedes aegypti* larvae 14
1.5.1. Transcellular transport mechanisms of the midgut 14
1.5.2. Transcellular transport mechanisms of the Malpighian tubules 19
1.5.3. Transcellular transport mechanisms of the hindgut 22
1.5.4. Transcellular transport mechanisms of the anal papillae 24

1.8. Objectives and hypotheses 27

2.0. Materials and Methods 29

2.1. Animal care and larval treatments 29

2.2. qPCR primer design 30

2.3. RNA Extraction and cDNA synthesis for qPCR analysis 34

2.4. Analysis of ion-transporter mRNA abundance in ion-regulating organs using quantitative PCR analysis (qPCR) 35

2.5. Localization of AeNHA1 with immunohistochemistry (IHC) 36

2.6. Western blotting analysis of AeNHA1 38

2.7. AeNHA1 and AeCA9 dsRNA synthesis and assessment of knockdown (KD) 40

2.8. Statistical Analysis 42

3.0. Results 43

3.1. Expression profile of *nha1*, *nha2*, *ca9* and *ccc3* in osmoregulatory organs of *Aedes aegypti* larvae 43

3.2. Immunolocalization and detection of AeNHA1 in osmoregulatory organs of *Aedes aegypti* larvae 45

3.3. Comparison of mRNA abundance of *nha1*, *nha2*, *ca9* and *ccc3* in the osmoregulatory organs of AFW vs BW *Aedes aegypti* larvae 47

3.4. Expression of AeNHA1 protein in osmoregulatory organs of AFW vs BW *Aedes aegypti* larvae 52

3.5. Protein abundance of AeNHA1 in the AP of AFW and BW exposed *Aedes aegypti* larvae 54

3.6. Assessment of *ca9*, *nha1* and AeNHA1 knockdown (KD) in larval *Aedes aegypti* 56

4.0. Discussion 59

4.1. Overview 59

4.2. AFW expression of ion-transporters and enzymes in larval osmoregulatory organs 61
4.2.1. AeCA9 61
4.2.2. AeCCC3 64
4.2.3. AeNHA2 66
4.2.4. AeNHA1 68

4.3. Expression of AeNHA1, AeNHA2, AeCA9 and AeCCC3 in *A. aegypti larvae* acutely exposed to salinity 76
4.3.1. Midgut 76
4.3.2. Malpighian tubules 77
4.3.3. Hindgut 77
4.3.4. Anal papillae 78

4.4. Conclusions and Future directions 80

5.0. References 82

Appendix and Supplementary Data 96

Appendix A. Antibody controls for immunohistochemistry and western blotting 96

List of Tables

Table 1. Primer sets tested and used to amplify larger fragments of *nha1*, *nha2* and *ca9* prior to qPCR primer design 32

Table 2. Primers used for gene amplification and dsRNA synthesis for AeNHA1 and AeCA9 KD 33

List of Figures

Figure 1. Lifecycle of the disease vector, *Aedes aegypti* 3

Figure 2. Osmoregulatory organs of the FW larval mosquito - *Aedes aegypti* 10

Figure 3. Proposed ion-transport model of the various segments of the midgut in the larval *Aedes aegypti* 18

Figure 4. Proposed model of larval Malpighian tubule (MT) ion secretion in larval *Aedes aegypti* 21

Figure 5. Ion transport model proposed for the hindgut (HG) of FW larval *Aedes aegypti* 23

Figure 6. Proposed ion-transport model for NaCl absorption across the anal papillae (AP) of FW *Aedes aegypti* larvae 26

Figure 7. Expression profile of *nha1*, *nha2*, *ca9* and *ccc3* in the midgut (MG), Malpighian tubules (MTs) and hindgut (HG) of artificial freshwater (AFW) *Aedes aegypti* larvae 44

Figure 8. Immunolocalization of AeNHA1 in the osmoregulatory organs of artificial freshwater (AFW) *Aedes aegypti* larvae 46

Figure 9. Effects of artificial freshwater (AFW) and brackish water (BW) exposure on the relative mRNA abundance of *nha1* in osmoregulatory organs of *Aedes aegypti* larvae..... 48

Figure 10. Effects of artificial freshwater (AFW) and brackish water (BW) exposure on the relative mRNA abundance of *nha2* in osmoregulatory organs of *Aedes aegypti* larvae..... 49

Figure 11. Effects of artificial freshwater (AFW) and brackish water (BW) exposure on the relative mRNA abundance of *ca9* in osmoregulatory organs of *Aedes aegypti* larvae..... 50

Figure 12. Effects of artificial freshwater (AFW) and brackish water (BW) exposure on the relative mRNA abundance of *ccc3* in osmoregulatory organs of *Aedes aegypti* larvae. 51

Figure 13. Immunolocalization and expression of AeNHA1 in artificial freshwater (AFW) and brackish water (BW) *Aedes aegypti* larvae 53

Figure 14. Protein abundance of AeNHA1 in aritifical freshwater (AFW) Malpighian tubules (MTs) and in 24-hour treated artificial freshwater (AFW) and brackish water (BW) anal papillae (AP) organs of larval *Aedes aegypti* 55

Figure 15. Whole-body AeCA9 and AeNHA1 knockdown (KD) attempts in *Aedes aegypti* larvae 57

Figure 16. Knockdown (KD) attempt assessing protein (A,B) and mRNA (C) abundance of AeNHA1 at larval anal papillae (AP) organs assessed 48-hours post dsRNA delivery 58

Figure 17. Updated proposed ion-transport model for the different segments of the midgut in larval *Aedes aegypti* 72

Figure 18. Updated proposed ion-transport model for the MTs in larval *Aedes aegypti* 73

Figure 19. Updated proposed ion-transport model for the hindgut (HG) in larval *Aedes aegypti* 74

Figure 20. Updated proposed ion-transport model for the anal papillae (AP) in larval *Aedes aegypti* 75

Figure A-21. Controls for secondary (VA & AeNHA1) and primary (AeNHA1) antibodies on tissue sections of *Aedes aegypti* larvae treated in artificial freshwater (AFW) 98

Figure A-22. Pre-immune serum-western blot (control) for AeNHA1 primary antibody 99

List of Abbreviations

AaCAT1 – *Aedes aegypti* cationic amino acid transporter 1

AeAE – *Aedes aegypti* anion exchanger

AeCA – *Aedes aegypti* carbonic anhydrase

AeCCC – *Aedes aegypti* cation-coupled chloride co-transporter

AMG – anterior midgut

AeNHA – *Aedes aegypti* Na^+/H^+ antiporter

AeNHE – *Aedes aegypti* Na^+/H^+ exchanger

AeNKCC – *Aedes aegypti* Na^+-K^+-$2Cl^-$ co-transporter

ADB – antibody dilution buffer

AFW – artificial freshwater

AgCA – *Anopheles gambiae* carbonic anhydrase

AgNAT – *Anopheles gambiae* nutrient amino acid transporter

AgNHA – *Anopheles gambiae* Na^+/H^+ antiporter

AP – anal papillae

BW – brackish water

CA – carbonic anhydrase

CCC – cation-coupled chloride cotransporter

cDNA – complementary deoxyribonucleic acid

DAPI – 4',6'-diamidino-2-phenylindole

ddH_2O – double distilled water

deH_2O – dechlorinated water

dsRNA – double stranded RNA

ECL – enhanced chemiluminescence

EGFP – enhanced green fluorescent protein

FW – freshwater

GC – gastric caeca

HG – hindgut

HRP – horseradish peroxidase

IHC – immunohistochemistry

kDa – kilodalton

MG – midgut

mRNA – messenger RNA

MT(s) – Malpighian tubule's

NAT – nutrient amino acid transporter

NCBI – National center for biotechnology information

NCC – Na^+-Cl- co-transporter

NHA – Na^+-H^+ antiporter

NHE – Na^+-H^+ exchanger

NKA – P-Type Na^+-K^+-ATPase

NKCC – Na^+-K^+-$2Cl^-$ co-transporter

PBS – phosphate-buffered saline

PCR – polymerase chain reaction

PMG – posterior midgut

PMSF – phenylmethylsulfonyl fluoride

PVDF – Polyvinylidene fluoride

qPCR – quantitative polymerase chain reaction

RNA – ribonucleic acid

RT – room temperature

rp49 –ribosomal protein 49

rps18 –ribosomal protein S18

SDS-PAGE – sodium dodecyl sulfate-polyacrylamide gel electrophoresis

SEM – standard error of mean

TBS-T – Tris-buffered saline with Tween-20®

VA –Vacuolar Type H^+-ATPase

Statement of Contributions

This thesis was written by Amber Reinsborough with valuable guidance and editorial support from Dr. Andrew Donini. Training in PCR, qPCR, and dsRNA synthesis were taught by Dr. Britney Picinic. Training in western blotting was taught and assisted by Dr. Britney Picinic. Larval dissections for RNA from the hindgut and both Malpighian tubule and anal papillae protein collection were assisted by Dr. Britney Picinic. All other experiments, compilation of results, analysis and presentation of data were performed by Amber Reinsborough.

1.0. Introduction

1.1. *Aedes aegypti* lifecycle, control and relevance

Aedes aegypti is a mosquito species commonly known for its ability to transmit several deadly diseases including the alphavirus, chikungunya and flaviviruses such as zika virus, yellow and dengue fever (Barrett and Higgs 2007; Halstead 2008; Ligon 2006; Wang et al. 2025). Female adult *A. aegypti* transmit these diseases within tropical and subtropical regions, with their distribution having broadened in more recent years, including into parts of North America and Europe (Kraemer 2015). The transmission of disease occurs through the blood feeding behaviour of the adult female, which is required for oviposition (Hossain et al. 2022). Within their distribution, *A. aegypti* are primarily adapted to oviposit near or on freshwater (FW) sources, where their eggs will hatch and develop into the aquatic larval stages (Figure 1) (Hossain et al. 2022). The larvae develop from 1st to 4th instar through feeding on organic material from the surrounding water. The final instar stage (4th) develops into the non-feeding pupae stage which continues to persist in the aquatic environment, before becoming the terrestrial adult (Figure 1) (Hossain et al. 2022).

Since these individuals have a direct impact on human health, many efforts have been made to control their population, targeting various stages of their lifecycle. For example, adults have been directly targeted through the application of insecticides and ovitraps which aim to reduce breeding efforts (Barrera et al. 2014; Devine et al. 2021; Wilke et al. 2021). Other strategies include attempts in releasing sterilized males into the environment to mate with females and ultimately reduce successful reproduction (Chen et al. 2023; Fay et al. 1963). RNAi methods have also been researched as a tool to control *A. aegypti* populations, although it is much less commercially available (Yadav et al. 2023). Alongside, employing methods targeting adults for vector control

purposes, early lifecycle stages such as the larval stage are often targeted as well. This is crucial since adults can disperse between environments with much greater ease than larvae, which are confined to their aquatic habitat. For example, one of the more common ways larval populations are targeted is through chemical based larvicides which are added to the water they inhabit (Tikar et al. 2008). Although, larvae have developed a resistance to various larvicides, making them an unreliable control strategy in some cases (Braga et al. 2005; Fernando et al. 2020; Rahman et al. 2021). Aquatic based larvicides are also not designed to specifically target only larval mosquitos and negatively influence other aquatic fauna inhabiting these same bodies of water, making them a less-than-ideal vector control candidate (Abe et al. 2014; Vieira Santos et al. 2017). Considering this, other control mechanisms such as botanical based larvicides and the use of RNAi have been studied for their effectiveness in targeting larval populations (Dias and Moraes 2014; Yadav et al. 2023). Ultimately, targeting the larvae of *A. aegypti* is advantageous since their success and survival is required for the terrestrial, arboviral adult to persist. Addressing the larval stages in vector control is also of value since adults are more difficult to target due to their ability to easily disperse within environments, while the larvae are restricted to an aquatic environment making them an easier target. Based on this, understanding ways at which control purposes can be tailored to *A. aegypti* larvae and their physiological adaptations which allow them to survive is of significance.

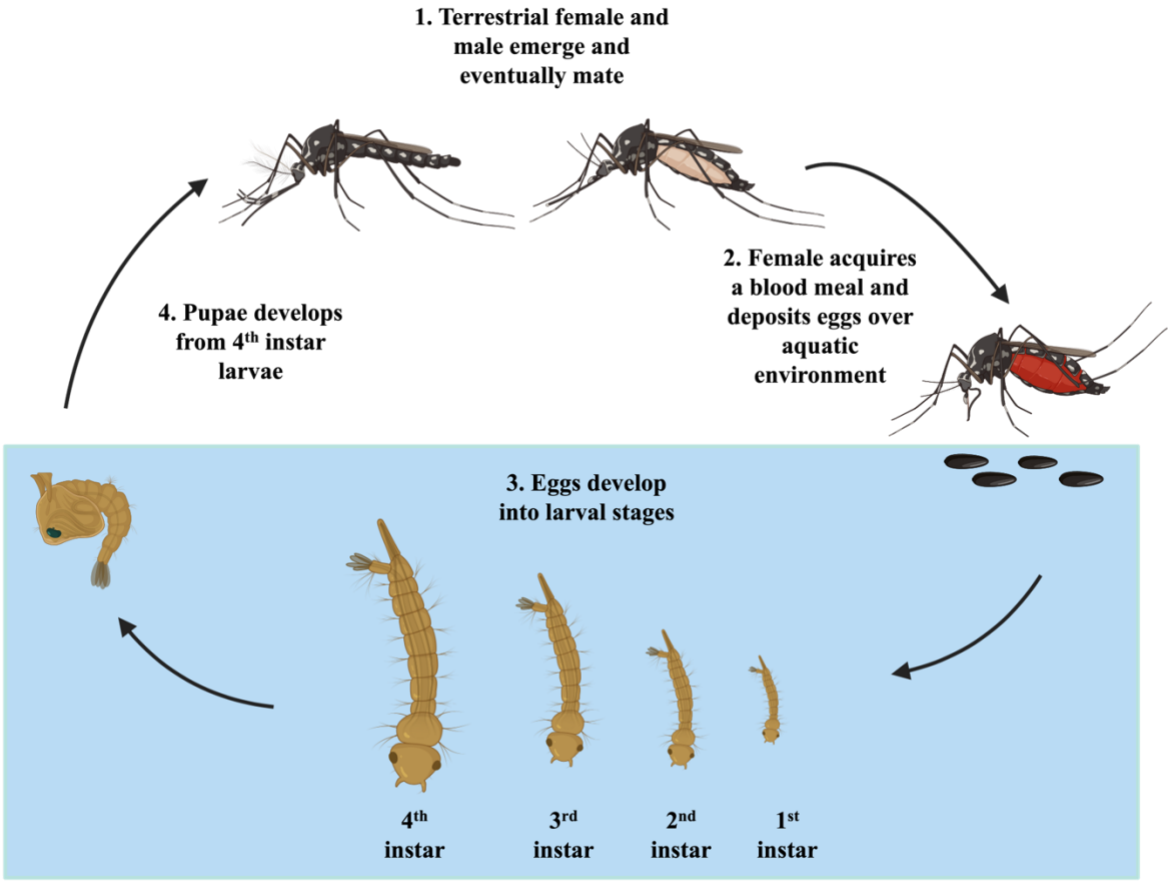

Figure 1. Lifecycle of the disease vector, *Aedes aegypti.* This figure illustrates the four major lifecycle stages of the mosquito, *Aedes aegypti* depicting the 1. Adult, 2. Egg, 3. Larval and 4. Pupae stage. As terrestrial adults (1) male and females will mate, allowing for the female to bear the fertilized eggs until acquiring a blood meal (2) where she can then lay her eggs on top of the surface of an aquatic environment. These eggs then hatch into the larval stages (3) first developing as the 1st instar, followed by the 2nd, 3rd and finally the 4th. The 4th larval instar then develops into the aquatic pupae (4) which eventually develops into the terrestrial adult within 2-3 days. This figure was modified from Hossain et al. 2022 using biorender.com.

1.2. Osmoregulation and salinity tolerance of *Aedes aegypti*

Larval *A. aegypti* are adapted for FW (Clements 1992). Generally, they have been found to reside in FW ponds, rock pools, and streams, but also inhabit man-made environments such as manholes and pits, plant pots, and wells which are often found in urban communities (Kay et al. 2000; McNaughton et al. 2018; Ramasamy et al. 2011). In FW, *A. aegypti* larvae are osmoregulators maintaining their hemolymph at a higher osmolarity (~300 mOsm) compared to the FW (~ 1 mOsm) (Bradley 1987). This creates a significant challenge where larvae are faced

with excess water gain and ion loss across permeable body surfaces (Bradley 1987). Under these conditions the regulation of salt and water balance involves physiological mechanisms that sequester ions and secrete excess water. Some FW habitats are subjected to chronic or acute salinization, which is when ambient salinity levels increase within these bodies of water (Kaushal et al. 2021). For *A. aegypti* larvae, the FW habitats where they reside in coastal regions of the world are subjected to rapid and varied adjustments in environmental salinity due to phenomena such as evaporation, tidal influx, increasing sea-levels, and saltwater intrusion (Ramasamy and Surendran 2011; Ramasamy et al. 2015). *A. aegypti* can tolerate some fluctuations in salinity and have been found residing in brackish water ranging from 2 to 15 ppt (Ramasamy et al. 2011; Surendran et al. 2012). Furthermore, in laboratory settings, larval *A. aegypti* develop successfully and regulate their internal osmotic pressure in up to ~ 10 ppt brackish water (BW) which is roughly iso-osmotic to their hemolymph (~300 mOsm) (Donini et al. 2007; Edwards 1982; Richards and Meier 1974). The ability to withstand these levels of salinity is ultimately linked to changes made in the osmoregulatory physiology of *A. aegypti* (Donini et al. 2007; D'Silva et al. 2017b; Jounsaite et al. 2016; Jonusaite et al. 2017a; Jonusaite et al. 2017b; Misyura et al. 2020). These changes can at least in part be attributed to the function of osmoregulatory organs such as the midgut, Malpighian tubules, hindgut and the external anal papillae (Bradley 1987) (Figure 2). Each of these organs play a unique and important role in maintaining salt and water balance.

1.3. The role of iono- and osmoregulating organs in *Aedes aegypti* larvae

1.3.1. Midgut

The midgut is a crucial organ involved in the digestion of ingested food, nutrient absorption and in regulating water, ion and pH balance (Barroso et al. 2025; Boudko et al. 2001a; Boudko et al. 2001b; D'Silva et al. 2017a; D'Silva et al. 2017b; Jagadeshwaran et al. 2010; Terra et al. 1990) (Figure 2). The midgut is divided into the gastric caeca, the anterior midgut, and the posterior

midgut where these distinct regions are functionally and morphologically different. The most anterior segment of the midgut, the gastric caeca, is composed of cuboidal and columnar epithelial cells which contain an apical brush border (Zhuang et al. 1999). The gastric caeca are morphologically distinguished as eight blind-ended bulbous-like sacs which are multifunctional, aiding in digestion, absorption of fluids, storage of nutrients and water and ion balance (Jones and Zeve 1968; Ramsay 1950; Volkmann and Peters 1989a; Volkmann and Peters 1989b). Different cell types are found in the gastric caeca linked to their functional characteristics. This includes cells involved in digestion and storage, secretion of the caecal membrane and imaginal cells (Volkmann and Peters 1989a). For ion and water balance, ion transporting cells have also been characterized, located in the distal third of the caeca (Volkmann and Peters 1989a). Furthermore, the gastric caeca have been found to facilitate the transport of ions such as Na^+, K^+ and H^+ in FW larvae along the proximal and distal surfaces (Boudko et al. 2001a; D'Silva et al. 2017b; Volkmann and Peters 1989a). Studies show that the transport of these ions at the gastric caeca become reduced when *A. aegypti* larvae are treated in brackish water (D'Silva et al. 2017b). In BW, larvae ingest the ions from the surrounding water into the gut, explaining the reduced need to secrete ions into the lumen when exposed to salinity (D'Silva et al. 2017b). Furthermore, morphological analysis of the gastric caeca supports this observed reduction in ion-transport in salinity, where mitochondrial abundance decreases and ion-transporting cells at the distal caecum become smaller and more dispersed (e.g., VA-rich cells), showing changes that are linked to reduced ion-transport (Volkmann and Peters 1989b). Alongside regulating ion levels, within the gastric caeca lumen, a relatively neutral pH is maintained (~8) which is like the posterior midgut, but more acidic than the anterior midgut based on the functional differences amongst these segments (Dadd 1975).

The anterior midgut is located just posterior to the gastric caeca, and is made of mostly columnar epithelial cells, in addition to the less abundant cuboidal cells (Zhuang et al. 1999). This segment of the midgut is primarily involved in the digestion and absorption of nutrients. This is supported by the highly alkaline luminal pH (~10-11) maintained in the anterior midgut, which aids in the breakdown of food, while the high pH also provides an environment that supports digestive enzyme activity (Dadd 1975). The establishment of this alkaline environment needed to digest food is driven by the transport of H^+ out of the lumen of the anterior midgut (Boudko et al. 2001b; Zhuang et al. 1999). The last distinct region of the midgut is the posterior midgut, which contains columnar, cuboidal and basal regenerative cells (Zhuang et al. 1999). The role of the posterior midgut is to absorb nutrients and ions from ingested food which explains the presence of an apical brush border, where surface area is optimized for nutrient and ion absorption (Zhuang et al. 1999). Furthermore, the posterior midgut plays an important role in reducing the alkalinization of the gut lumen presented by the anterior region (Jagadeshwaran et al. 2010). This is done by reducing the luminal pH of the posterior midgut to ~7.6-8.5, where the alkalinized lumen from the anterior segment is no longer required along the posterior segment as the functional motives differ (Dadd 1975). Furthermore, despite there being an understanding on the response of the gastric caeca to salinity, less is known on how the anterior and posterior midgut cope with a changed environmental salinity despite larval *A. aegypti* being adaptive to these conditions.

1.3.2. Malpighian tubules

The Malpighian tubules are critical iono- and osmoregulatory organs involved in the secretion of water and ions to produce a primary urine. In *A. aegypti,* there are five structurally and functionally identical Malpighian tubules which are described by having a blind-ended distal segment and a proximal segment that opens into the alimentary canal, where the midgut and

hindgut meet (Figure 2) (Beyenbach and Piermarini 2011). Each Malpighian tubule is composed of cuboidal principal cells and squamous stellate cells that intercalate between these principal cells. Furthermore, the lumen facing, apical membrane of the Malpighian tubules contains an apical brush border, where the microvilli are dense and contain enhanced elongation on principal cells compared to stellate cells for increased secretory abilities (Beyenbach and Piermarini 2011). Both cell types are involved in the secretion of ions and water, but a vast majority of the secretion occurs through the more abundant principal cells (Beyenbach et al. 2010). To produce a primary urine for excretion, the tubules facilitate the transepithelial secretion of ions by active transport mechanisms, which creates an osmotic pressure that promotes water secretion across the tubule membrane through aquaporin water channels (Marusalin et al. 2012; Misyura et al. 2017; Misyura et al. 2020). The secretion of water and ions (e.g., Na^+, K^+, Cl^-) into the tubule lumen compromises part of the primary urine produced by the tubules that is approximately iso-osmotic to the hemolymph (Piermarini 2016). This urine product is then further processed at the hindgut for ion reabsorption, while excess water remains and becomes excreted from the rectum. When *A. aegypti* larvae are reared in salty conditions, the tubules have been found to increase secreted [Cl^-] while maintaining overall fluid secretion rates (Donini et al. 2006; Jonusaite et al. 2017b). Ultimately, the role of the tubules in FW conditions is well studied, with less being known on their role in response to salinity. Although, in the SW-adapted mosquito larvae, *Aedes taeniorhynchus,* the Malpighian tubules exhibit higher secretion rates, with more Na^+ and K^+ being secreted compared to FW-adapted larvae (*A. aegypti*) (Donini et al. 2006). This illustrates that there are physiological differences exhibited by the Malpighian tubules of FW compared to SW adapted larval mosquitoes.

1.3.3. Hindgut

The hindgut is characterized by two distinct regions, the anterior ileum and the more posterior rectum. Both segments are composed of a single layer of epithelial cells, where the rectum is composed of thick columnar cells and contains an apical brush border, maximizing cell surface area (Meredith and Phillips 1973; Edwards and Harrison 1983). Furthermore, the basolateral membrane of the rectal epithelial cells contains many basal infoldings for increased surface area, which is characteristic of ion-transporting epithelia (Meredith and Phillips 1973; Edwards and Harrison 1983). The rectal segment is the site primarily responsible for the reabsorption of ions from the luminal fluid which originates mostly from the secretion of water and ions by the Malpighian tubules (Figure 2) (Bradley 1987; Phillips 1981; Phillips et al. 1987; Ramsay 1950). This process results in a hypotonic fluid to be excreted thereby helping to conserve ions that were initially secreted by the tubules and enabling excess water removal in FW environments (Bradley 1987). Understanding how the hindgut adjusts its osmoregulatory physiology in response to salinity is lacking in FW mosquitoes. However; in SW mosquitoes, the rectum has been shown to actively secrete salts to produce a hyperosmotic urine (Beadle 1939; Patrick et al. 2024; Ramsay 1950). In *A. taeniorhynchus*, the rectal secretion of ions has been linked to V-Type H^+-ATPase which establishes a gradient that facilitates Na^+ secretion through a cation proton exchanger across the apical membrane (Patrick et al. 2024). Nonetheless, these differences observed in the rectum of saline mosquitoes illustrates the physiological changes required to maintain osmotic homeostasis in raised salinities.

1.3.4. Anal papillae

Another set of organs crucial to maintaining ion and water balance, are the anal papillae (papillae). These organs are found in select dipteran larval species, including *A. aegypti.* The papillae are four identical and distinguishable organs based on their long ovoid shape and posterior

location, where they protrude from the body surface and come into direct contact with the surrounding environment (Figure 2). Ultra-structurally, the papillae of *A. aegypti* are characterized by their multinucleate, syncytial epithelium with an apical (environment facing) membrane possessing microvilli and a basal membrane (hemolymph/lumen facing) with extensive infoldings and a high abundance of closely associated mitochondria (Edwards and Harrison 1983; Sohal and Copeland 1966). This ultrastructure is indicative of an epithelium that functions in solute transport and subsequent studies confirmed that papillae absorb ions from the water in which the larvae reside (Sohal and Copeland 1966; Donini and O'Donnell 2005; Koch 1938; Ramsay 1953; Stobbart 1959; Stobbart 1960). Specifically, in FW the papillae take up Na^+, K^+ and Cl^-, while secreting H^+ and NH_4^+ (Donini and O'Donnell 2005). Through understanding the role of the papillae in dilute FW conditions, morphological and functional changes have been characterized in these organs when exposed to varying salinities. For example, when treated in NaCl compared to dilute media, the papillae face reductions in their size, surface area, membrane infoldings and mitochondrial abundance (Edwards and Harrison 1983; Sohal and Copeland 1966; Wigglesworth 1938). On a functional level the papillae have been shown to experience reductions in the uptake of NaCl when exposed to BW which should aid in stabilizing hemolymph ion content in *A. aegypti* larvae (Donini et al. 2007). Furthermore, in other dipteran larvae possessing anal papillae like the midge, *Chironomus riparius,* the papillae can actively secrete Na^+ when acutely exposed to elevated levels of NaCl (e.g., 7g/L) (Reinsborough and Donini 2025). Overall, the papillae can adjust their function in response to changes in ambient salinity to support internal ion-balance within aquatic larvae.

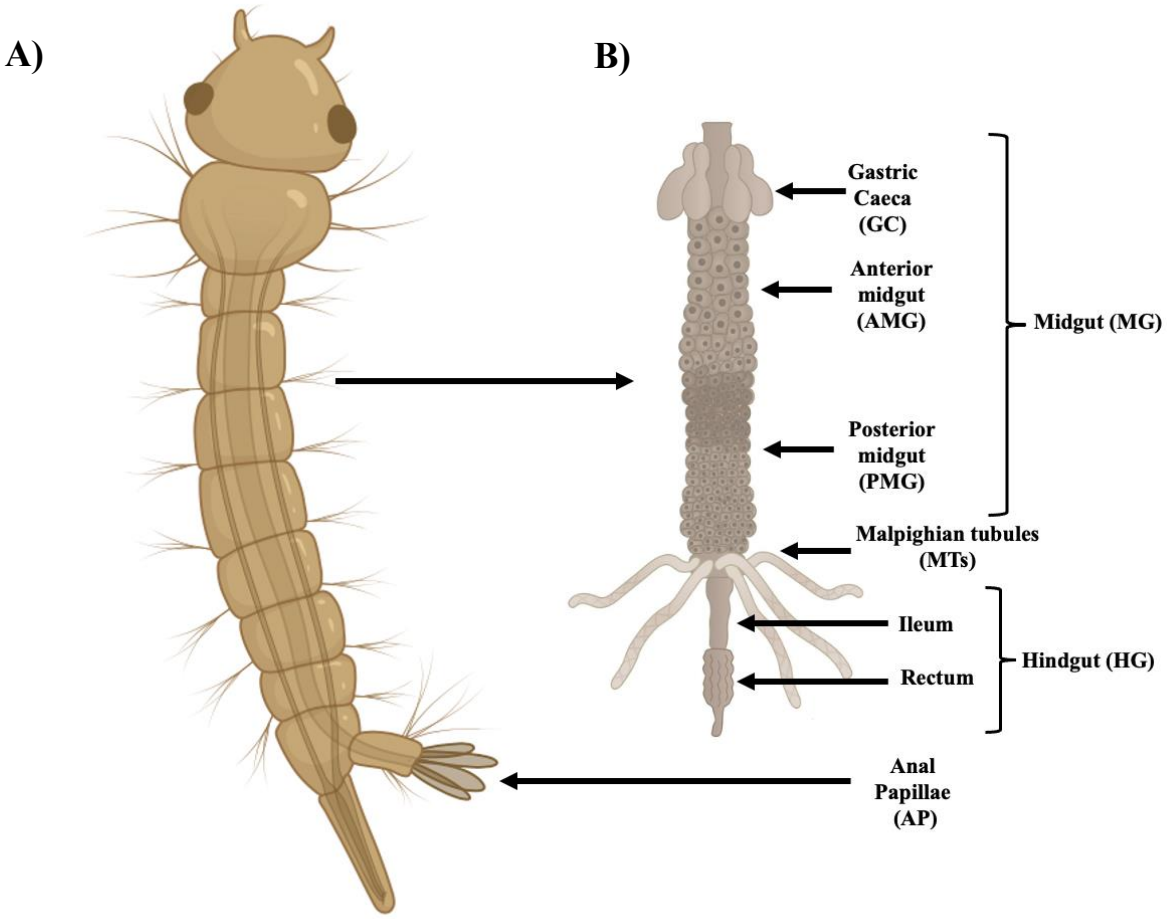

Figure 2. Osmoregulatory organs of the FW larval mosquito - *Aedes aegypti*. (A) Shows an illustration of a mosquito larvae, where the external anal papillae organs are shown, which come into direct contact with the aquatic habitat. (B) Demonstrates an isolated larval whole-gut where the distinct regions of the gut are highlighted. Most anterior is the gastric caeca (GC), followed by the anterior midgut (AMG), then the posterior midgut (PMG). These distinct segments make up the entirety of the midgut (MG). Located where the midgut and hindgut meet, are the five Malpighian tubules (MTs). Posterior to the tubules is the start of the hindgut (HG), first composed of the ileum, and posterior to that is the rectum. (A) is a larval mosquito illustration made with BioRender (biorender.com) (B) is a modified illustration from Lecia Szyca.

1.4. Active transporters in ion-regulatory epithelia

Transcellular ion transport across epithelia occurs through transport proteins expressed in the plasma membrane of epithelial cells. Transport is energized by ATP consuming transporters, P-Type Na^+-K^+-ATPase (NKA) and the V-Type H^+ ATPase (VA) which set up electrochemical gradients that power solute transport (Patrick et al. 2006). The VA transports H^+ out of cells in most ion-regulatory epithelia establishing a negative electrochemical potential which promotes the uptake of ions such as Na^+ and K^+ (Klein 1992; Wieczorek et al. 1999). For example, in *A. aegypti* VA is often regarded for its role in pumping H^+ into the lumen of the MTs which drives ion secretion, and for pumping H^+ into the aquatic habitat in papillae promoting ion absorption (Del Duca et al. 2011; Weng et al. 2003). NKA transports $3Na^+$ out of the cell in exchange for $2K^+$ establishing the cell's membrane potential in virtually all cells of animals, and in ion regulatory epithelia that is directly responsible for regulating Na^+ levels in body fluids (Sáez et al. 2009; Skou 1999; Weihrauch and O'Donnell 2015; Wieczorek et al. 1999). The role for NKA in ion-regulation in *A. aegypti* is less clear throughout the midgut and hindgut, but in the MTs it has been shown to promote steady rates of fluid secretion, and it is implicated in Na^+ uptake by the papillae (Hegarty et al. 1991; Del Duca et al. 2011). Nonetheless, despite the role of NKA being more elusive in the other ion-regulatory organs, its localization and presence suggest its importance in energizing ion-transport (Patrick et al. 2006).

Working in conjunction with these primary active transporters are various secondary transporters and enzymes that rely on the gradients produced by the primary transporters. A superfamily of transporters involved in ion-transport and pH balance are the monovalent cation/proton antiporters (CPAs) which are involved in exchanging monovalent ions (e.g., Na^+, K^+ or Li^+) in exchange for H^+ (Brett et al. 2005). This super family is divided into two groups - CPA1 and CPA2 (Brett et al. 2005). CPAs belonging to the CPA1 category are known as Na^+/H^+

exchangers (NHEs) which are electroneutral, transporting cations in exchange for H^+ (Brett et al. 2005; Putney et al. 2002). Meanwhile, Na^+/H^+ antiporters (NHAs) are categorized into the CPA2 family, where they have been found to be electrogenic driving the exchange of nH^+ with nNa^+/nK^+ (Brett et al. 2005; Taglicht et al. 1993). Other examples such as in mammals and in fruit flies illustrate that NHAs can facilitate the electroneutral transport of ions as well (Chintapalli et al. 2015; Usdavinys et al. 2017). NHEs have been characterized in epithelial tissue of both adult and larval *A. aegypti* including in the Malpighian tubules, midgut, the gastric caeca and the anal papillae (Chasiotis et al. 2016; Kang'ethe et al. 2007; Pullikuth et al. 2006). In the FW mosquito *Anopheles gambiae,* NHAs have been characterized in larvae (Rheault et al. 2007; Xiang et al. 2012). AgNHA1 was localized in larval gastric caeca, midgut, Malpighian tubules and rectal tissue (Okech et al., 2008a; Rheault et al. 2007). Furthermore, in the Malpighian tubules AgNHA1 and AgNHA2 were both found to be apically localized in the principal and stellate cells, respectively (Xiang et al. 2012). No characterization of NHAs have been established in *A. aegypti,* although, RNA sequencing studies have detected relevant transcript levels for two putative NHAs, AeNHA1 and AeNHA2 (Akbari et al. 2013; Durant et al. 2021; Li et al. 2017; Matthews et al. 2018).

Another group of secondary transporters involved in ion-transport in osmoregulatory epithelial tissues are known as cation coupled chloride co-transporters (CCCs). These transporters are responsible for the electroneutral transport of Na^+ and or K^+ with Cl^- (Arroyo et al. 2013). The superfamily of CCCs, includes $Na^+/K^+/2Cl^-$ cotransporters (NKCCs), Na^+/Cl^- cotransporters (NCCs) and K^+/Cl^- cotransporters (KCCs) (Hartmann et al. 2014). Ultimately, CCCs are involved in both ion secretion and absorption depending on the organ, organism and environmental conditions (Haas and Forbush III 2000; Hwang et al. 2011; McNamara and Faria 2012). Compared to vertebrate models, less is known on the role of CCCs in insect ion-regulating epithelia. In

Drosophila melanogaster and *A. aegypti* Malpighian tubules, NKCCs (e.g., AeNKCC1) have been linked to basolateral uptake (into the cell) of Na^+, K^+ and $2Cl^-$ to allow for these ions to be secreted apically for primary urine production (Beyenbach and Piermarini 2011; Rodan et al. 2012). Other CCCs have been characterized in *A. aegypti* such as AeCCC2 and AeCCC3 which are proposed to be linked to ion secretion and absorption, respectively (Piermarini et al. 2017). This is based on the findings that *ccc3* mRNA abundance was high in the ion-absorptive anal papillae organs while *ccc2* abundance was higher in the ion-secretory Malpighian tubules (Piermarini et al. 2017). However; in the ion-absorptive hindgut, both *ccc2* and *ccc3* transcripts have been detected in larval *A. aegypti* (Durant and Donini 2024).

Working in conjunction with primary active transporters (e.g., NKA and VA) and secondary transporters (e.g., NHEs/NHAs and CCCs) are the metalloenzymes found in many different cell types and tissues known as carbonic anhydrases (CAs). These enzymes are responsible for catalyzing the reversible reaction of $CO_2 + H_2O \leftrightarrow H^+ + HCO_3^-$ (Lindskog 1997). The production of H^+ by CAs can be used by transporters (e.g. VA, NHE) to drive Na^+ transport while HCO_3^- can be exchanged for Cl^- and these processes have been implicated in the ion-absorptive papillae of *A. aegypti* larvae (Del Duca et al. 2011). CAs may also contribute to pH regulation by the buffering capacity of HCO_3^- as seen in the midgut lumen (Dixon et al. 2017). There are five evolutionarily distinct CAs including alpha, beta, gamma, zeta and eta, with the α-CAs found more commonly in animals (Dixon et al. 2017; Lindskog 1997). The location of CAs in cells varies as follows: through glycosylphosphatidylinositol (GPI)- anchorage to the plasma membrane; soluble in the cytoplasm; integrated as a transmembrane protein; mitochondrial or they can be secreted (Hewett-Emmet and Tashian 1996; Linser et al. 2009). Within the larval midgut of *A. aegypti* a CA isoform with GPI-anchorage to the membrane was detected primarily in the

gastric caeca, with some detection in the anterior/posterior midgut and the Malpighian tubules (Seron et al. 2004). Following this discovery, 14 CA genes were characterized in *A. aegypti*, where the transcript expression of a specific soluble cytoplasmic CA designated as AeCA9 was enriched throughout all developmental stages (Dixon et al. 2017). AeCA9 protein was also expressed throughout the midgut (including gastric caeca) and Malpighian tubules of both larvae and adults (Dixon et al. 2017). Furthermore, a transcriptome study detected high levels of *ca9* transcript in *A. aegypti* papillae (Durant et al. 2021).

1.5. Ion-transport models in the ion-regulating organs of *Aedes aegypti* larvae

Thus far, previous work has highlighted the types of active transporters that may be involved in facilitating ion-absorption or secretion in the osmoregulatory organs of larval *A. aegypti.* However, the localization and types of different transcellular transporters have been found to vary across these organs based on their function which provides valuable insight on how the larvae are capable of osmoregulation in dilute media as well as in response to changes in external salinity.

1.5.1. Transcellular transport mechanisms of the midgut

The midgut is divided into the gastric caeca, the anterior region and the posterior region, based on differences in the function of these distinct segments. Similarly, the types of transcellular transporters and their localizations vary across these regions. In the gastric caeca both NKA and VA are expressed (Patrick et al. 2006). VA is found on the apical membrane in all epithelial cells of the gastric caeca and in the cells that make up the distal third of the caeca, it is also on the basal membrane (D'Silva et al. 2017b; Patrick et al. 2006). NKA is found on the basal membrane of the epithelial cells that make up the proximal two-thirds of the caeca (Figure 3A, B) (D'Silva et al. 2017b; Patrick et al. 2006). In all the cells of the gastric caeca AeCA9 is expressed in the cytoplasm

and AeCCC (AaeCG1277) which shares homology with a *Drosophila* CCC, is expressed on the basal membrane (Figure 3A, B) (Dixon et al. 2017; Filippov et al. 2003). There is no functional characterization of AeCCC, but it is suggested to help drive the secretion of Na^+ and or K^+ with Cl^- (D'Silva et al. 2017b). An anion exchanger AeAE1 expresses on the basal membrane with pronounced staining on the distal segments of the gastric caeca (Linser et al. 2012). The AeAE1 has been characterized to facilitate the antiport of Cl^- into cells for HCO_3^- out (Figure 3A, B) (Piermarini et al. 2010). The CPA1 variants, AeNHE3 and AeNHE8 are expressed on the basal membrane of the distal caeca and apically across the entire caeca, respectively (Figure 3A, B) (Kang'ethe et al. 2007; Pullikuth et al. 2006). The basal expression of AeNHE3 is proposed to drive the secretion of Na^+ or K^+ into the epithelial cell from the hemolymph (D'Silva et al. 2017b). The apically located AeNHE8 is suggested to be linked to the secretion of Na^+ or K^+ from the cell into the gastric caecal lumen (D'Silva et al. 2017b).

The anterior and posterior midgut possess small variations in the transporters they express, and their localization based on the functional differences between these regions. Despite its apical localization in the majority of epithelial cells involved in ion-transport, VA is on the basal membrane of the anterior midgut where H^+ transport into the hemolymph maintains a negative transepithelial lumen potential and a highly alkaline luminal fluid (Figure 3C) (Patrick et al. 2006; Boudko et al. 2001b; Clark et al. 2000; Onken et al. 2008; Zhuang et al. 1999). CAs have been found to be involved in luminal alkalinization likely providing VA with H^+ for acid efflux and more recently AeCA9 protein has been detected in the anterior midgut (Figure 3C) (Boudko et al. 2001a; Boudko et al. 2001b; Dixon et al. 2017). Localized along the basal membrane of the anterior midgut with VA is the AeNHE3 (Figure 3C) (Pullikuth et al. 2006). The role for the basal AeNHE3 in the anterior midgut has not been exclusively studied, but the function of this

transporter has been shown to restore intracellular pH levels in a cell line known to not express endogenous NHEs (e.g., PS120) by exchanging H^+ for Na^+ or K^+ (Pullikuth et al. 2006). Furthermore, pharmacological inhibition of NHEs has been found to reduce luminal alkalinization suggesting its role for removing H^+ from the anterior midgut (Figure 3C) (Onken et al. 2008). Other transporters localized along the basal membrane are AeCCC and AeAE1, although how they contribute to ion flux at the anterior midgut has not been determined (Figure 3C) (Filippov et al. 2003; Linser et al. 2012). On the apical side of the anterior midgut, thus far only NKA has been expressed where based on its transport characteristics, would be transporting $3Na^+$ into the lumen for $2K^+$ (Figure 3C) (Patrick et al. 2006).

At the posterior midgut VA is apical while NKA is basal, the opposite to that of the anterior midgut (Figure 3D) (Patrick et al. 2006). VA has been shown to be responsible for maintaining the positive lumen potential and the re-acidification of the lumen by H^+ secretion (Jagadeshwaran et al. 2010). The posterior midgut of larval *A. aegypti* also exhibits CA activity and its inhibition causes a reduced positive luminal potential (Corena et al. 2002; Jagadeshwaran et al. 2010). Recently AeCA9 was shown to be expressed in the posterior midgut, suggesting its involvement in acidification through providing H^+ to VA for apical secretion (Figure 3D) (Dixon et al. 2017). Apically it is also proposed that the posterior midgut contains a nutrient amino acid transporter (NAT) which drives Na^+ and amino acids into the cell from the lumen (Figure 3D) (Jagadeshwaran et al. 2010). An NHA is also proposed to be transporting Na^+ into the cell for $2H^+$, and Na^+ is then further transported into the hemolymph by the basal NKA (Jagadeshwaran et al. 2010; Patrick et al. 2006). The exact NAT or NHAs involved in this process is unknown in larval *A. aegypti*. Although, in the FW mosquito larvae *A. gambiae* NATs and NHAs proposed to be involved in this process have been localized to the apical membrane of the posterior midgut (e.g., AgNAT8 and

AgNHA1) (Okech et al. 2008a; Rheault et al. 2007). On the basal side of the posterior midgut is the AeNHE3, AeAE1, AeCCC (Linser et al. 2012; Pullikuth et al. 2006) (Figure 3D). How these transporters serve the posterior midgut has not been studied but based on their function observed thus far, AeNHE3 exchanges Na^+ or K^+ for H^+, while AeAE1 exchanges Cl^- for HCO_3^- (Figure 3D) (Piermarini et al. 2010; Pullikuth et al. 2006).

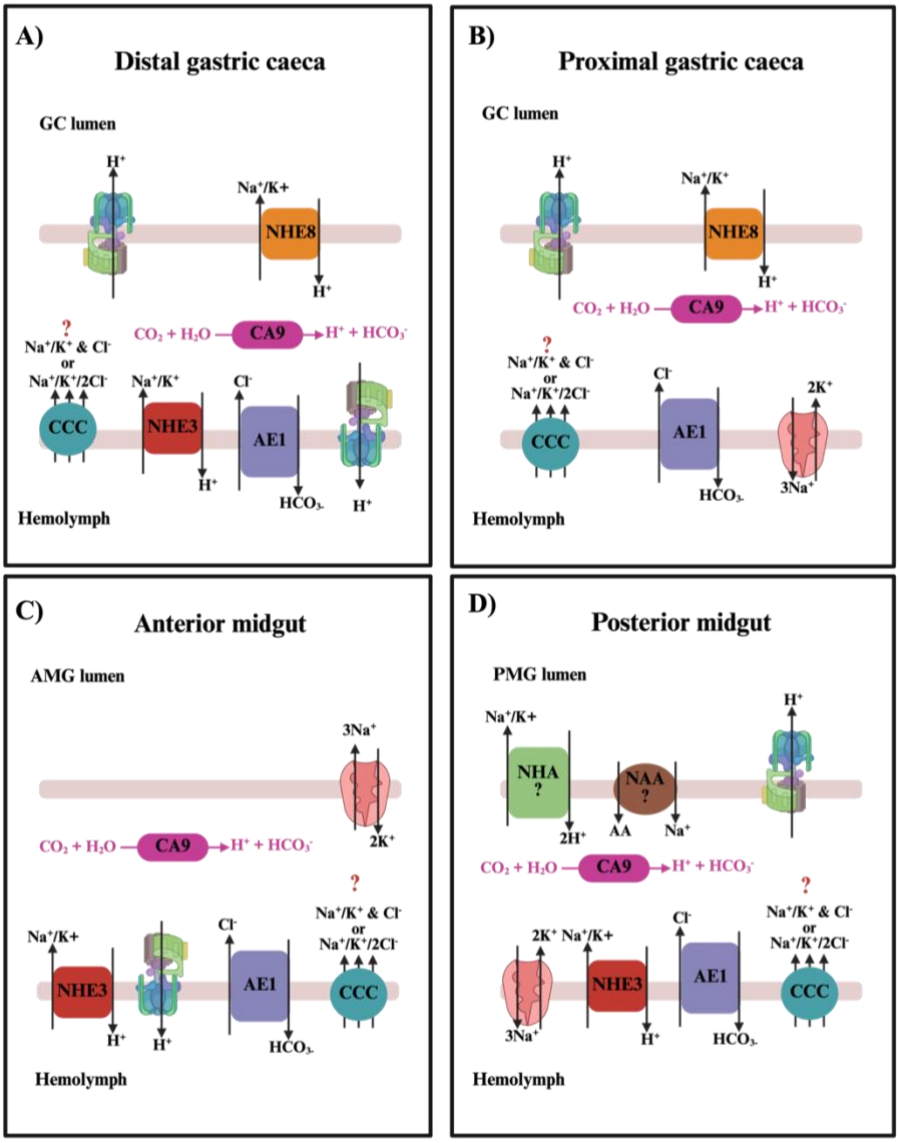

Figure 3. Proposed ion-transport model of the various segments of the midgut in the larval *Aedes aegypti*. (A) Illustrates the ion-transporters localized to the distal gastric caeca of larval *A. aegypti*, where the apical membrane faces the GC (gastric caeca) lumen, and the basolateral membrane faces the hemolymph of the larvae. (B) Shows the ion-transporters localized to the proximal gastric caeca. (C) and (D) show the proposed ion-transport models for the anterior and posterior midgut respectively, where the apical membrane faces the AMG (anterior midgut) lumen and PMG (posterior midgut) lumen. Basal membranes also face the hemolymph for the AMG and PMG. In A, B, C and D, the transporter pumping H^+ is the V-Type H^+-ATPase, and the Na^+-K^+-ATPase is shown transporting $3Na^+$ for $2K^+$. NHE3 and NHE8 are Na^+/H^+ exchangers, CCCs are cation-coupled chloride co-transporters and CA9 is the characterized carbonic anhydrase 9. In (D) NAA is a proposed nutrient amino acid (aa) co-transporter, and NHA is a proposed Na^+/H^+ antiporter. Transporters shown with a black '?' indicate that they have not been localized, with their localization being proposed. Ion movements with a red '?' indicate that the function is proposed (see main text). This figure was made using BioRender (biorender.com).

1.5.2. Transcellular transport mechanisms of the Malpighian tubules

The ion transport mechanisms in tubules of *A. aegypti* are often based on adult female studies. Although, the ion-transporters involved in secretion at the MTs of larvae has become more developed. Along the basal membrane of the principal cells AeNHE3 has been expressed, where it is proposed to drive Na^+/K^+ secretion into the cell for H^+ out (Figure 4) (Li et al. 2017; Pullikuth et al. 2006). AeCCC2 protein has also been expressed in the MTs of larvae, where it is localized on the basal membrane and has been shown to transport Na^+ alone when expressed in a heterologous system (Figure 4)(Duong et al. 2022; Kalsi et al. 2019). Other cation-coupled chloride co-transporters such as AeNKCC1 have been expressed on a transcript level in larval MTs like adult MTs, where it is proposed to be basal and secreting Na^+, K^+ and Cl^- like what has been proposed for adult *A. aegypti* (Li et al. 2017; Scott et al. 2004). On the apical membrane of principal cells, VA has been localized in both adult and larval tubules, where it is proposed to provide H^+ for apical NHAs/NHEs which will then exchange H^+ for Na^+/K^+ (Figure 4) (Patrick et al. 2006). Indeed, in the larvae NHE8 has been localized to the apical membrane of principal cells (Figure 4) (Kang'ethe et al. 2007). In larval *A. aegypti,* the presence of CAs to hydrate CO_2 to produce H^+ and HCO_3^- has been evaluated, with AeCA9 being the probable candidate for facilitating this exchange, due to its localization in the cytoplasm of larval principal cells (Dixon et al. 2017).

In the stellate cells, NKA and AeAE1 have been localized on the basal membrane of larval *A. aegypti* (Figure 4) (Linser et al. 2012; Patrick et al. 2006). Here, NKA would transport $3Na^+$ into the hemolymph for $2K^+$ into the stellate cell, likely establishing a negative membrane potential to energize other transporters (Figure 4) (Patrick et al. 2006). The basal AeAE1 facilitates Cl^- influx into the stellate cell, for HCO_3^- out, driving basal Cl^- secretion (Figure 4) (Piermarini et al. 2010). Furthermore, transcripts for several Cl^- channels have been detected in larval tubules, where they are proposed to facilitate the transepithelial secretion of Cl^- across the apical membrane of the

stellate cells, like what has been found in adult *A. aegypti* (Figure 4) (Li et al. 2017; O'Connor and Beyenbach 2001). Ultimately, when in conditions of increased salinity (e.g., BW), understanding the response or role of transcellular transporters has not yet been evaluated despite the ability of larvae to maintain osmotic homeostasis (Bradley 1987; Donini et al. 2007; Edwards 1982; Richards and Meier 1974).

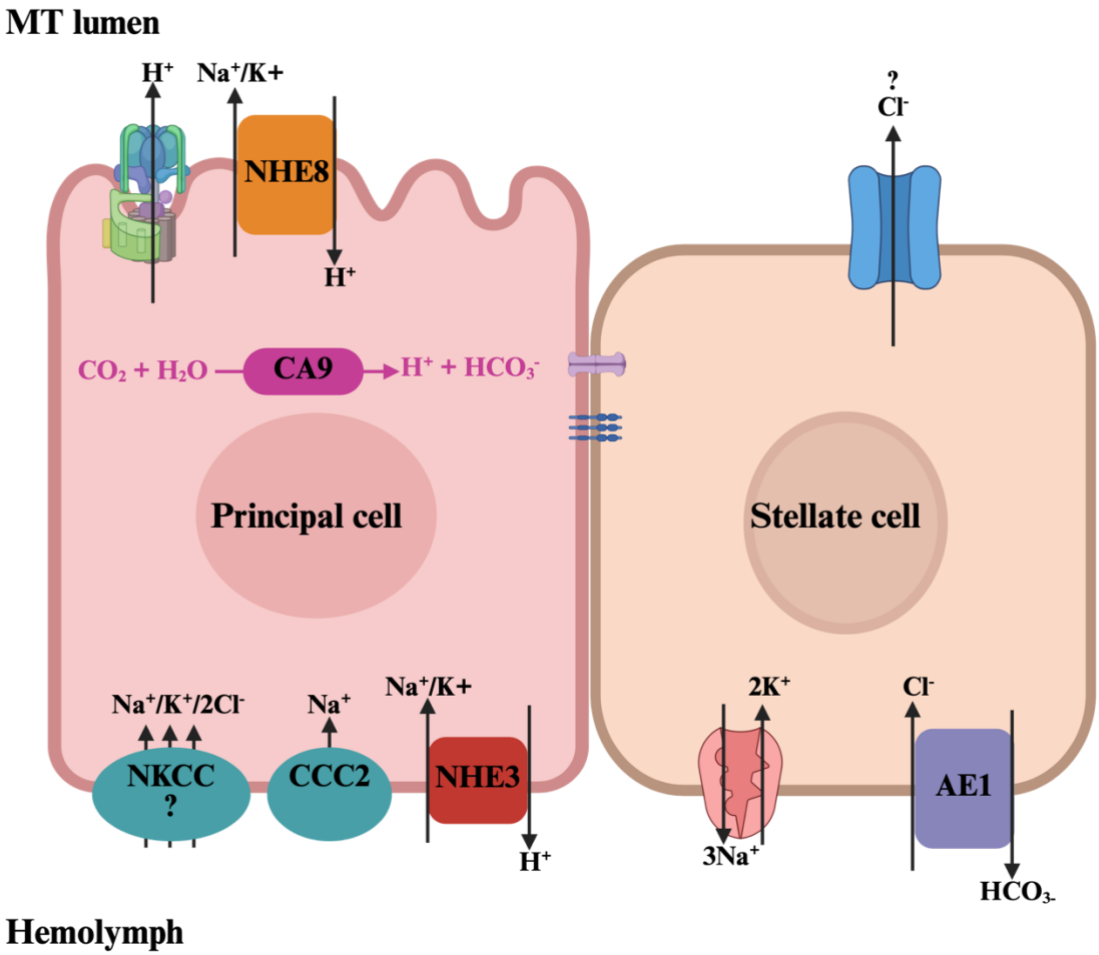

Figure 4. Proposed model of larval Malpighian tubule (MT) ion secretion in larval *Aedes aegypti*. The apical membrane faces the MT lumen, where in principal cells, the V-Type H^+-ATPase has been localized (extrudes H^+) a Na+/H+ exchanger (NHE8) as well. Within the cytoplasm of principal cells is the carbonic anhydrase (CA9) catalyzing the reversible reaction of hydrating CO_2. The basal membrane of principal cells is proposed to contain a $Na^+/K^+/2Cl^-$ cotransporter (NKCC) (see main text). Adjacent to the principal cell is the stellate cell, where on the basal membrane the Na^+-K^+-ATPase has been localized, transporting $2K^+$ out of the hemolymph for $3Na^+$, alongside an anion exchanger (AE) which exchanges Cl^- for HCO_3^-. On the apical membrane of stellate cells, Cl^- channels are proposed to be facilitating Cl^- secretion. Any '?' symbolizes that the transporters shown have not be localized in larvae, with their proposed localization based on evidence for their role in larval MTs. This figure was made using BioRender (biorender.com).

1.5.3. Transcellular transport mechanisms of the hindgut

Thus far, VA has been immunolocalized to the apical membrane of the hindgut, pumping H^+ into the lumen (Figure 5) (Patrick et al. 2006). Additionally, NKA is located on the basal side of the hindgut, transporting Na^+ into the hemolymph in exchange for K^+ into the cell (Figure 5) (Patrick et al. 2006). Based on the localization of these transporters, they are presumed to play a role in energizing ion re-absorption; however, the direct ion-transporters involved in re-absorption remains unclear. A transcriptome study on the hindgut of larval *A. aegypti* showed high expression of transcript levels for inwardly rectifying K^+ channels (e.g., *kir2*), *ccc2 and ca9* (Figure 5) (Durant and Donini 2024). Although, their roles in ion-absorption at the hindgut have not been studied. Furthermore, the role of both primary and secondary active transporters in the hindgut when exposed to conditions of salinity has not been uncovered.

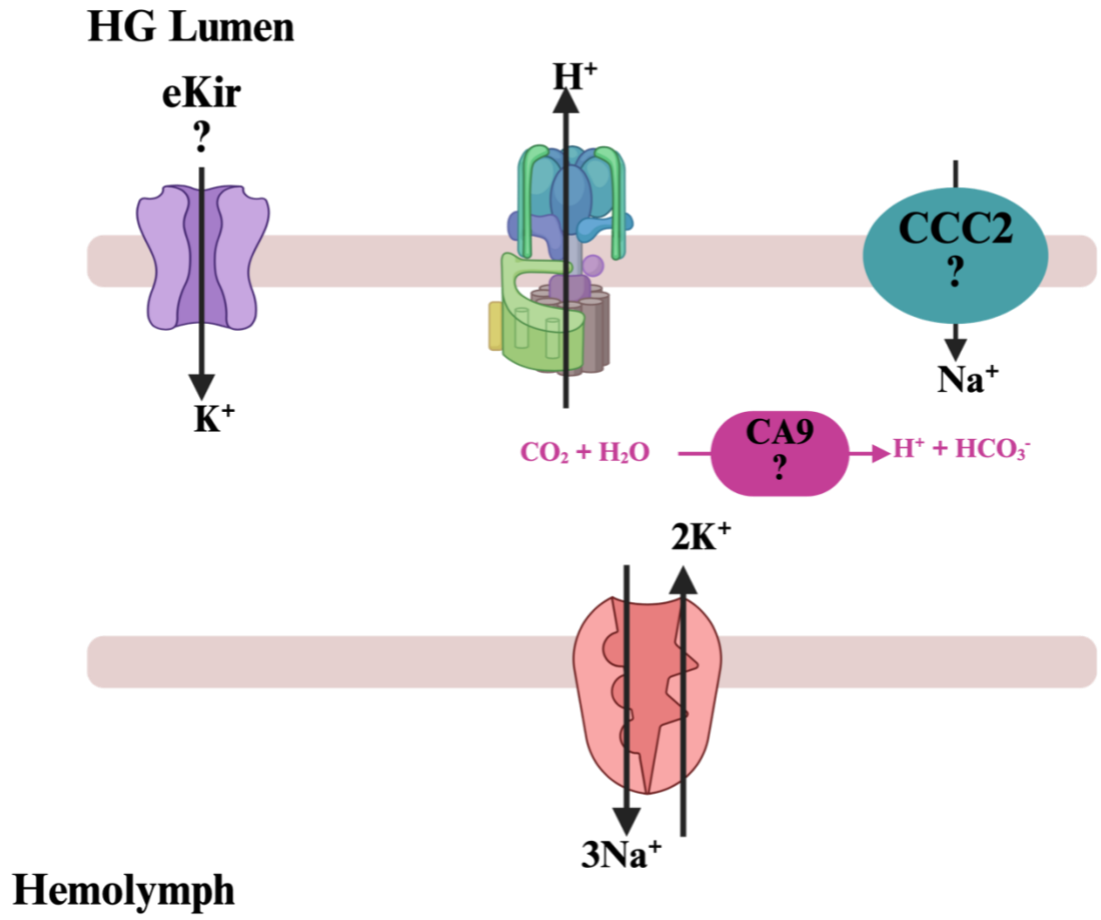

Figure 5. Ion transport model proposed for the hindgut (HG) of FW larval *Aedes aegypti*. The apical membrane of the HG faces the HG lumen, whereas the basal membrane is hemolymph facing. Both the V-Type H^+-ATPase (extrusion of H^+) and Na^+-K^+-ATPase (exchange of $3Na^+$ for $2K^+$) are localized to the apical and basal membrane respectively. The remaining transporters shown such as a cation-couple chloride cotransporter (CCC2), carbonic anhydrase (CA) and inwardly rectifying K^+ channels (Kir) are proposed to be involved in ion-transport with their functional implications unclear in the HG (see main text). This figure was made using BioRender (biorender.com).

1.5.4. Transcellular transport mechanisms of the anal papillae

Understanding the transport mechanisms by which NaCl/KCl are absorbed from the external environment through the papillae has not been fully established. VA is expressed on the apical (water facing side) where H^+ secretion is thought to drive Na^+ uptake (Figure 6) (Del Duca et al. 2011; Patrick et al. 2006; Stobbart 1965; Stobbart 1967). The apical application of pharmacological inhibitors targeting CPAs had no effect on Na^+ uptake, whereas inhibition of Na^+ channels reduced Na^+ uptake, suggesting that Na^+ channels mediate its apical absorption (Del Duca et al. 2011). Although, a recent transcriptome study on the papillae of *A. aegypti* shows relevant transcript levels for putative NHAs (e.g., AeNHA1 and AeNHA2) while no known Na^+ channel transcripts were present (Durant et al. 2021). AeNHE3 is expressed on the apical membrane of the papillae, where it is suggested to transport NH_4^+ or H^+ into the environment, in exchange for Na^+ (Figure 6) (Chasiotis et al. 2016). Therefore, the transport mechanism for apical uptake of Na^+ in these organs remains to be determined. On the basal side (lumen facing), NKA has been localized where it helps establish a negative membrane potential and drive Na^+ into the lumen for its absorption (Figure 6) (Patrick et al. 2006).

In addition to understanding Na^+ uptake, Cl^- absorption has also been studied in the papillae. For example, inhibition of both CA and HCO_3^-/Cl^- antiporters reduce the total Cl^- absorption across isolated papillae (Del Duca et al. 2011). Transcript levels of *ca9* are relatively high in the papillae which supports the pharmacological results implicating HCO_3^-/Cl^- exchange (Durant et al. 2021). However; like with Na^+ uptake, no transcripts of known HCO_3^-/Cl^- antiporters were detected (Durant et al. 2021). On the other hand, transcripts of several annotated Cl^- channels were detected, as were *ccc3* transcript (Durant et al. 2021; Piermarini et al. 2017). Neither Cl^- channels nor AeCCC3 proteins have been localized in the papillae so how these transporters participate in ion uptake is speculative.

When larvae are exposed to BW the transcript levels of *ca9* and *nha1* decreased in the papillae, suggesting that they may be involved in NaCl uptake in FW (Durant et al. 2021). Meanwhile the transcript levels of *nha2* increase with salinity while *ccc3* transcript levels remain unchanged (Durant et al. 2021). Overall, this suggests that in salinity, there is likely a complex array of necessary changes that occur to facilitate adjustments to the transport functions of the papillae.

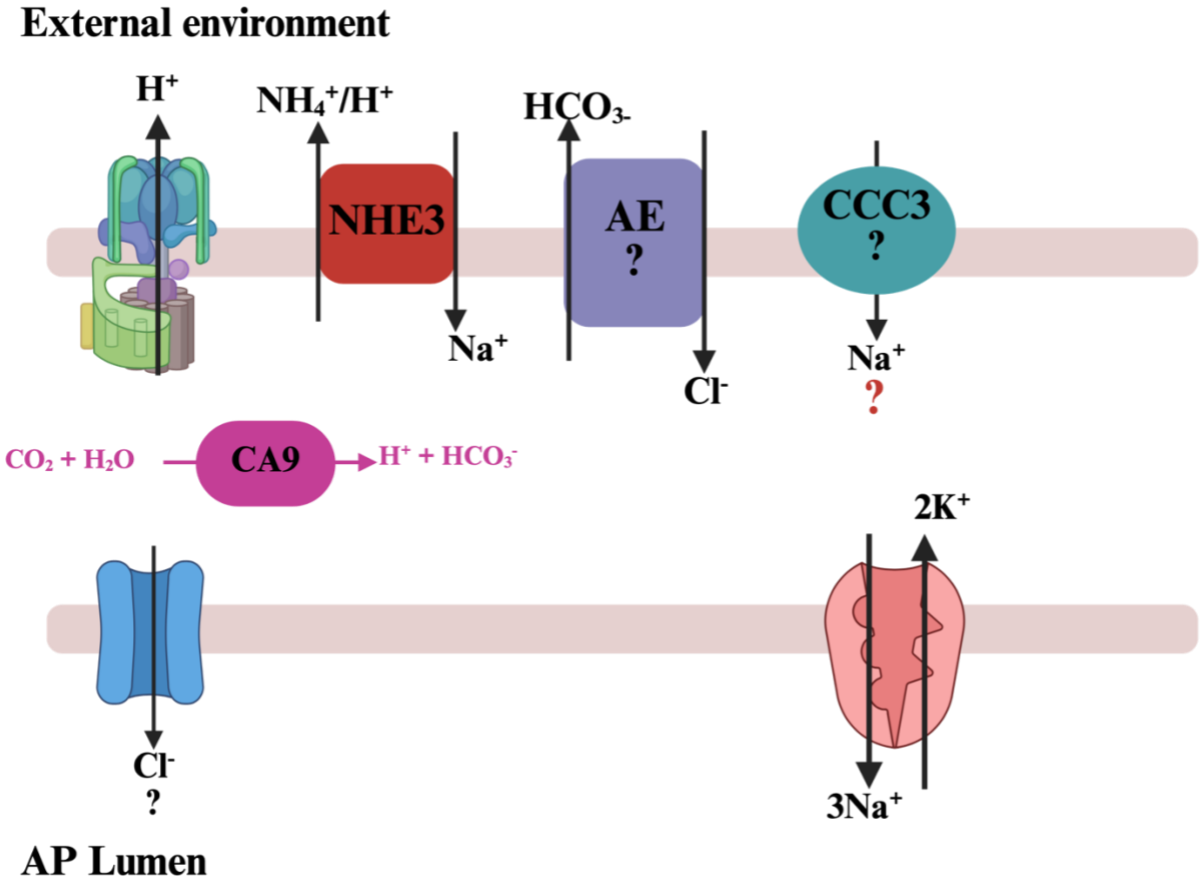

Figure 6. Proposed ion-transport model for NaCl absorption across the anal papillae (AP) of FW *Aedes aegypti* larvae. In the AP, the basal membrane faces the AP lumen, where the apical membrane faces the external environment. Apically, the V-Type H^+-ATPase (extrudes H^+) and Na^+/H^+ exchanger (NHE3) have been localized. The localization of an anion exchanger (AE) and a cation-coupled chloride co-transporter (CCC3) are proposed to be apical as well. On the basal membrane, the Na^+-K^+-ATPase (exchange of $3Na^+$ for $2K^+$) has been localized, with Cl^- channels proposed to be localized here as well. Furthermore, carbonic anhydrases such as CA9 are proposed to be cytoplasmic in the AP. Any black '?' symbolizes proposed transporter localization and red '?' indicates that the ion-specificities have not been determined for the respective transporters. This figure was made using BioRender (biorender.com).

1.8. Objectives and hypotheses

Since *A. aegypti* is an arboviral disease vector, studying the mechanisms which allow them to osmoregulate in aquatic environments throughout early lifecycle stages (e.g., larval) is of significance. Understanding which ion-transporters are involved in osmoregulation in FW but also, salinized environments (e.g., BW) can serve as possible future larval control targets. Specifically, little is known regarding the mediation of NaCl uptake in absorptive organs such as the hindgut and of particular interest – the papillae. As mentioned, a previous transcriptome compared the expression of different ion-transporters and enzymes in the anal papillae when acutely exposed (e.g., 24-hours) to FW or BW (Durant et al. 2021). In FW, the papillae have elevated transcripts of genes such as *ca9* and *nha1* which are reduced in salinity, meanwhile some transporters remain unchanged in either condition (e.g., *ccc3*) or become elevated when exposed to salinity such as the putative *nha2* (Durant et al. 2021). Therefore, the first objective of this research was to confirm the abundance of *ca9*, *ccc3* and the putative *nha1* and *nha2* using qPCR in the anal papillae of 24-hour treated AFW and BW larvae (Durant et al. 2021). Based on antibody availability, AeNHA1 protein localization was assessed in the papillae and protein expression in freshwater vs salinated water was evaluated. The second objective was to determine the functional role for AeCA9 and AeNHA1 in NaCl transport at the papillae of larval *A. aegypti* in FW and BW using dsRNA knockdown. It was hypothesized that based on their high transcript expression in FW which decreases in BW these transporters contribute to NaCl uptake at the anal papillae in dilute conditions (Durant et al. 2021). Furthermore, CAs have been found to be involved in NaCl uptake through pharmacological inhibition at the papillae and therefore, AeCA9 is hypothesized to be the candidate CA facilitating this transport (Del Duca et al. 2011).

In addition to confirming the abundance of *nha1*, *nha2*, *ca9* and *ccc3* in the papillae, the next objective of this study was to compare their transcript expression across the alimentary canal

(e.g., midgut, MTs, hindgut) of FW larval *A. aegypti* to add to the current body of knowledge on which ion-transporters may be serving these organs. Thus far, AeCA9 protein has been shown to be expressed along the alimentary canal, the putative *nha1* and *nha2* have been detected in a transcriptome done on the MTs, and another transcriptome showed evidence for transcripts of *ccc3* in the larval hindgut of *A. aegypti* (Dixon et al. 2017; Durant et al. 2021; Durant and Donini 2024; Li et al. 2017). Based on this, it is hypothesized that each of these genes will be expressed in the mentioned osmoregulatory organs, with differential expression patterns based on their functional differences. To further evaluate which ion-transporters may be salinity responsive, the next aim of this study is to assess their transcript expression in the midgut, MTs and hindgut in larvae treated in FW or salinated water (e.g., BW) for 24-hours, alongside assessing the protein localization and staining for AeNHA1 in these organs. It is hypothesized that each of the genes will show decreased abundance in BW based on the reduced need for hyperregulation, as the osmotic fluxes in BW are less than those faced in FW. Overall, this research aims to provide further insights on the transporters involved in FW vs BW osmoregulation of the larval *A. aegypti* to better understand how they withstand changes in environmental salinity with specific focus on the absorptive anal papillae.

2.0. Materials and Methods

2.1. Animal care and larval treatments

Aedes aegypti larvae (Liverpool) were maintained from a colony established in the lab at York University in Toronto, Canada. Adult mosquitoes were kept in mesh mosquito cages and were provided sugar water (10% sucrose) *ad libitum* through a soaked-cotton ball that was changed weekly. Females were periodically fed sheep's blood in Alsever's solution (Cedarlane Laboratories, ON, Canada). Small containers filled with ddH_2O and lined with filter paper were placed in each cage to allow for blood-fed adult females to deposit their eggs on the filter paper provided. Once eggs were laid, the filter paper was removed and left to dry before they were stored for later use. Eggs were hatched by placing egg strips in a large plastic container filled with dechlorinated tap water (deH_2O). Larval food, consisting of a 1:1 mixture of liver and yeast powder dissolved in ddH_2O was added to the plastic container with egg strips. The water was replaced with fresh deH_2O, and the hatched and growing larvae were fed with larval food every other day. The containers with growing larvae were kept in a temperature and light controlled incubator on a 12:12 hour light to dark cycle at 25°C. For experiments, larvae were starved for at least 24-hours and 4th instar larvae were taken from the colony and were placed in containers in either artificial freshwater (AFW: pH=7.6, 0.6g KCl, 0.35g NaCl, 0.5g NaOH, 0.84g $CaCl_2$, dissolved in 20L of 18.2 MΩ water) or in salinated water which is referred to as brackish water from here onwards (BW: 10.5g/L Instant Ocean Salt dissolved in AFW). For qPCR and western blotting organ collections, ~100 larvae were transferred to 500mL plastic containers with 250mL of either AFW or BW. For immunohistochemistry, ~10-15 larvae were placed in 100mL plastic containers, containing 50 mL of either AFW or BW. Additionally, to test out primers, obtain partial clones of genes and synthesize dsRNA template, larvae were treated as mentioned for

immunohistochemistry but only in AFW. For each experimental set up, larvae were maintained at 25°C and kept on a 12:12 hour light: dark cycle for 24 hours without feeding.

2.2. qPCR primer design

To examine the transcript abundance of *nha1*, *nha2*, *ca9* and *ccc3* in the different ion-regulating organs in AFW and when individuals were acutely exposed (24 hours) to AFW or BW, PCR was used to clone relatively large fragments of each gene for sequencing and subsequent design of primers for qPCR. PCR primers that spanned a relatively large fragment of each gene were designed based on mRNA sequences obtained from the National Centre for Biotechnology Information (NCBI) nucleotide database for *nha1* (accession number: AAEL011109-RC), *nha2* (AAEL000137-RD) and *ca9* (AAEL004930-RA), while the *ccc3* (AAEL009886-RA) primer set used was from a previous research study on *A. aegypti* larval MTs and AP (Piermarini et al. 2017). Using these mRNA sequences for each respective gene, primer sets spanning ~600-700 bp were then designed within these sequences using the Primer3 software (v. 0.4.0.) (Table 1). To confirm the partial mRNA sequences of these genes using these primer sets, total RNA was collected from 4-5 whole larvae of the 4th instar stage were treated in AFW for 24-hours using the PureLink RNA minikit (Invitrogen, MA, USA). These larvae that were treated in AFW were then placed in 300 µl of lysis buffer containing 1% β-mercaptoethanol kept on ice and samples were homogenized for 3 x 10 s at 5 watts using the XL 2000 Ultrasonic Liquid Processor (QSONICA LLC, Newton, CT, USA). RNA extraction was then conducted as per the manufacturer's instructions provided in the PureLink RNA minikit (Invitrogen). The RNA samples were then further purified with the TURBO DNA-*free*™ kit (Ambion®, Life Technologies Inc., Burlington, ON, Canada) and RNA quality and concentration was evaluated with a NanoDrop 2000 spectrophotometer (Thermo Scientific, DE, USA) before downstream application. Using the whole-body RNA (1 µg), template

cDNA was made for PCR reactions using the iScript™ cDNA synthesis kit (Bio-Rad Laboratories, Mississauga, ON, Canada) following the protocol provided by the manufacturer. The cDNA template made from whole-body tissue was then amplified in a PCR reaction with the different primer sets designed (Table 1) using the Q5® High-Fidelity DNA Polymerase (New England Biotechnology, Ipswich, MA, USA) at annealing temperatures ranging from 49.4°- 67°C to find suitable annealing temperatures (see Table 1). PCR amplicon band and size were confirmed by running an agarose gel electrophoresis, and the most optimal bands for each primer set were gel extracted and purified with the QIAquick PCR Purification Kit (Qiagen, Toronto, ON, Canada). Following purification, the concentration and purity of each product was verified using a NanoDrop 2000 spectrophotometer (Thermo Scientific, DE, USA). The purified product was then sent for sequencing (The Centre for Applied Genomics, Sick Kids, ON, Canada) and specificity of the sequenced product for *nha1*, *nha2* and *ca9* were confirmed using the NCBI nucleotide blast tool. Sequences were then aligned using the alignment tool on SnapGene (Dotmatics, San Diego, CA, USA) to confirm base pair matches from the NCBI mRNA sequence to that obtained through PCR amplification. Using these partial mRNA sequences, qPCR primers spanning ~100-200 bp of the genes were then designed and were later tested and used in qPCR application (Table 2).

Table 1. Primer sets tested and used to amplify larger fragments of *nha1*, *nha2* and *ca9* prior to qPCR primer design. The gene column depicts which gene was tested and are labelled according to how many primer sets were tested (e.g., 1-3 primer sets for each gene). For each gene, these different primer sets were designed from the same FASTA sequence derived by the GenBank accession number listed in the last column. This was done to obtain partial mRNA sequences for each of the genes (e.g., *nha1*, *nha2* and *ca9*). Both the forward and reverse primer sequences listed are oriented in the 5' to 3' direction and the respective amplicon size amplified by these primers is also listed. The tested annealing temperatures column illustrates the different annealing temperatures that were run using PCR for each of the different primer sets.

Gene	Forward primer sequence (5' to 3')	Reverse primer sequence (5' to 3')	Amplicon size	Tested annealing temperatures	GenBank accession number
***nha1*-1**	GGATGGGTCACGATAACTTGGGC	GGTCCATTTCCAACCCAGCTCG	671 bp	67°, 64.6°, 59.6°, 55.5°	AAEL011109-RC
***nha1*-2**	AATTGGAGATTCGGCAGCGC	AGACCTCCAAGAACGCAAACC	609 bp	67°, 64.6°, 59.6°, 55.5°	AAEL011109-RC
***nha1*-3**	CACTTTGAAGGGGCTGGTCC	TTCACGCTCCTCCTCTTCGTC	600 bp	67°, 64.6°, 59.6°, 55.5°	AAEL011109-RC
***nha2*-1**	AGGTTGTGGTTTCTGTTCGTCGG	GTAAGCTCGCTCCACATGCACC	601 bp	65.3°, 62.1°, 59.8°, 56.7°, 55°, 53.8°, 51.3°, 49.4°	AAEL000137-RD
***nha2*-2**	TGAAGGAAGAACGTCTCGGCATG	AAGAGCAGCTGGGCCCAAAG	662 bp	65.3°, 62.1°, 59.8°, 56.7°, 55°, 53.8°, 51.3°, 49.4°	AAEL000137-RD
***ca9*-1**	GTCTGGCCGGAAATGTACCCAC	AGCAGCGCATCTCACGGAAC	658 bp	65.3°, 62.1°, 59.8°, 56.7°	AAEL004930-RA
***ca9*-2**	AAAACACACGCAGCCTGGTC	AGTTGTTGACCACCTTGCCG	609 bp	65.3°, 62.1°, 59.8°, 56.7°	AAEL004930-RA

Table 2. Primers used for gene amplification and dsRNA synthesis for AeNHA1 and AeCA9 KD. This table highlights the gene being amplified, with its respective forward and reverse primer sequences, amplicon size, the experiment the primers were used for and the respective GenBank accession number used to source each gene sequence for primer design. For *egfp*, 'n/a' is listed since the sequence derived was not submitted to GenBank. Primer sets for (1) *ccc3* housekeeping genes (2) *rp49* and *rps18* and a dsRNA KD control (3) *egfp* were used from previous studies ((1) Piermarini et al. 2017, (2) Paluzzi and Vanderkeen 2014, (3) Sajadi and Paluzzi 2024).

Gene	Forward Primer Sequence (5' to 3')	Reverse Primer Sequence (5' to 3')	Base pair length	Experiment	GenBank accession number
ca9	TCACACACAAGGGCGACAAAG	CGGTGGAGTGGTCAACGAAC	109 bp	qPCR	AAEL004930-RA
ccc3 **(Piermarini et al. 2017)**	GGCCTCATGCCGGTCA	TTCTCGCGGAATATGTTAAGTTCC	125 bp	qPCR	AAEL009886-RA
nha1	GCATCCCAACATCGGTCTGAG	ACTTCGTCGCCAGCCTTCTG	176 bp	qPCR	AAEL011109-RC
nha2	GCTGTTTTGGGGCGTTCTG	CGTCGGAATCAAGGTTAGTTGC	183 bp	qPCR	AAEL000137-RD
rp49 **(Paluzzi and Vanderkeen 2014)**	ACAAGCTTGCCCCCAAC	GCGATTTCGGCACAGTAGA	214 bp	qPCR	AY539746
rps18 **(Paluzzi and Vanderkeen 2014)**	TAAAAATGTCGCTCGTGATCC	AATCGGGGATCTTGTACTGG	249 bp	qPCR	XM_001657661
nha1 **dsRNA**	GGATGGGTCACGATAACTTGGGC	GGTCCATTTCCAACCCAGCTCG	671 bp	dsRNA synthesis	AAEL011109-RC
nha1 **dsRNA Forward T7**	TAATACGACTCACTATAGGGAGA GGATGGGTCACGATAACTTGGGC	GGTCCATTTCCAACCCAGCTCG	694 bp	dsRNA synthesis	AAEL011109-RC
nha1 **dsRNA Reverse T7**	GGATGGGTCACGATAACTTGGGC	TAATACGACTCACTATAGGGAGA GGTCCATTTCCAACCCAGCTCG	694 bp	dsRNA synthesis	AAEL011109-RC
ca9 **dsRNA**	TGTCTGGCCGGAAATGTACCCAC	AAACTCCCAACACCGCTAGCCC	400 bp	dsRNA synthesis	AAEL004930-RA
ca9 **dsRNA Forward T7**	TAATACGACTCACTATAGGGAGA TGTCTGGCCGGAAATGTACCCAC	AAACTCCCAACACCGCTAGCCC	423 bp	dsRNA synthesis	AAEL004930-RA
ca9 **dsRNA Reverse T7**	TGTCTGGCCGGAAATGTACCCAC	TAATACGACTCACTATAGGGAGA AAACTCCCAACACCGCTAGCCC	423 bp	dsRNA synthesis	AAEL004930-RA
egfp **(Sajadi and Paluzzi 2024)**	ACTCGTGACCACCCTGACCTACG	AGATCTTGAAGTTCACCTTGATG CC	324 bp	dsRNA synthesis	n/a

2.3. RNA Extraction and cDNA synthesis for qPCR analysis

Total RNA from AFW and BW 24-hour treated 4th instar larvae was extracted for the midgut (midgut collected with gastric caeca; MG), Malpighian tubules (MTs), hindgut (HG) and the anal papillae (AP) using the Monarch® Total RNA Miniprep Kit (New England Biolabs, Ipswich, MA, USA) following the manufacturers protocol. Individual larvae were dissected for the different organs in a Sylgard® lined petri dish under larval *A. aegypti* physiological saline (Clark and Bradley 1996) and the respective organ was then placed in a 1.5 ml centrifuge tube containing 1X DNA/RNA Protection reagent chilled on ice. Each organ type was pooled for a single biological replicate which consisted of organs from ~50 larvae for MG collections, ~75 larvae for MTs and HG and ~100 larvae for AP collections. The MT, HG and AP organ samples were placed in 200 µl of 1X DNA/RNA Protection reagent, and MG collections were placed in 300 µl of 1X DNA/RNA Protection reagent. Tissues were stored at -80°C until processing for RNA was completed. To homogenize the organs before RNA extraction, each collection tube containing either MG, MTs or HG organs with the respective volume of 1X DNA/RNA Protection reagent were sonicated for 3 x 8 s at 5 watts, whereas AP organs were sonicated for 3 x 5 s at 5 watts using an XL 2000 Ultrasonic Liquid Processor (QSONICA). The purity and concentration of the extracted RNA for each organ sample was assessed using a NanoDrop 2000 spectrophotometer (Thermo Scientific). Once total RNA was extracted, cDNA was synthesized using 0.5 µg of RNA for downstream use as the template product in a qPCR reaction, using the iScript^{TM} cDNA synthesis kit (Bio-Rad Laboratories) following the manufacturer's instructions.

2.4. Analysis of ion-transporter mRNA abundance in ion-regulating organs using quantitative PCR analysis (qPCR)

For this study, qPCR was utilized to compare the relative mRNA abundance of *nha1*, *nha2*, *ca9* and *ccc3* in different ion-regulating organs, the MG, MTs and HG in 24-hour AFW treated *A. aegypti* larvae. The mRNA abundance of the transporters in the AP could not be compared with the other organs because of differential expression of housekeeping genes. The mRNA abundance of these same transporters in AFW vs BW within each organ was also compared through qPCR analysis. The cDNA template used for these assays was collected based on previously outlined methods (see RNA Extraction and cDNA synthesis for qPCR analysis). After designing qPCR primers for each gene of interest (see Table 2) a dilution curve was run for each set of primers using whole-body cDNA from AFW larvae which underwent a series of increasing template dilution to ensure primer efficiency and to determine an optimal dilution of template cDNA. Each qPCR reaction was carried out using SsoAdvanced Universal SYBR Green Supermix (Bio-Rad Laboratories) and 2X diluted cDNA template was used for each organ mentioned. These reactions were completed using the CFX Duet Real-Time PCR System (Bio-Rad Laboratories), where the annealing temperature for each primer set used was 60°C. After each reaction a melting-curve analysis was conducted to ensure that the primer binding was specific throughout the amplification process. The relative gene abundance of *nha1*, *nha2*, *ca9* and *ccc3* in the different organs in AFW and in the AFW and BW comparison was quantified using the $2^{-\Delta\Delta C_T}$ method (Livak and Schmittgen 2001). Transcript abundance was normalized to the geometric means of both *rp49* and *rps18* for each organ analyzed in this study. These reference genes were designed and previously studied by Paluzzi and Vanderkeen 2014 (see Table 2). The expression profile of *nha1*, *nha2*, *ca9* and *ccc3* in the AFW ion-transporting organs consisted of 4-5 biological replicates. For transcript abundance comparison between the 24-hour AFW and BW treated larvae, 6 biological replicates

were used for testing the mRNA abundance of each gene in the AP, and 5 biological replicates were used for each gene for the MG, MTs and HG.

2.5. Localization of AeNHA1 with immunohistochemistry (IHC)

Through immunohistochemistry, the localization and expression of AeNHA1 was detected in various ion and water regulating organs in 4th instar *A.aegypti* larvae exposed to either AFW or BW for 24-hours. This includes the MG, MTs, HG and AP. Whole gut samples which contained the MG, MTs and HG were dissected from the differentially treated larvae under *A. aegypti* physiological saline (Clark and Bradley 1996) and were left to fix in Bouin's fixative solution (RICCA, Arlington, TX, USA) for 1 hour at room temperature. Furthermore, whole body larvae were placed in Bouin's fixative for 2 hours at room temperature where they were used to obtain AP organ sections, as well as whole-body organ sections which contained the whole gut (e.g., MG, MTs, HG). Once the organs from intact, whole-body larvae and isolated whole gut organs were fixed, they were then left in 70% ethanol for 24-hours at 4°C. The organs and whole-body samples were then dehydrated through a series of ethanol incubations of 45 minutes each (70%, 95% and 100%) followed by a 45-minute incubation in a 1:1 ratio of ethanol to xylene and then subsequently incubated for 45 minutes in 100% xylene. Following the series of ethanol and xylene incubations, larvae were then exposed to a 1:1 solution of xylene and paraffin wax at 60°C for 1 hour, followed by 100% paraffin wax for another 1 hour at 60°C. These organ and whole-body samples were then left in fresh 100% paraffin wax for at least 24-hours at 60°C and were embedded in new paraffin wax. Once solidified, 3µm thick tissue sections of embedded samples were obtained using an Epredia HM325 manual microtome (Epridia, MI, USA) and were positioned on a double frosted microscope slide (Fisherbrand, Pittsburgh, PA) with a droplet of 30% ethanol. The sections placed on the slide were gently submerged in a water bath (39°C) repositioned onto the slide, and then

subsequently placed on a slide warmer set to 50°C for 24 hours. Slides containing an AFW and BW section were then processed which consists of deparaffinization and hydration, heat induced epitope retrieval, followed by a series of 1X PBS washes based on a previously established protocol (Akhter et al. 2017). Sections were then probed with an anti-AeNHA1 affinity purified primary antibody (64.52 g/L) rabbit polyclonal antibody against SHSEDGPVRRKSNL, Genscript, NJ, USA). Acting as a membrane marker to better establish the localization of AeNHA1, the same sections were also probed with guinea pig anti-V_1 complex of the V-Type H^+-ATPase primary antibody (Ab 353-2, 1: 5000 dilution, generously donated by Dr.H. Wieczorek, Osnabruck, Germany). To visualize AeNHA1 in the different organs of the *A. aegypti* larvae, a goat anti-rabbit AlexaFluor 594 antibody (Jackson Immunoresearch, Westgrove, PA, USA) was used at a 1:400 dilution. To visualize VA, a goat anti-guinea pig antibody AlexaFluor488 antibody (Jackson Immunoresearch) was used at 1:500. After the sections were probed with the described antibodies mounting media was applied made with 500µL of 1X PBS, 500 µL of glycerol (Bio shops, Burlington, ON, Canada) and 4µg/mL of DAPI (Life Technologies, Burlington, ON, Canada) and a double frosted slide cover was used to cover the slide (Fisherbrand, Pittsburgh, PA, USA). The slides were then left to dry for 24-hours. Sections were viewed with an Olympus IX81 inverted fluorescence microscope using the CellSens® 1.12 digital imaging software (Olympus, Richmond Hill, ON, Canada). Negative antibody controls were also processed to ensure primary and secondary antibody specificity (see Appendix A). Images were then overlayed using the ImageJ 1.54 Software. Biological replicates obtained for both AFW and BW conditions were as follows: MG n=5, MTs n= 4, HG n= 3, AP n=4, and ~3-5 technical replicates for each treatment and organ type.

2.6. Western blotting analysis of AeNHA1

AeNHA1 protein abundance was assessed in the MTs of AFW 4th instar larvae for antibody validation. Protein abundance of AeNHA1 was then determined in the AP of 4th instar larvae exposed to either AFW or BW for 24-hours. Organs from larvae were dissected in a Sylgard® dish containing physiological saline (Clark and Bradley 1996) and were then placed in a 1.5 ml centrifuge tube of saline kept on ice. A total of ~100 larvae (~400 individual AP organs) were collected for each biological replicate for each treatment, with a total of 5 biological replicates processed for each treatment. For MT collections, a total of ~75 larvae (~375 MT organs) were collected for each biological replicate in AFW, for a total of 3 replicates. Following the collection of each individual sample, the tube was centrifuged at 16,000 x g for 30 s to force the organs into a pellet and the saline was gently pipetted out of the tube, leaving only the organs. The samples were then stored at -80°C until later use for protein processing. To test AeNHA1 protein abundance, AP AFW and BW samples as well as AFW MT samples were thawed and mixed with a homogenization buffer [pH = 7.5, 50mmol l^{-1} Tris-HCl, 1 mmol l^{-1} PMSF and 1:200 protease inhibitor cocktail (Sigma-Aldrich, St. Louis, MO, USA)]. Once mixed with the homogenization buffer, papillae samples were sonicated 3 x 5 s at 5 watts and MT samples were sonicated 3 x 8 s at 5 watts. After homogenization, the samples were centrifuged at 16,000 x g for 15 minutes at 4°C and the supernatants were collected. A Bradford assay was used to quantify protein in samples. The quantity of protein in each sample was measured relative to bovine serum albumin (BSA) standards. To prepare the samples for SDS-PAGE they were combined with 50 mM Tris buffer and 6x loading buffer [pH = 6.8, 225 mmol l^{-1} Tris-HCl, 2.5% SDS, 35% glycerol, 12.5% β-mercaptoethanol and 0.01% bromophenol blue] and were heated for 5 minutes at 100°C. Following heating, samples were immediately placed back on ice for 30 s and then briefly spun down in a centrifuge. After protein samples were prepared, 10 µg of AP or MT protein was loaded in a 12%

resolving SDS-PAGE and a 4% stacking gel for each biological replicate. Once the samples were loaded, gel electrophoresis was conducted at 80V for 45 min followed by 120V for approximately 1.5hr. The transfer of AP and MT proteins onto a PVDF membrane using the wet transfer method was then completed at 100mV for 1hr in a chilled 1X transfer buffer (0.225g Tris, 1.05 g glycine and 20% methanol in 1 L of ddH_2O). The PVDF membranes were then incubated in 5% milk blocking buffer (5g skim milk powder, 100 ml 1X Tris-buffered saline (TBS-T; pH=7.4 9.9 mmol l-1 Tris, 0.15 mmol L-1 NaCl, 1% Tween-20, 0.1 mmol l-1 NP-40) for 2 hr at room temperature on a rocker. Membranes were then probed with anti-AeNHA1 affinity-purified primary antibody (6.452 g/L) in blocking buffer, and were left to incubate overnight on a rocker kept at 4°C. After primary antibody incubation, the membranes were washed in 1X TBS-T for 15 minutes X 4 (replacing with fresh TBS-T for each wash) the next day prior to incubation with the horseradish peroxidase (HRP)-conjugated goat anti-rabbit antibody (1:10000 in 5% skim milk in TBS-T) (Bio-Rad Laboratories). The antibody was left to incubate for 1 hr at room temperature and was then washed with TBS-T for 15 minutes X 4 (replacing with fresh TBS-T for each wash). Once the membranes were washed, the chemiluminescent reaction was conducted, applying 2 mL of the Clarity™ Western ECL substrate (Bio-Rad Laboratories) to each blot for 5 mins. The membranes were then assessed using a Chemi-Doc MP Imaging System (BioRad Laboratories) to visualize the respective protein bands. After visualization, the membranes were then washed in TBS-T for 1 minute and were incubated with Coomassie blue as a loading control to determine total protein content. The Image J 1.54 software was used to quantify the protein abundance in AFW vs BW AP samples, where the treatment groups were normalized to total protein, followed by the AFW values to obtain the relative protein abundance. A pre-immune serum blot was also conducted to confirm specificity of the detected AeNHA1 protein bands (see Appendix A).

2.7. AeNHA1 and AeCA9 dsRNA synthesis and assessment of knockdown (KD)

To design dsRNA, a similar approach was taken as outlined above for designing qPCR primers (see qPCR primer design, section 2.2). Primer sets targeting a large portion of each gene (e.g., *nha1* and *ca9*) were designed and tested through PCR, gel electrophoresis, and were sent for sequencing (The Centre for Applied Genomics, Sick Kids, ON, Canada). Specificity of the sequences were then confirmed through an NCBI nucleotide blast search. The primer sets used to synthesize dsRNA product for *nha1* and *ca9* are shown in Table 2. To synthesize template for dsRNA synthesis, RNA was extracted from 4-5 larvae using the Monarch® Total RNA Miniprep Kit (New England Biolabs), and cDNA was synthesized from this whole-body RNA as previously described (see RNA Extraction and cDNA synthesis for qPCR analysis, section 2.3). This whole-body cDNA was then utilized to amplify the *nha1* and *ca9* in PCR using the Q5® High-Fidelity DNA Polymerase (New England Biotechnology) with the respective primer sets (Table 2). A portion of the enhanced green fluorescent protein (*egfp*; see Table 2) from a pcDNA 3.1 vector was amplified in PCR which acted as the knockdown (KD) control in this study (kind gift from Dr. Jean-Paul Paluzzi, York University). PCR products were then purified using the Monarch PCR Purification Kit (New England BioLabs) and the concentration and purity were determined using a Nanodrop 2000 spectrophotometer (Thermo Scientific). The respective purified template for each gene was then amplified in another PCR reaction with the addition of the T7 promoter sequence to the 5' end of either the forward or reverse primer for *nha1*, *ca9* or *egfp* (see Table 2). The products were then purified using the Monarch PCR Purification Kit (New England BioLabs). Using these products, the final dsRNA was synthesized using the T7 RiboMAX™ Express RNAi System (Promega, Madison, WI, USA) based on the manufacturer's instructions. The dsRNA was then purified using the Monarch RNA Cleanup Kit (New England Biolabs). After purification,

dsRNA concentration and purity was assessed using a Nanodrop 2000 spectrophotometer (Thermo Scientific) before administering the dsRNA to larvae.

To administer the dsRNA for *nha1*, *ca9*, or *egfp*, previous dipteran larval dsRNA KD protocols were adapted with some modifications to assess KD efficiency on both a whole-body and organ level (e.g., at the papillae) (Chasiotis et al. 2016; Durant and Donini. 2018; Picinic et al. 2026). To test whole-body KD, 12-15 third instar larvae were collected from the lab colony and placed in 150 µl of RNAse-free water containing 0.5 µg/µl of dsRNA for *nha1*, *ca9* or *egfp*. Individuals were then left in open centrifuge tubes with the respective dsRNA and RNAse-free water for 2 hours at room temperature to take up the surrounding dsRNA. Larvae were starved for at least 24 hours prior to having been exposed to the dsRNA treatments. After dsRNA exposure, individuals were placed in 100 ml plastic containers containing 50 ml of AFW at 25 °C for 24 or 48 hours, to assess when KD occurs. These whole-body larvae were then used for RNA extraction and cDNA synthesis which was used for downstream qPCR application to assess KD using the previous qPCR primer sets for *nha1* and *ca9* (see Table 2). A single biological replicate consisted of total RNA extracted from 4-5 whole body larvae.

Whole body KD assessed through qPCR at 24 and 48 hours was not achieved for both *nha1* and *ca9* so some method-based modifications were made, and KD was assessed at the papillae instead of from the perspective of the whole-larvae. These modifications included only assessing *nha1* KD, incubating the larvae with the dsRNA for 3 hours, starving the larvae for 48-hours instead of 24-hours before administering the dsRNA and testing KD at only 48-hours post-dsRNA delivery based on constraints with time and feasibility with organ collections. Furthermore, to test *nha1* KD at the papillae, both qPCR and western blotting were used. For both assays, after individuals were exposed to dsRNA (*nha1* or *egfp*) as outlined above, ~90 larvae were transferred

to a container with 250 ml of AFW for 48 hours. For qPCR, ~90 larvae were used to harvest AP organs, where total RNA was extracted and cDNA was synthesized as previously described, using the established qPCR primer set for *nha1* (see Table 2). Any changes in gene abundance in the KD compared to the *egfp* control groups was assessed. For western blotting, ~90 larvae were used to dissect the anal papillae organs of AeNHA1 KD or the EGFP KD control. The protein from these samples were then processed and assessed through western blotting methods as described previously (see Western blotting analysis of AeNHA1). For assessing KD with qPCR, 2 biological replicates were collected for the *nha1* KD group and *egfp* KD control. A total of 5 biological replicates were assessed in western blotting for both treatments mentioned.

2.8. Statistical Analysis

The statistical analyses were performed using the Prism® software (GraphPad Software Inc., CA, USA). For the AFW expression profile of the various genes in different ion-regulating tissues a Welch's ANOVA test was run, with a Dunnett's T3 multiple comparison analysis when the conditions were significant ($p < 0.05$). For comparing relative mRNA abundance in the MG, MTs, HG and AP, AP protein abundance in AFW vs BW larvae and KD success, a Welch's t-test was conducted to evaluate differences between the treatments. Data are expressed as mean± SD for the freshwater expression profile and as mean± SEM for AFW vs BW comparisons and for the KD analyses.

3.0. Results

3.1. Expression profile of *nha1*, *nha2*, *ca9* and *ccc3* in osmoregulatory organs of *Aedes aegypti* larvae

The relative mRNA abundance of *nha1*, *nha2*, *ca9* and *ccc3* in the MG, HG and MTs were compared. The AP were excluded from this comparison because of differential expression of the housekeeping genes; however, transcripts of all genes were detected. The HG possessed the greatest mRNA levels of *nha1*, *ca9* and *ccc3* compared to the MTs and MG. For *nha1*, mRNA is significantly higher in the HG compared to the MG and the MTs (Figure 7A). The mRNA abundance for *ca9* were the highest in the HG compared, although not statistically different from the MTs and MG which showed lower mRNA levels (Figure 7C). Abundance of *ca9* mRNA were statistically higher in MG compared to the low levels detected in the MTs (Figure 7C). The mRNA levels of *ccc3* were not statistically different between organs despite the HG having ~ 600 times more mRNA compared to the MG and MTs (Figure 7D). The mRNA levels of *nha2* were significantly higher in the MTs compared to MG and the levels in HG were between the other two organs (Figure 7B).

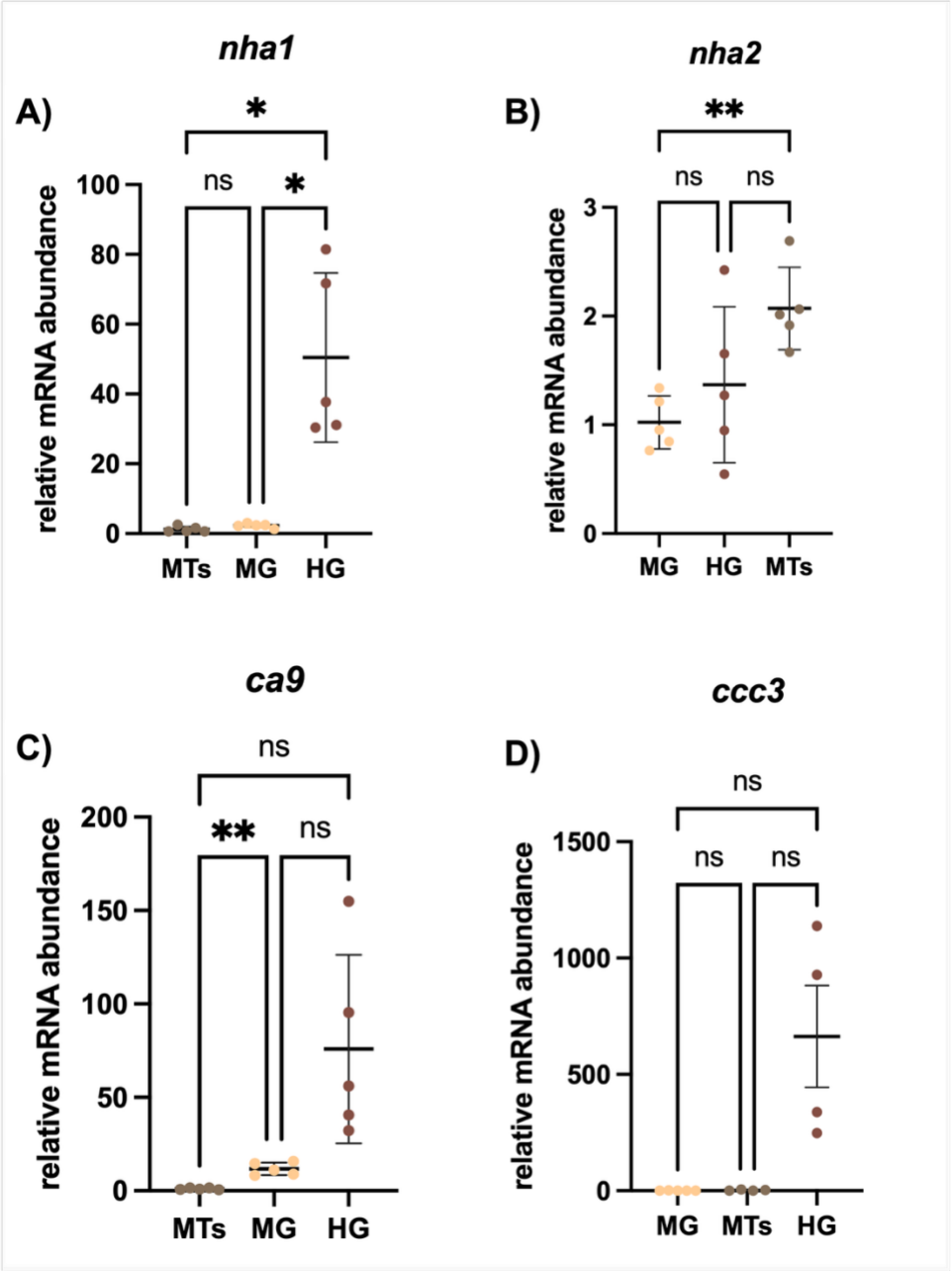

Figure 7. Expression profile of *A. aegypti nha1*, *nha2*, *ca9* and *ccc3* in the midgut (MG), Malpighian tubules (MTs) and hindgut (HG) of artificial freshwater (AFW) *Aedes aegypti* larvae. The relative mRNA abundance of *nha1* (A), *nha2* (B), *ca9* (C) and *ccc3* (D) were detected and compared in the studied osmoregulatory organs using quantitative PCR. All the genes were normalized to housekeeping genes, *rp49* and *rps18* and were expressed relative to an organ calibrator assigned a value of 1, that showed the highest ΔCt values. A single asterisk (*) denotes a significant difference where $p < 0.05$ and a set of asterisks (**) indicates that $p < 0.01$. Relationship between data sets marked with 'ns' indicated no significant differences between the data sets. All data sets were analyzed with a Welch's ANOVA, followed by a Dunnett's T3 multiple comparisons. Values are graphed as mean ± SD, n = 5.

3.2. Immunolocalization and detection of AeNHA1 in osmoregulatory organs of *Aedes aegypti* larvae

Immunohistochemistry was used to detect AeNHA1 protein expression in the gastric caeca (GC) + MG (PMG), MTs, HG and AP of *A. aegypti* larvae. AeNHA1 protein was detected in all osmoregulatory organs assessed with VA staining used as an apical membrane marker in the mentioned epithelia evaluated (Figure 8). In all the organs, AeNHA1 was localized to the basal (hemolymph facing) membrane (Figure 8). Within the MTs, cytosolic staining of AeNHA1 appears in addition to its basolateral position (Figure 8C). No AeNHA1 or VA staining was shown in control slides where both primary antibodies were omitted (see Appendix A). Pre-absorption of the AeNHA1 primary antibody with immunogenic peptide showed no AeNHA1 staining in sections of the MG, MTs, HG and AP of larvae (see Appendix A).

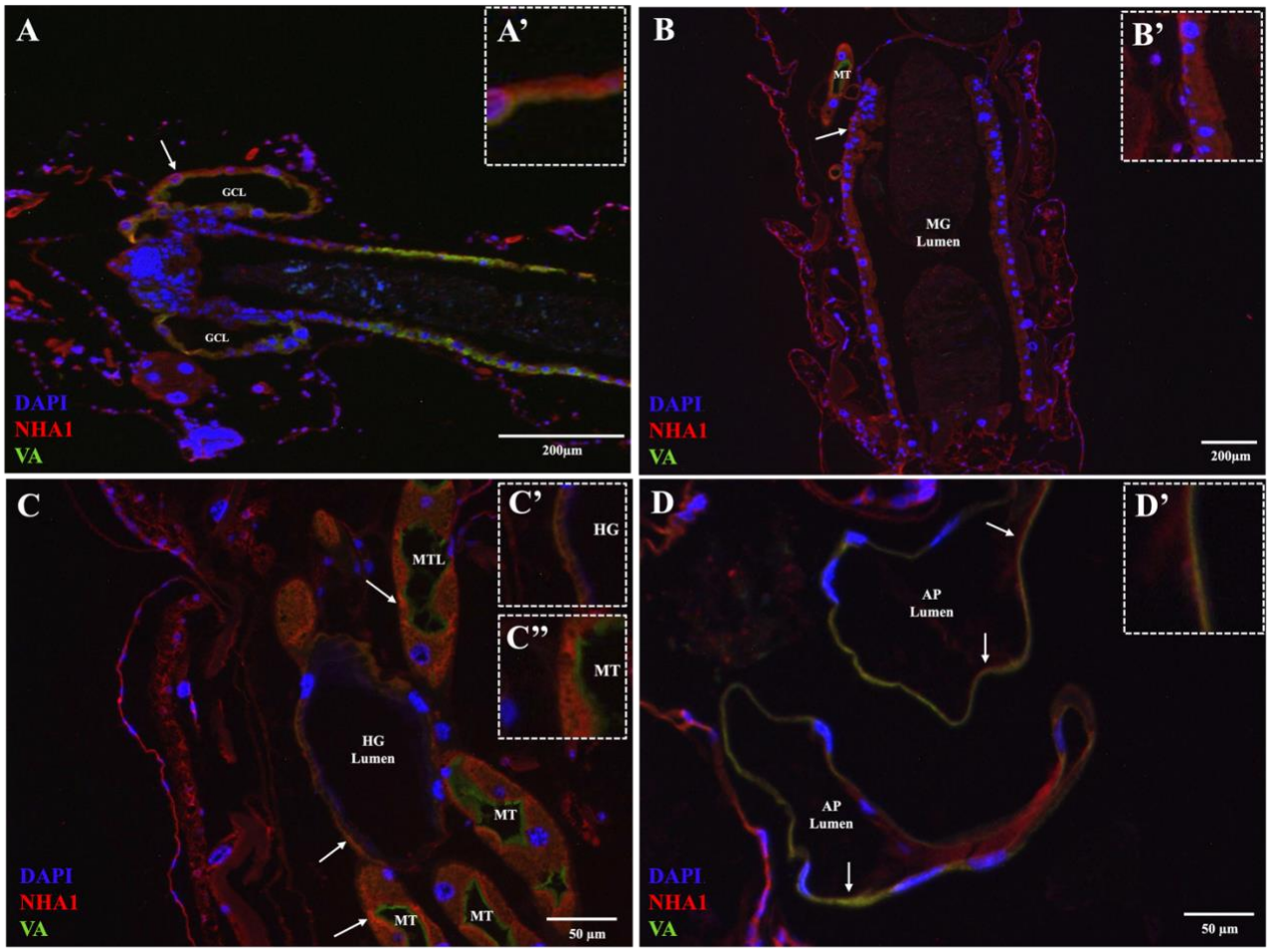

Figure 8. Immunolocalization of AeNHA1 in the osmoregulatory organs of artificial freshwater (AFW) *Aedes aegypti* larvae. This figure illustrates the localization of AeNHA1 in the gastric caeca (GC; BW representative image) (A), posterior midgut (PMG) (B), Malpighian tubules (MTs)/hindgut (HG) (C) and the anal papillae (AP) (D). Each image shows the overlayed images with AeNHA1 (red), V-Type H^+-ATPase (green; membrane marker) and DAPI (blue; stains nuclei) staining. Each figure contains a respective inset image (A', B', C' & C'', D') showing a close-up image of the localization of AeNHA1 on the membranes of the different tissues being examined. A total of 3-5 biological and technical replicates were assessed for each organ type, aside for GC where n=1.

3.3. Comparison of mRNA abundance of *nha1*, *nha2*, *ca9* and *ccc3* in the osmoregulatory organs of AFW vs BW *Aedes aegypti* larvae

The relative mRNA abundance of *nha1*, *nha2*, *ca9* and *ccc3* was measured in *A. aegypti* larval osmoregulatory organs after larvae were exposed to AFW or BW for 24-hours. For *nha1*, mRNA abundance was similar in the MG, MTs and HG of larvae treated in AFW vs BW (Figure 9A, B, C). Meanwhile, the AP exhibit a decrease in the mRNA abundance of *nha1* when exposed to BW (Figure 9D). No changes were observed in *nha2* and *ca9* mRNA abundance in AFW vs BW in all the osmoregulatory organs tested (Figure 10 and Figure 11). The mRNA abundance of *ccc3* is unchanged in AFW and BW-treated MTs, HG and AP, but is reduced in the MG of BW larvae (Figure 12).

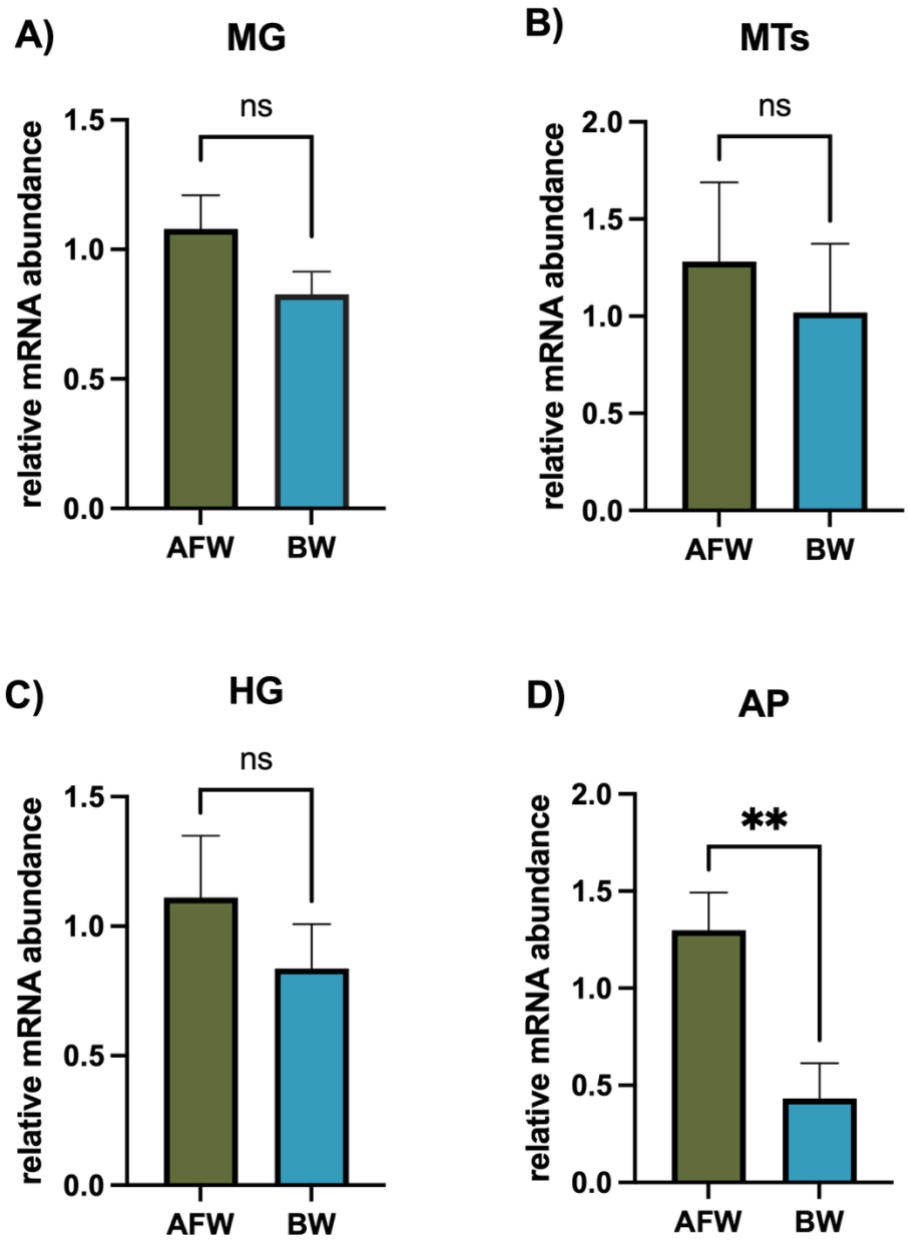

Figure 9. Effects of artificial freshwater (AFW) and brackish water (BW) exposure on the relative mRNA abundance of *nha1* in osmoregulatory organs of *Aedes aegypti* larvae. Using real-time quantitative PCR (qPCR) the relative mRNA abundance of *nha1* was compared in 24-hour AFW vs BW treated larvae looking at changes under these conditions in the (A) midgut (MG), (B) Malpighian tubules (MTs), (C) hindgut (HG) and anal papillae (AP). Abundance of *nha1* was normalized to *rp49* and *rps18* and the data is represented as mean ± SEM and 5 biological replicates were collected for AFW and BW for all the organs, except the AP where 6 biological replicates were used. Data was analyzed using a Welch's t-test, where 'ns' denotes no significant difference, and a pair of asterisk indicates $p < 0.01$.

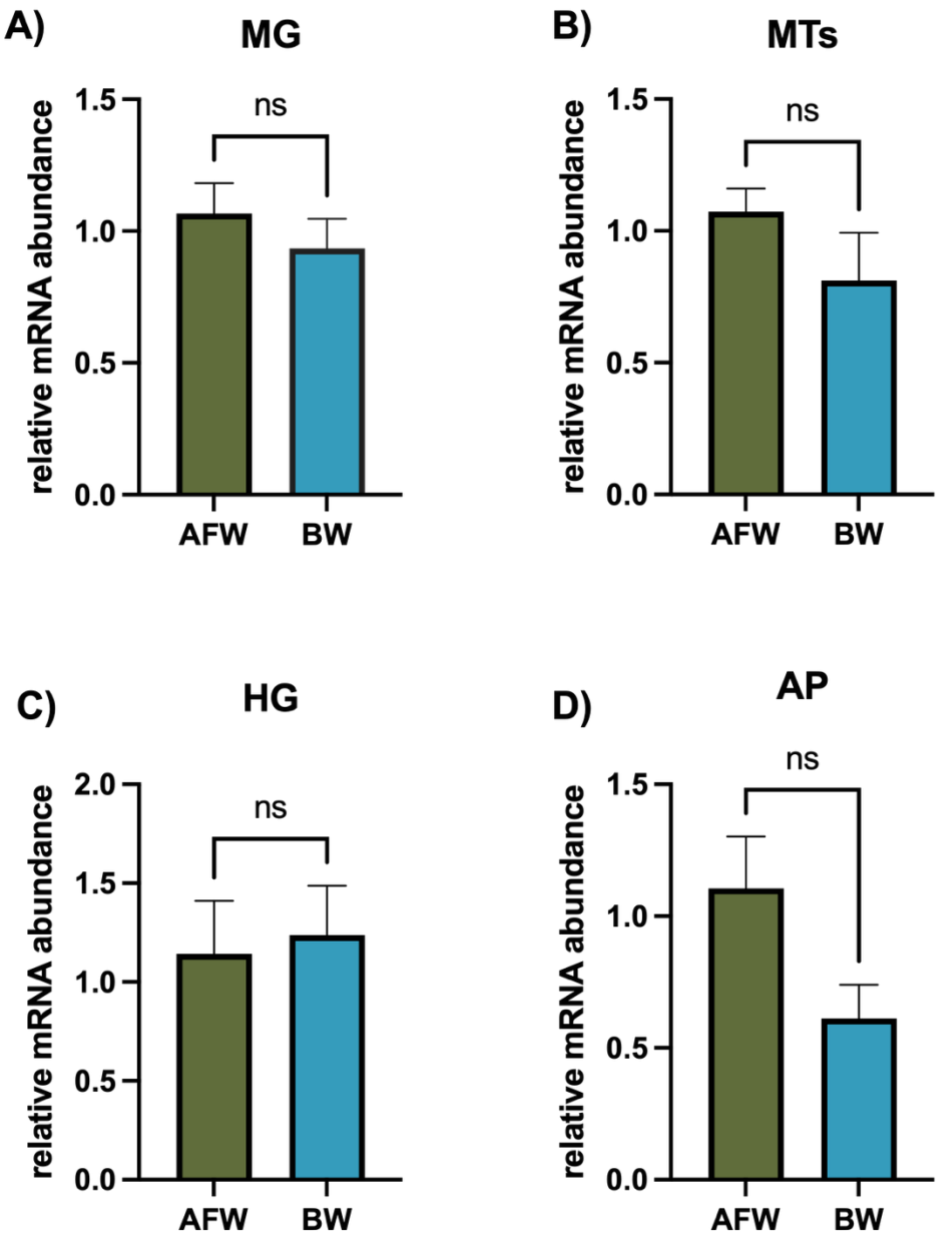

Figure 10. Effects of artificial freshwater (AFW) and brackish water (BW) exposure on the relative mRNA abundance of *nha2* in osmoregulatory organs of *Aedes aegypti* larvae. Relative mRNA abundance of *nha2* was compared in larvae that were treated in AFW vs BW for 24-hours for the different osmoregulatory organs such as the (A) midgut (MG), (B) Malpighian tubules (MTs), (C) hindgut (HG) and anal papillae (AP). Abundance of *nha2* was normalized to *rp49* and *rps18* and the data is represented as mean ± SEM. A total of 5 biological replicates were collected for AFW and BW for the MG, MTs and HG. The mRNA data for the AP represents a total of 6 biological replicates. Data was analyzed using a Welch's t-test, where 'ns' denotes no significant difference.

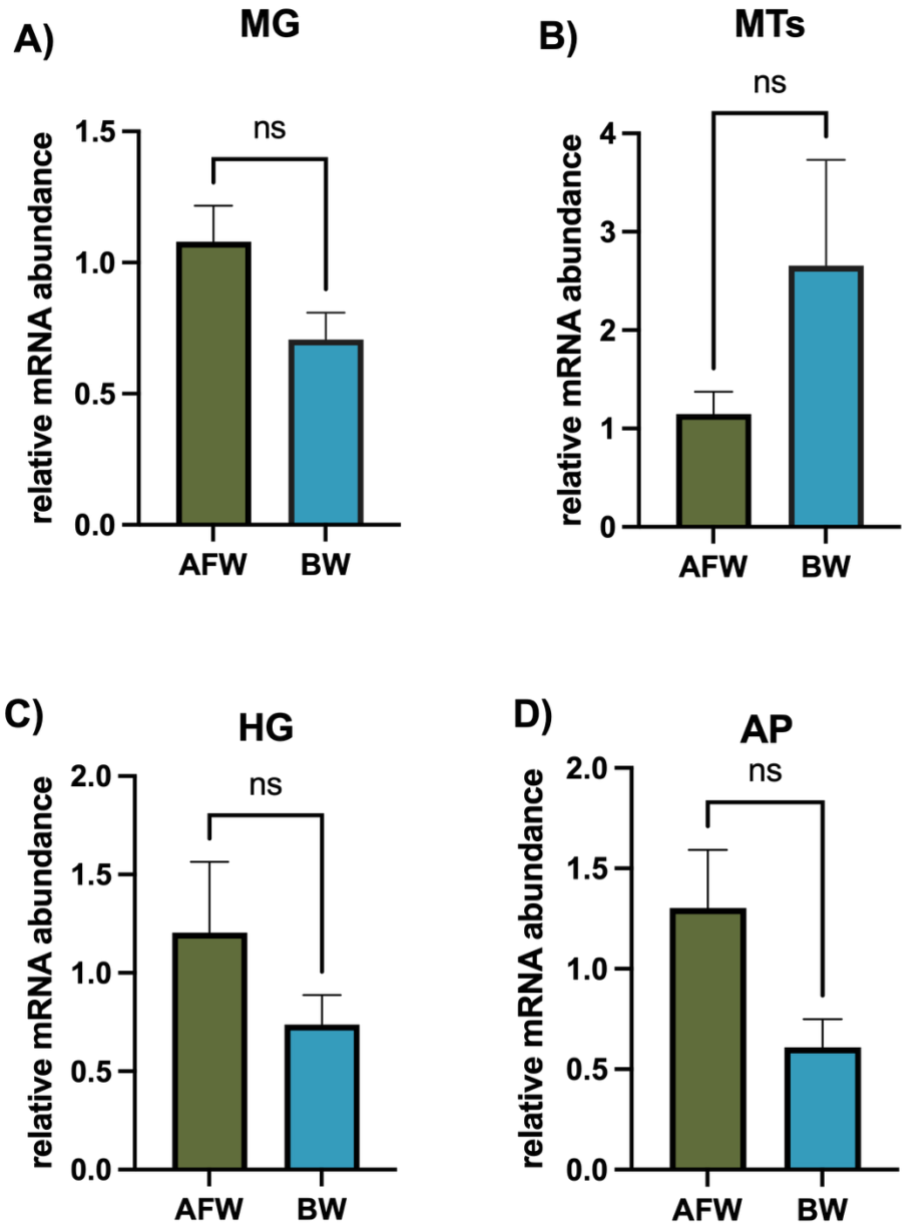

Figure 11. Effects of artificial freshwater (AFW) and brackish water (BW) exposure on the relative mRNA abundance of *ca9* in osmoregulatory organs of *Aedes aegypti* larvae. Relative mRNA abundance of *ca9* was compared in the (A) midgut (MG), (B) Malpighian tubules (MTs), (C) hindgut (HG) and anal papillae (AP) of larvae treated in AFW or BW for 24-hours. Abundance of *ca9* was normalized to *rp49* and *rps18* and the data is represented as mean ± SEM. For the MG, MTs and HG, 5 biological replicates were collected for AFW and BW, and 6 biological replicates were used for both treatments in AFW for the AP. Data was analyzed using a Welch's t-test, where 'ns' denotes no significant difference.

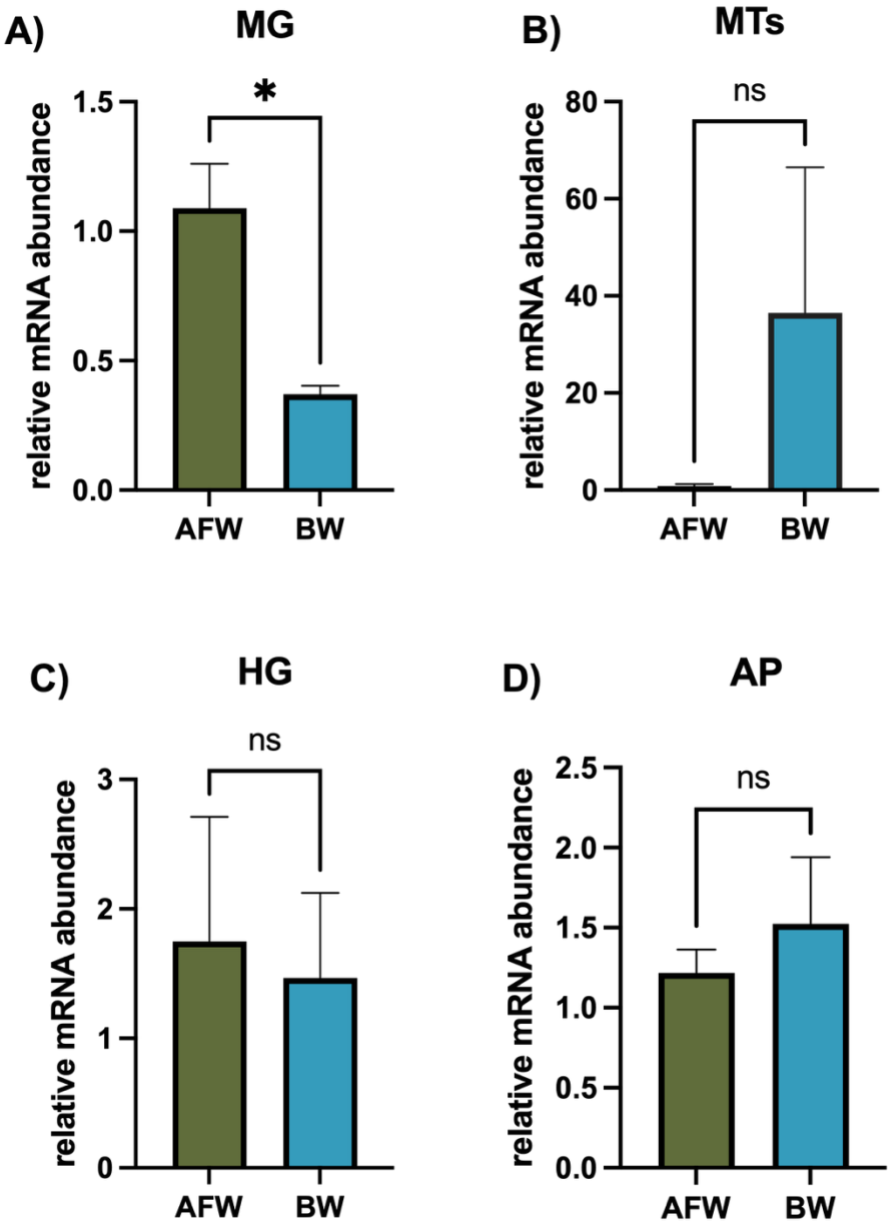

Figure 12. Effects of artificial freshwater (AFW) and brackish water (BW) exposure on the relative mRNA abundance of *ccc3* in osmoregulatory organs of *Aedes aegypti* larvae. Relative mRNA abundance was compared in 24-hour AFW vs BW treated larvae in the (A) midgut (MG), (B) Malpighian tubules (MTs), (C) hindgut (HG) and anal papillae (AP). For each organ, 5 biological replicates were analyzed except for the papillae where 6 were analyzed for both AFW and BW. Abundance of *ccc3* was normalized to *rp49* and *rps18* and the data is represented as mean ± SEM. Data was analyzed using a Welch's t-test, where a single asterisk (*) indicates a significant different of $p < 0.05$ and 'ns' denotes no significant difference.

3.4. Expression of AeNHA1 protein in osmoregulatory organs of AFW vs BW *Aedes aegypti* larvae

AeNHA1 protein is detected and localized to the basolateral membrane of the osmoregulatory organs assessed in this study and BW treatment had no effect on this localization in the organs (see Figure 8 and Figure 13). Cytosolic staining of AeNHA1 was also detected in the MTs in addition to its basolateral location for AFW and BW treated larvae (Figure 13C, D). Furthermore, when comparing AFW and BW-treated organ sections no qualitative changes in staining intensity were observed in any of the organs (Figure 13).

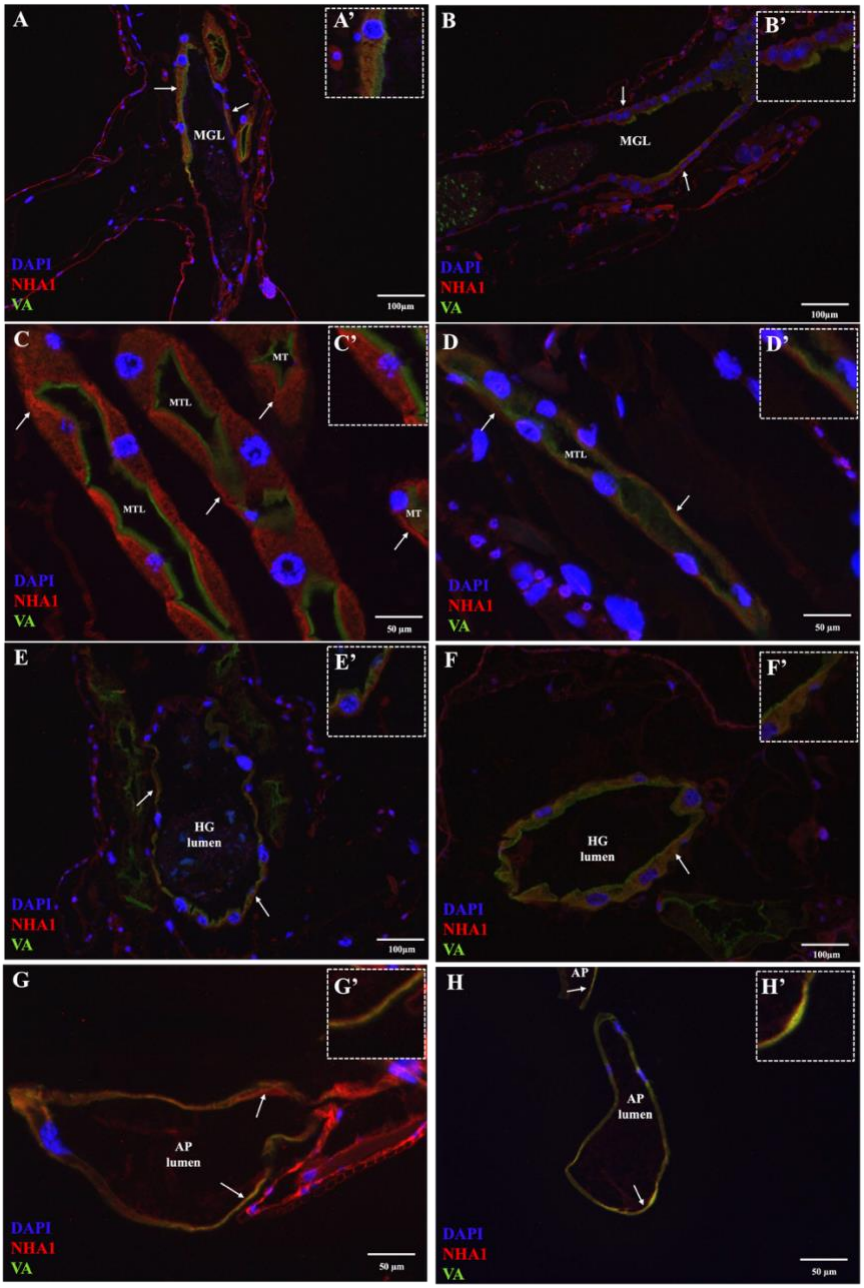

Figure 13. Immunolocalization and expression of AeNHA1 in artificial freshwater (AFW) and brackish water (BW) *Aedes aegypti* larvae. AeNHA1 was compared in expression in localization in the (A, B) midgut (MG), (C, D) Malpighian tubules (MTs), (E, F) hindgut (HG) and (G, H) anal papillae (AP). Expression of AeNHA1 (red staining) is compared in these organs in AFW (A, C, E, G) and BW (B, D, F, H). The V-Type H^+-ATPase was used as a membrane marker (green staining) to better illustrate the localization of AeNHA1 in AFW and BW conditions which is further illustrated in A', B', C', D', E', F', G', H'. Nuclei are stained with DAPI, illustrated by blue-staining in each figure. White arrows point to the basolateral location of AeNHA1 in the various organs in AFW and BW. In (A, B) 'MGL' indicates the midgut lumen and 'MTL' in (C, D) describes the Malpighian tubules lumen. Biological replicates for AFW and BW were as followed: MG n=5, MTs n= 4, HG n= 3, AP n=4, with ~3-5 technical replicates.

3.5. Protein abundance of AeNHA1 in the AP of AFW and BW exposed *Aedes aegypti* larvae

Using western blotting AeNHA1 protein abundance was assessed in the anal papillae (AP) organs of 4th instar *A. aegypti* larvae. Validation of the antibody was performed using MT protein samples from AFW larvae where bands at ~71 and 140 kDa were detected (Figure 14A). The band shown at ~71 kDa is proposed to be the putative monomer of AeNHA1 since this is the expected mass of the AeNHA1 monomer. Meanwhile, the band that appeared at ~140 kDa is proposed to be the putative dimer of AeNHA1, being detected as roughly double the mass of the putative monomer (Figure 14A). After assessing that the antibody successfully binds to AeNHA1 in the MTs, AP protein samples from larvae treated in AFW vs BW for 24-hours was tested (Figure 14B, C). For measuring AeNHA1 protein abundance in the AP samples of AFW and BW-treated larvae, the putative-dimer was detected and analyzed. In both AFW and BW, the mass of this putative dimer appeared at ~140 kDa and generally, no bands were detected for the putative monomer at ~71 kDa (Figure 14B). No changes in the protein abundance was observed in AP of AFW and BW larvae (Figure 14C). Pre-incubating the AeNHA1 antibody with pre-immune serum confirmed the specificity of this antibody since neither the ~71 kDa or ~140 kDa band were detected (see Appendix A).

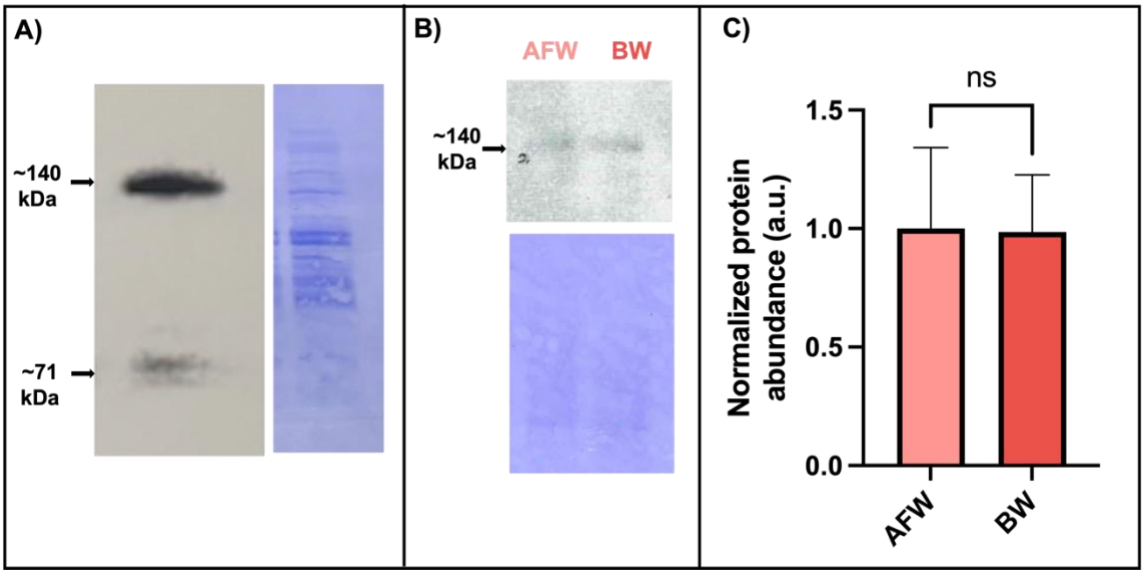

Figure 14. Protein abundance of AeNHA1 in aritifical freshwater (AFW) Malpighian tubules (MTs) and in 24-hour treated artificial freshwater (AFW) and brackish water (BW) anal papillae (AP) organs of larval *Aedes aegypti*. Protein abundance of AeNHA1 in AFW treated MTs (A) is shown where a band appears at ~71 kDa (putative monomer) and ~140 kDa (putative dimer). No non-specific binding of the antibody was found using AFW MT samples as only these two bands were detected. Approximately 75 sets of MTs were collected from AFW larvae for a total of 3 biological replicates. After assessing the specificity of the AeNHA1 antibody, normalized protein abundance of AeNHA1 in AFW and BW AP samples was assessed (B, C). The values were normalized to AeNHA1 band detected in AFW AP samples, where ~100 larvae were collected per one biological replicate (FW n=5; BW n=5). In (C) a Welch's t-test was run to compare AeNHA1 normalized protein abundance in AFW to BW treated AP. No significant differences were found as denoted by 'ns' ($p < 0.05$).

3.6. Assessment of *ca9*, *nha1* and AeNHA1 knockdown (KD) in larval *Aedes aegypti*

The KD of *ca9* and *nha1* was evaluated in whole-body larval *A. aegypti* after administering dsRNA for the respective genes. For the *ca9* whole-body KD attempt, there was no significant difference between the relative mRNA abundance of this gene to the *egfp* control at both 24 and 48-hours post dsRNA delivery (Figure 15A,B). Similarly, *nha1* mRNA abundance was unchanged in larvae treated with dsRNA for *nha1* compared to individuals treated with the *egfp* dsRNA (KD control) (Figure 15C,D). Additionally, it was found that 48-hours post dsRNA delivery, no changes were observed in both the mRNA and protein abundance of AeNHA1 compared with the EGFP group for isolated anal papillae organs (Figure 16). No changes in the abundance of *nha1* and *ca9* mRNA and protein (AeNHA1 only) compared to the KD control (EGFP) shows that KD was unsuccessful as expression was maintained in the KD groups compared to the control.

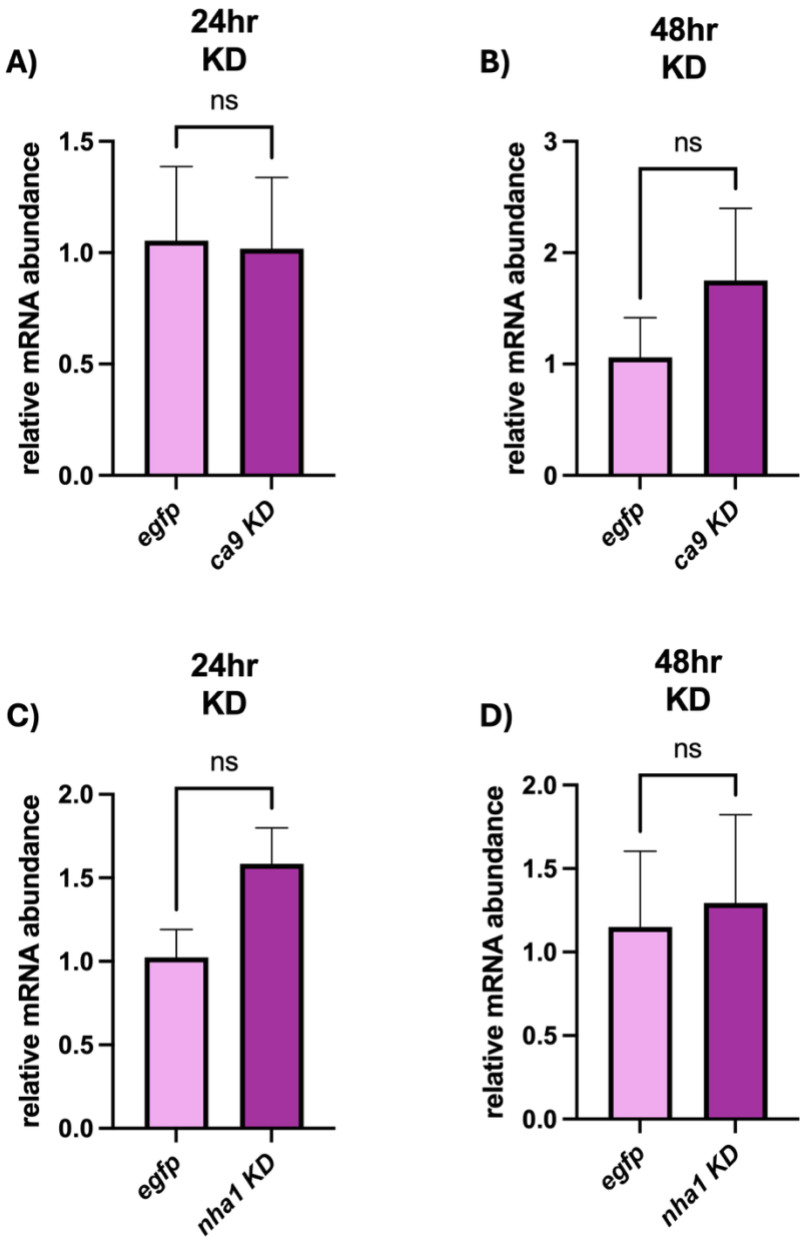

Figure 15. Whole-body *ca9* and *nha1* knockdown (KD) attempts in *Aedes aegypti* larvae. The assessed KD for *ca9* (A, B) and *nha1* (C, D) was evaluated at both 24 (A, C) and 48-hours (B, D) after 3rd instar larval *A. aegypti* were treated with dsRNA. This was assessed by measuring the relative mRNA abundance of whole-body cDNA from larvae treated with the KD control – *egfp* and *ca9* dsRNA to see if gene KD occurred (A, B). The same was done for evaluating the success of *nha1* whole-body KD (C, D). The data displayed was normalized to housekeeping genes *rp49* and *rps18* and was analyzed using a Welch's t-test, where graphs shown with 'ns' denotes no significant differences between compared data sets ($p > 0.05$). KD of *ca9* and *egfp* KD data is represented with n = 2, whereas *nha1* and *egfp* KD data is represented as n = 3. All data is shown as mean ± SEM.

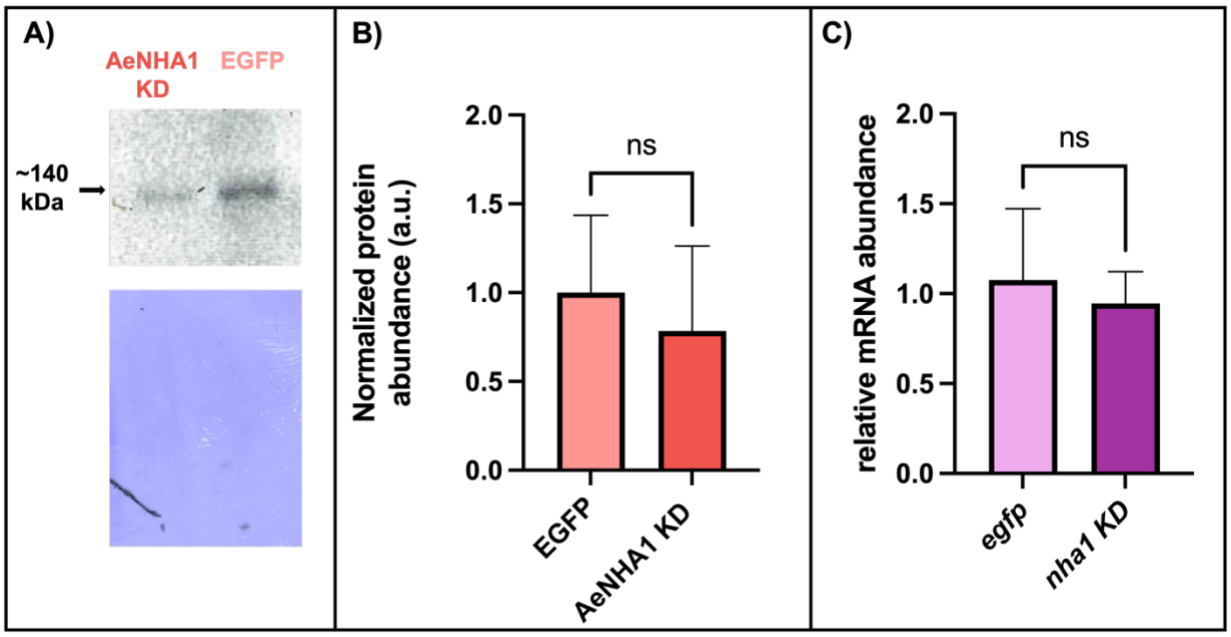

Figure 16. Knockdown (KD) attempt assessing protein (A, B) and mRNA (C) abundance of AeNHA1 at larval anal papillae (AP) organs assessed 48-hours post dsRNA delivery. Success of AeNHA1 knockdown in the AP organs of *A. aegypti* was assessed by both mRNA and protein abundance of larvae treated with EGFP (KD control) or AeNHA1 dsRNA. (A) Shows the putative dimer of AeNHA1 appearing at ~140 kDa for both the AeNHA1 KD larvae and EGFP KD control with the respective Coomassie blot shown. (B) Shows the normalized protein abundance of EGFP (n=5) and AeNHA1 KD (n=5). In (C) the relative mRNA abundance of collected anal papillae organs through qPCR is shown for the control – *egfp* (n=2) and the *nha1* KD group (n=2). One biological replicate consisted of 4 anal papillae organs collected from ~90 larvae. In (B, C) the data was analyzed using a Welch's t-test, where 'ns' shows no statistical changes between the AeNHA1 KD to the EGFP KD control. All data are represented as mean ± SEM.

4.0. Discussion

4.1. Overview

The ability of larval *A. aegypti* to maintain a desirable internal osmolarity in a FW environment has been studied and observed through techniques utilized at the midgut, Malpighian tubules, hindgut and the external anal papillae (Bradley 1987; Donini and O'Donnell 2005; Donini et al. 2006; D'Silva et al. 2017b; Ramsay, 1950). These ion-regulating techniques can be altered when larvae are exposed to conditions of salinity such as BW, allowing them to persist in these environments (Donini et al. 2007; D'Silva et al. 2017b; Jonusaite et al. 2017a). A vital organ responsible for FW osmoregulation are the anal papillae, which absorb NaCl from the surrounding water in dilute media, but switch to reducing uptake when faced with salinized environments (Donini and O'Donnell 2005; Donini et al. 2007; Koch 1938; Stobbart 1959; Stobbart 1960). Understanding which ion-transporters drive anal papillae NaCl uptake in FW and adjust ion-uptake when in salinity remains an area of study. Roles for different ion-transporters have been implicated in previous studies, but transporters directly involved in Na^+ or Cl^- absorption remain unclear as does an understanding on which transporters aid in responding to elevated environmental salinities (Del Duca et al. 2011). More recently, RNA-sequencing analysis on the papillae of *A. aegypti* larvae provided preliminary evidence for different ion-transporters responsible for mediating NaCl uptake in FW, but also in regulating ion-transport when faced with BW exposure (Durant et al. 2021). Based on this, the first aim of this present study was to confirm the transcript results from the transcriptome study by Durant et al., 2021 on the papillae of larval *A. aegypti* in AFW and BW on ion-transporters; *nha1*, *nha2*, *ccc3* and the enzyme – *ca9* using qPCR. To better understand NaCl uptake in FW and alterations made to this transport in BW, knockdown of AeNHA1 and AeCA9 was attempted to determine how these transporters serve ion-transport at the anal papillae. Ultimately, since the K.D. of these transporters was unsuccessful (see Figure 9 and Figure 10) no

functional determinations could be attempted regarding how AeNHA1 and AeCA9 participate in ion uptake by the papillae in this current study.

Alongside assessing the mRNA abundance of *nha1*, *nha2*, *ccc3* and *ca9* in the papillae, this study also aimed to compile an expression profile of each of these genes in the other osmoregulatory organs and how their expression is impacted by BW. The ion-transporters serving the MTs has been well studied compared to the midgut, and much less is known on the hindgut and how it mediates NaCl absorption. Furthermore, how secondary ion-transporters respond to salinity in larval *A. aegypti* in these organs is virtually unknown to the best of my knowledge. Ultimately, it was predicted that all four genes would be detected throughout the midgut, MTs and hindgut of larvae based on the previous characterization or RNA-sequencing studies detecting these transporters but differential expression across these organs was hypothesized based on their functional differences (Akbari et al. 2013; Dixon et al. 2017; Durant and Donini 2024; Li et al. 2017; Matthews et al. 2018; Piermarini et al. 2017). The findings from this study showed that the hindgut consistently showed elevated expression of these transporters compared to the MTs and midgut, aside for *nha2* which is highest in the MTs. With salinity-exposure it was predicted that these different genes would be downregulated in the various organs. The results from the freshwater vs salinity comparison illustrate that only some changes are seen in transporter mRNA expression with salinity exposure. Alongside this, the putative AeNHA1 has been unexplored in *A. aegypti* mosquitoes, with our understanding on this transporter being restricted to RNA-sequencing detecting this gene in different developmental stages, larval and adult MTs and in the anal papillae (Akbari et al. 2013; Durant et al. 2021; Li et al. 2017; Matthews et al. 2018). Based on this, the present study localized AeNHA1 protein throughout the different ion-regulatory organs of the *A. aegypti* larvae for the first time. With these findings altogether, this study has provided a

more comprehensive overview on which ion-transporters may be involved in the different organs assessed in both freshwater and saline water conditions, while providing preliminary evidence for the role of the putative AeNHA1 in the different ion-transporting organs of larval *A. aegypti* for the first time based on its localization.

4.2. AFW expression of ion-transporters and enzymes in larval osmoregulatory organs

4.2.1. AeCA9

An expression profile of *ca9* on the midgut, MTs and hindgut is presented in this study. Transcript for *ca9* was detected in these osmoregulatory organs, where there was greater abundance in the hindgut compared to the MTs and midgut (Figure 7C). These results align with what has been found with another FW larval mosquito *A. gambiae* where the mRNA abundance of the *A. gambiae ca9* (AgCA9) is highest in the ion-absorptive segment of the hindgut, known as the rectum, compared to the rest of the alimentary canal (e.g., gastric caeca, anterior and posterior midgut, MTs) (Smith et al. 2007). An RNA-sequencing analysis of the rectum of *A. aegypti* larvae has found that *ca9* exhibits high transcript reads, which also aligns with the high transcript levels detected in the present study (Durant and Donini 2024). Conversely, previous studies assessing AeCA9 protein signal on a qualitative basis in the alimentary canal of larval *A. aegypti* show a lack of staining in the rectum with expression in the midgut and MTs (Dixon et al. 2017; Smith et al. 2008). Therefore, the high transcript abundance of *ca9* in the hindgut found in this and previous studies contradicts the lack of protein expression previously reported in the rectum of larval *A. aegypti* (Durant and Donini 2024; Dixon et al. 2017; Smith et al. 2008). Based on these conflicting findings in *ca9* mRNA compared to protein detection, it is possible that at least for the hindgut, this gene is under post-transcriptional regulation. For example, other genes in larval *A. aegypti* display differential expression on a transcript and protein level such as the cationic amino acid transporter (AaCAT1) which has elevated mRNA abundance at the 3rd and 4th larval instar stages,

where protein is not detected (Hansen et al. 2011). In 4th instar larval *A. aegypti,* transcripts are expressed for nine CAs (e.g., AeCA9, AeCA7-RA, unannotated CA – AAEL009330, AeCA3-RA, AeCAβ, AeCA3-RB, AeCA4, AeCA10, AeCA7-RB, AeCA6) (Dixon et al. 2017). Therefore, it is possible that one or several of these detected CAs are translated into protein aiding in the larval hindgut's role in ion-absorption, whereas AeCA9 may be under some sort of post-transcriptional control and regulation. CAs, and in particular, cytosolic CAs like AeCA9 can participate in the ion-absorptive function of the hindgut by producing H^+ and HCO_3^- through the hydration of CO_2. The H^+ and HCO_3^- could then be utilized by the apically located VA to facilitate the uptake of ions such as Na^+, and in exchange for Cl^- by anion exchangers (AE), respectively (Figure 19) (Patrick et al. 2006). Although, through whole mount immunolocalization studies, the anion exchanger AeAE1, was not successfully detected in the rectal segment of the hindgut, other AE transcripts have been detected in the rectum of *A. aegypti* larvae (Durant and Donini 2024; Linser et al. 2012).

The midgut had significantly higher mRNA abundance of *ca9* compared to the MTs and this verifies previous studies that showed AeCA9 protein expression throughout the midgut of larval *Aedes aegypti* (Dixon et al. 2017) (Figure 7C). Throughout the midgut, including the gastric caeca, and both the anterior and posterior midgut, the pH of the lumen is regulated to support digestive function in *A. aegypti* larvae (Dadd 1975; Onken et al. 2008). The ability to regulate luminal pH along the midgut has been linked to CAs in all the regions of the midgut regardless of the regulated luminal pH (e.g. highly alkaline or neutral to alkaline). When larval *A. aegypti* are treated with CA inhibitors such as methazolamide, the highly alkaline pH (~10-11) of the anterior midgut is reduced (Boudko et al. 2001a; Corena et al. 2002). CA activity is highest in the gastric caeca and posterior midgut, regions that have neutral to alkaline pH (Corena et al. 2002). More recently, protein expression of AeCA9 was detected in the midgut, with strong

immunohistochemical signals found in the gastric caeca and qualitatively lower detection in the anterior and posterior midgut (Dixon et al. 2017). These results together with the detection of *ca9* mRNA found in the midgut in this present study suggest that this CA is at least in part involved in regulating luminal pH throughout the midgut (Dixon et al. 2017) (see Figure 17). Nonetheless, the expression and function of AeCA9 in the midgut of *A. aegypti* larvae exposed to salinity has not been examined.

In this study it was found that *ca9* transcript abundance was relatively low in the MTs but, a previous study reported a considerable amount of AeCA9 protein expression in the MTs of larval *A. aegypti* (Figure 7C) (Dixon et al. 2017). Furthermore, it was reported that AeCA9 is not expressed in the hindgut; however, this study detected arguably, the highest level of *ca9* transcript in the hindgut (see Dixon et al. 2017; Smith et al. 2008 and Figure 7). The discrepancy in these results remains to be resolved as does the functional significance of any expression of AeCA9 in *A. aegypti* larvae.

The role for CAs in the MTs have been functionally demonstrated in insects such as the fruit fly (*Drosophila*). For example, when *Drosophila* larval tubules are treated with CA inhibitors (e.g., acetazolamide and hydrochlorothiazide), K^+ and Cl^- content becomes significantly reduced within the apical and basal cytoplasm of the MTs suggesting a role for this enzyme in facilitating transepithelial ion-secretion (Wessing et al. 1997). Although, the functional role for CAs in the MTs of larval *A. aegypti* have not been evaluated, studies have shown that the MTs display CA activity, with higher activity compared to the anterior midgut, but lower than that shown in the gastric caeca and posterior midgut (Corena et al. 2002). At least part of this CA activity can be attributed to AeCA9 because immunohistochemical studies demonstrated pronounced staining in the MTs (as well as the gastric caeca) compared to the anterior and posterior midgut (Dixon et al.

2017). It is therefore likely that AeCA9 plays a role in transepithelial ion transport in the MTs (see Figure 18). The expression of AeCA9 in MTs and hindgut of salinity exposed larvae has not been examined.

Transcript of *ca9* was detected in the anal papillae which aligns with a previous RNA-sequencing study of the anal papillae of *A. aegypti* (Durant et al. 2021). A functional role for CAs in ion transport by anal papillae has been shown with the application of the CA inhibitor, methazolamide, which decreases Cl^- uptake and H^+ secretion (Del Duca et al. 2011). Since CA catalyzes the reversible hydration of CO_2 to yield HCO_3^- and H^+, it was hypothesized that Cl^- uptake occurs through exchange for HCO_3^- and that H^+ is used by VA to establish an electrochemical gradient that favours Na^+ uptake (Del Duca et al. 2011). Based on the findings from this present study and previous RNA-sequencing analyses, it is plausible that the CA facilitating NaCl uptake at the papillae is AeCA9 (Figure 20) (Durant et al. 2021).

4.2.2. AeCCC3

Previous studies have detected mRNA of *ccc3* in the MTs and hindgut of *A. aegypti* larvae using qPCR and RNA-sequencing (Durant and Donini 2024; Li et al. 2017; Piermarini et al. 2017). In this study *ccc3* transcript expression was also detected in these organs with the hindgut having an apparent, but not statistically higher level of transcript (Figure 7D). Previous studies have suggested that AeCCC3 is involved primarily in ion-absorption, since it is highly detected in larval organs such as the papillae, with comparatively low expression in the MTs which are secretory, suggesting it may not play a role in ion secretion by the MTs (Piermarini et al. 2017). In the MTs of larval *A. aegypti* transcript expression of other cation-coupled chloride co-transporters such as *nkcc1*, *kcc* and *ccc2* has been discovered (Li et al. 2017). Furthermore, relatively abundant expression of the *ccc2*, has been shown in the MTs compared to *ccc3* (Piermarini et al. 2017).

There is no functional characterization of AeCCC3 but, AeCCC2 has been evaluated for its function where it was found to differ from other cation-coupled chloride co-transporters (Duong et al. 2022; Kalsi et al. 2019). When expressed in a heterologous system (e.g., *Xenopus* oocytes), AeCCC2 has a high conductance for Na^+ independent from Cl^-, suggesting it functions differently than traditional NCCs/KCCs and NKCCs (Duong et al. 2022; Kalsi et al. 2019). This is of significance because the predicted transmembrane domain sequences of AeCCC3 are very similar to those of AeCCC2, suggesting that they may share similar transport functions (Piermarini et al. 2017). Most interestingly, AeCCC2 and AeCCC3 differ in amino acid sequences compared to AeNKCC1 along sites where a putative ion and inhibitor binding site is proposed to be located (Piermarini et al. 2017). These findings together suggest that AeCCC2 as well as AeCCC3 have different transport properties from AeNKCC1 (Piermarini et al. 2017). If this is the case, then AeCCC3 may be facilitating Na^+ transport into the hindgut cells from the hindgut lumen for Na^+ absorption (Figure 19).

Expression of *ccc3* in the midgut has not been previously examined. In this study, transcript for *ccc3* was detectable but at comparatively low levels. Other cation-coupled chloride co-transporters are expressed in the midgut. For example, AaeCG1277 is abundantly expressed throughout the midgut of larval *A. aegypti* (Filipov et al. 2003).

Previous studies have detected high transcript abundance of *ccc3* in the anal papillae of *A. aegypti* in comparison to other organs (e.g., MTs) and other cation-coupled chloride co-transporters (e.g., *ccc2*) (Durant et al. 2021; Piermarini et al. 2017). In this study, *ccc3* transcript was detected in the anal papillae. From a functional perspective the involvement of cation-coupled chloride cotransporters in NaCl uptake by the papillae was cautiously excluded because the inhibitor bumetanide did not affect NaCl uptake (Del Duca et al. 2011). However, other cation-

coupled chloride co-transporters such as NCCs can be insensitive to bumetanide, but sensitive to other inhibitors such as thiazide which has not been tested on papillae (Zhao et al. 2024). Since AeCCC2 and probably AeCCC3 do not function like NKCCs it is plausible that AeCCC3 may participate in NaCl uptake by the papillae (Figure 20). Therefore, *ccc3* is expressed primarily in the absorptive osmoregulatory organs (e.g. hindgut and anal papillae) where it may participate in sodium absorption but the expression and function of this transporter in mosquitoes that encounter salinity has not been studied.

4.2.3. AeNHA2

No previous studies have compared the expression of AeNHA2 in the osmoregulatory organs of larvae or adult *A. aegypti*, with the exception of a study that compared the gene's expression between larval and adult female MTs (Li et al. 2017). It was found that larval MTs have higher transcript levels than adult female MTs suggesting a greater role for AeNHA2 in larval MT function (Li et al. 2017). In this study *nha2* transcript levels were highest in the MTs of the larvae. These levels were apparently higher than those found in the hindgut and significantly higher than in the midgut (Figure 7B). These findings align with *nha2* expression in the osmoregulatory organs of adult *Drosophila*, where the MTs show the highest *nha2* transcript expression, followed by the hindgut, with the lowest mRNA abundance detected in the midgut (Chintapalli et al. 2015). The transport function of AeNHA2 has not been studied; however, heterologous expression systems have been used to study the function of AgNHA2, a homolog from the freshwater mosquito *Anopheles gambiae*, and also of *Drosophila* NHA2, another homolog. Both transporters exchanged cations for H^+, where AgNHA2 transported Na^+ or K^+ while *Drosophila* NHA2 transported Na^+ with the caveat that H^+ was transported outward by AgNHA2 and inward by *Drosophila* NHA2 (Xiang et al. 2012; Chintapalli et al. 2015). The electroneutral NHE8 has been

localized to the apical membrane of the principal cells of larval *A. aegypti* where it could be a candidate cation-proton antiporter coupled to VA and promoting Na^+ or K^+ secretion (Kang'ethe et al. 2007). If AeNHA2 functions similarly to AgNHA2 transporting Na^+ into cells, it could be basal, exchanging Na^+ from the hemolymph with H^+ for subsequent Na^+ apical excretion by other transporters (e.g. NHE8) (Figure 18). If AeNHA2 is expressed apically, it may function like AgNHA2 which is located on the apical side of the stellate cells in *A. gambiae* (Xiang et al. 2012). Here, it is proposed to exchange Na^+ into the stellate cells for H^+ where it could be electrically coupled to the adjacent principal cell through Na^+ cycling, where the AgNHA1 is located apically and is suggested to be driving Na^+ secretion (Figure 18) (Xiang et al. 2012).

The mRNA expression of *nha2* in the hindgut of *A. aegypti* suggests it is involved in Na^+ or K^+ re-absorption. Two plausible mechanisms can be proposed. First, if transporting Na^+ out of the cell for H^+, AeNHA2 is proposed to be basal, where Na^+ could be transported into the hemolymph facilitating the absorption of this ion (Figure 19). If AeNHA2 functions in the opposite direction, like AgNHA2, then it could be apically driving Na^+ into the cells for later absorption within the hemolymph across the basal surface of the hindgut (Figure 19).

Transcript expression of *nha2* was also found in the midgut but at this stage it is unclear if the gene is expressed in all segments of the midgut since the samples used contained gastric caeca, anterior midgut and posterior midgut combined. Nevertheless, some transport models can be cautiously proposed. In the anterior midgut, AeNHA2 could contribute to the high luminal pH through the apical removal of H^+ from the lumen in exchange for Na^+ if it were to function like the *Drosophila* NHA2 (Figure 17). On the other hand, if AeNHA2 functions like AgNHA2, then it may be proposed to basally remove H^+ from the cell in exchange for Na^+ (Figure 17). In the posterior midgut of larval *A. aegypti*, it was proposed that a nutrient amino acid transporter (NAT)

is expressed to absorb amino acids from the gut lumen with Na^+ (Jagadeshwaran et al. 2010). This led to the proposal that an NHA would be needed to exchange Na^+ back into the lumen, for $2H^+$ to prevent luminal Na^+ depletion by the NAT (Jagadeshwaran et al., 2010). In another FW mosquito *A. gambiae*, NHAs and NATs co-localize to the apical membrane of the posterior midgut (Okech et al. 2008a) Therefore, AeNHA2 could serve this purpose if it were expressed in the posterior midgut.

A previous transcriptome study has shown expression for *nha2* in the papillae and the present study has confirmed its expression with qPCR (Durant et al. 2021). A proposed model for NaCl uptake by the papillae suggests that AeNHA2 transports Na^+ across the apical membrane in exchange for H^+ (Figure 20) (Durant et al. 2021; Xiang et al. 2012). Another possible candidate for apical Na^+ uptake is NHE3 which was localized to the apical membrane of papillae (Chasiotis et al. 2016). Furthermore, pharmacological inhibitors of Na^+ channels were shown to reduce Na^+ uptake, suggesting that apical Na^+ channels are involved (Del Duca et al. 2011). Nonetheless, the molecular mechanism for NaCl uptake by papillae is a work in progress.

4.2.4. AeNHA1

Previous transcriptome studies completed on larval MTs and papillae of *A. aegypti* detected transcript for *nha1* but expression has not been previously assessed in the midgut or hindgut (Li et al. 2017; Durant et al. 2021). The present study confirmed *nha1* transcript in the MTs and detected transcript in the midgut and hindgut where abundance was by far greater in the hindgut than the other two organs (Figure 7A). These findings align with what was found in adult *Drosophila* and larval *A. gambiae* larvae where the rectum portion of the hindgut had the highest transcript expression of *nha1*, followed by the midgut then the MTs in both insects (Chintapalli et al. 2015; Rheault et al. 2007).

This present study also detected AeNHA1 protein through western blot analysis, where immunoreactive bands for AeNHA1 were detected in the MTs and anal papillae of larval *A. aegypti* (Figure 14). In the MTs, a band at ~71 kDa, corresponds to the expected mass of AeNHA1 but, an additional band was also detected at ~140 kDa. In the AP only the ~140 kDa band was consistently detected in both AFW and BW treated larvae (Figure 14). This band is approximately double the expected weight of the AeNHA1 monomer and therefore could represent a putative dimer. In *A. gambiae* larvae an antibody against AgNHA1, a homolog of AeNHA1 detected only a putative monomer in several different organs (Okech et al. 2008a; Rheault et al. 2007). However, in many organisms from prokaryotes to unicellular eukaryotes, to metazoans, NHAs have been consistently found to possess dimer domains (Herz et al. 2009; Lee et al. 2013; Matsouka et al. 2022; Rimon et al. 2007; Williams et al. 1999). Therefore, it is possible that AeNHA1 forms dimers in the membranes of the osmoregulatory organs of mosquito larvae.

The same antibody was used to localize AeNHA1 in tissue sections of osmoregulatory organs of larval *A. aegypti*. AeNHA1 staining was found in the midgut (gastric caeca and posterior midgut), MTs, hindgut and the anal papillae with no obvious qualitative differences in staining intensity between organs. In all the organs, AeNHA1 was consistently located on the basal side of the epithelium (Figure 8). Putative transport roles for AeNHA1 in these organs are proposed below.

Interestingly, in *A. gambiae* larvae AgNHA1, a homolog of AeNHA1 was localized to the apical membrane of the midgut as well as the MTs, in contrast to the basal localization shown here for AeNHA1 (Okech et al. 2008a; Xiang et al. 2012). In *A. gambiae* it was proposed that AgNHA1 drives Na^+ into the lumen of the midgut and MTs in exchange for H^+ (Okech et al. 2008a; Xiang et al. 2012). However; the homolog *Drosophila* NHA1, was shown to be functionally different

from traditional NHAs, including the *Drosophila* NHA2 and AgNHA2 (Chintapalli et al. 2015). When expressed in *Xenopus* oocytes, *Drosophila* NHA1 was found to either symport Cl^- and H^+ or exchange Cl^- for OH^- (Chintapalli et al. 2015). To the best of my knowledge, no other studies have functionally characterized NHA1s in Dipterans. Furthermore, AeNHA1 shares protein sequence similarity to both AgNHA1 (77.9%) and the *Drosophila* NHA1 (63.2%). The AgNHA1 is also similar to the *Drosophila* NHA1 (62.4%). Therefore, in the absence of other functional studies on NHA1s in Dipterans besides *Drosophila* NHA1 and the similarity in protein identity amongst these homologs, it is reasonable to assume that AeNHA1 (and AgNHA1) share similar ionic transport specificities.

In the gastric caeca, Na^+ and K^+ are secreted across both the distal and proximal surfaces, while H^+ is secreted at the proximal surface and absorbed at the distal surface (D'Silva et al. 2017b). Assuming that the overall transepithelial flux of H^+ is predominantly determined by the action of VA this would not be a reliable indicator of how AeNHA1 may be functioning in the gastric caeca. However, the direction of cation flux is a reliable indicator of the direction of Cl^- flux (Kirschner et al. 1983). Therefore, it stands to reason that Cl^- is being secreted across the gastric caeca and that AeNHA1 may mediate cellular uptake of Cl^- from the hemolymph across the basal side of the gastric caeca epithelium. This mechanism would be more feasible in the distal gastric caeca where a basal VA can provide the proton motive force for Cl^-/H^+ symport by AeNHA1 (Figure 17A) (Patrick et al. 2006). The process is less clear in the proximal gastric caeca where VA is only on the apical side and NKA is on the basal side (Figure 17A) (Patrick et al. 2006). For the remainder of the midgut, this present study only localized AeNHA1 to the posterior segments of the midgut, with the anterior region not having been assessed. This is apparent based on the apical VA staining shown in this study, which is characteristic of the posterior midgut,

unlike the anterior midgut which exhibits basal VA localization (Patrick et al. 2006). In the posterior midgut AeNHA1 may transport Cl^-/H^+ into the cell (Figure 17D). This would support the transport of H^+ that may be needed to aid in luminal acidification of the posterior midgut. The basal localization of AeNHA1 is logical in the MTs if it functions like the *Drosophila* NHA1, transporting Cl^- and H^+ across the basal surface into the cells for secretion into the lumen (Figure 18) (Chintapalli et al. 2015). However, the basal localization of this transporter in the ion-absorptive organs, hindgut and papillae is not as logical unless the electrochemical gradients are such that AeNHA1 transports Cl^- and H^+ out of the cell and into the hemolymph (Figure 19 and Figure 20). Previous studies have shown that cation-proton antiporters can switch the direction of Na^+/H^+ exchanged based on the external Na^+ or H^+ available in the extracellular and intracellular fluid (Demaurex et al. 1995). It is therefore possible that AeNHA1 switches the direction of transport in different epithelia based on the electrochemical gradients inherent in these epithelia.

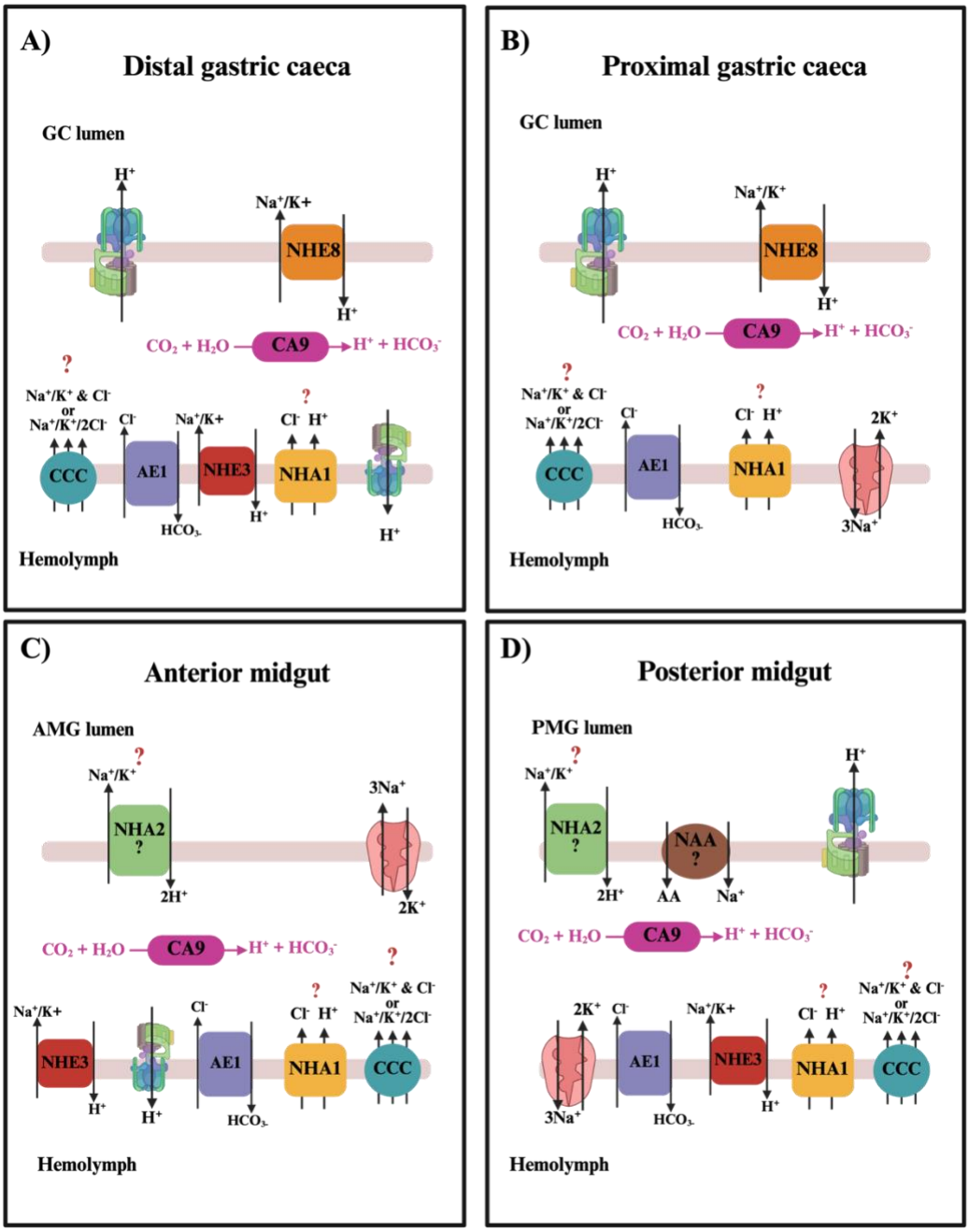

Figure 17. Updated proposed ion-transport model for the different segments of the midgut in larval *Aedes aegypti*. (A) Illustrates the ion-transporters localized to the distal and (B) proximal gastrica caeca, (C) and (D) show the proposed ion-transport models for the anterior and posterior midgut respectively, where the apical membrane faces the AMG (anterior midgut) lumen and PMG (posterior midgut) lumen. Transporters shown with a black '?' indicate that they have not been localized, with their localization being proposed and ion routes with a red '?' indicate the proposed function of these ion-transporters (see main text). This figure was made using BioRender (biorender.com).

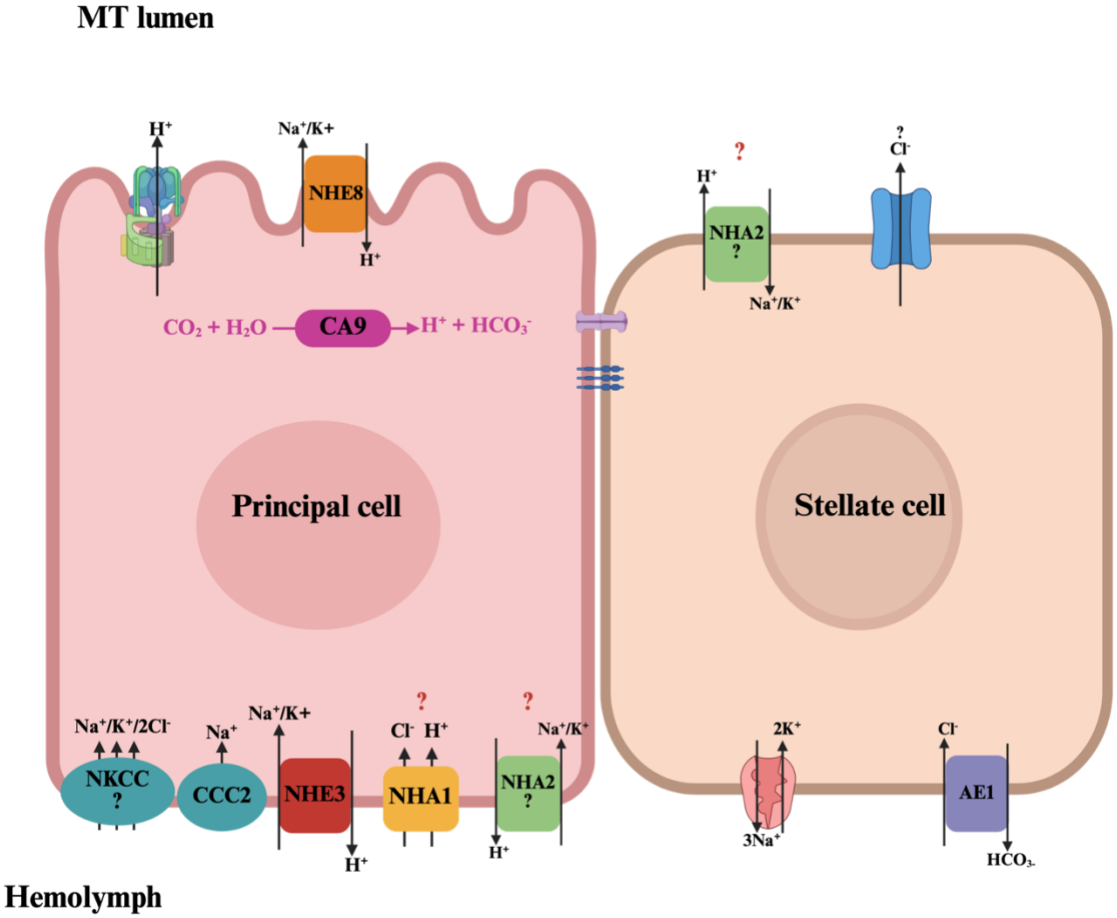

Figure 18. Updated proposed ion-transport model for the MTs in larval *Aedes aegypti*. This figure represents an updated MT larval ion-transport model for *A. aegypti* based on the expression findings reported in this present study. This includes the proposed localization/function of AeNHA2 and proposed function of AeNHA1. Any black '?' associated with ion-transporters suggests the localization hasn't been evaluated and a red '?' associated with ion routes indicate the proposed function of these transporters (see main text). This figure was made using BioRender (biorender.com).

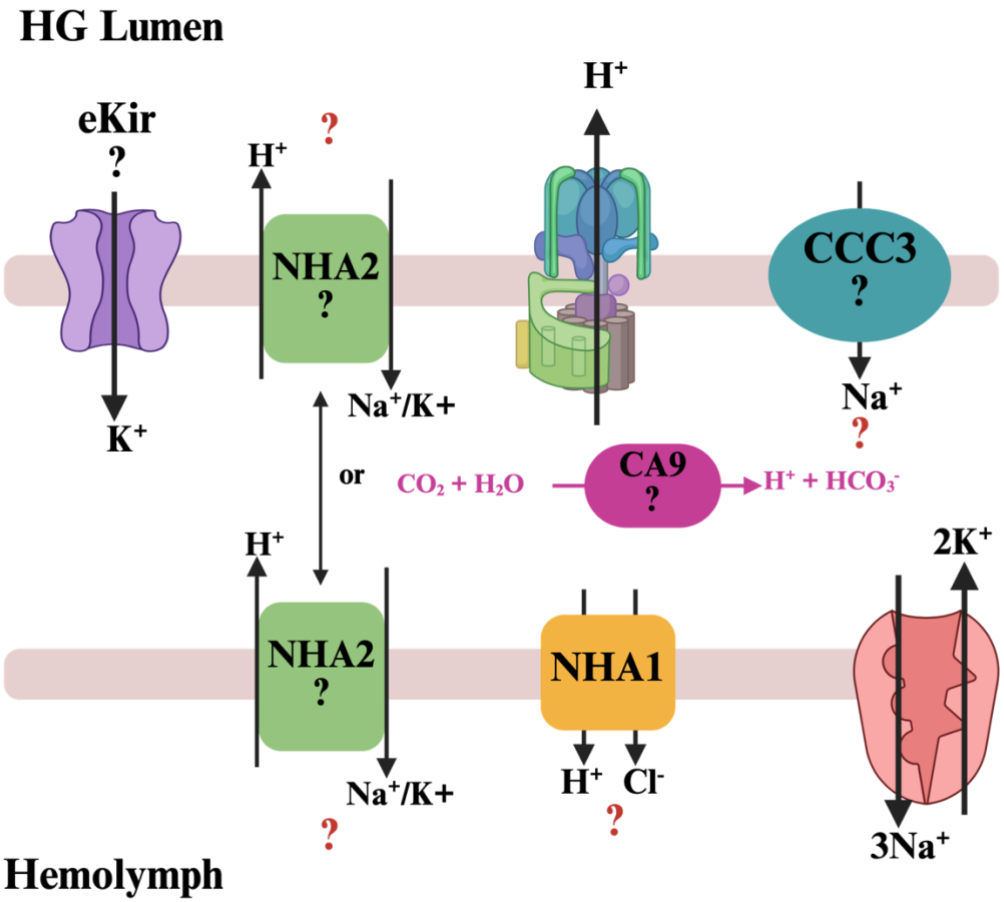

Figure 19. Updated proposed ion-transport model for the hindgut (HG) in larval *Aedes aegypti.* This figure represents an updated HG larval ion-transport model for *A. aegypti* based on the expression findings reported in this present study. This includes the proposed localization/function of AeCA9, AeCCC3, AeNHA2 and proposed function of AeNHA1. Any black '?' associated with ion-transporters suggests the localization hasn't been evaluated and a red '?' associated with ion routes indicate the proposed function of these transporters (see main text). This figure was made using BioRender (biorender.com).

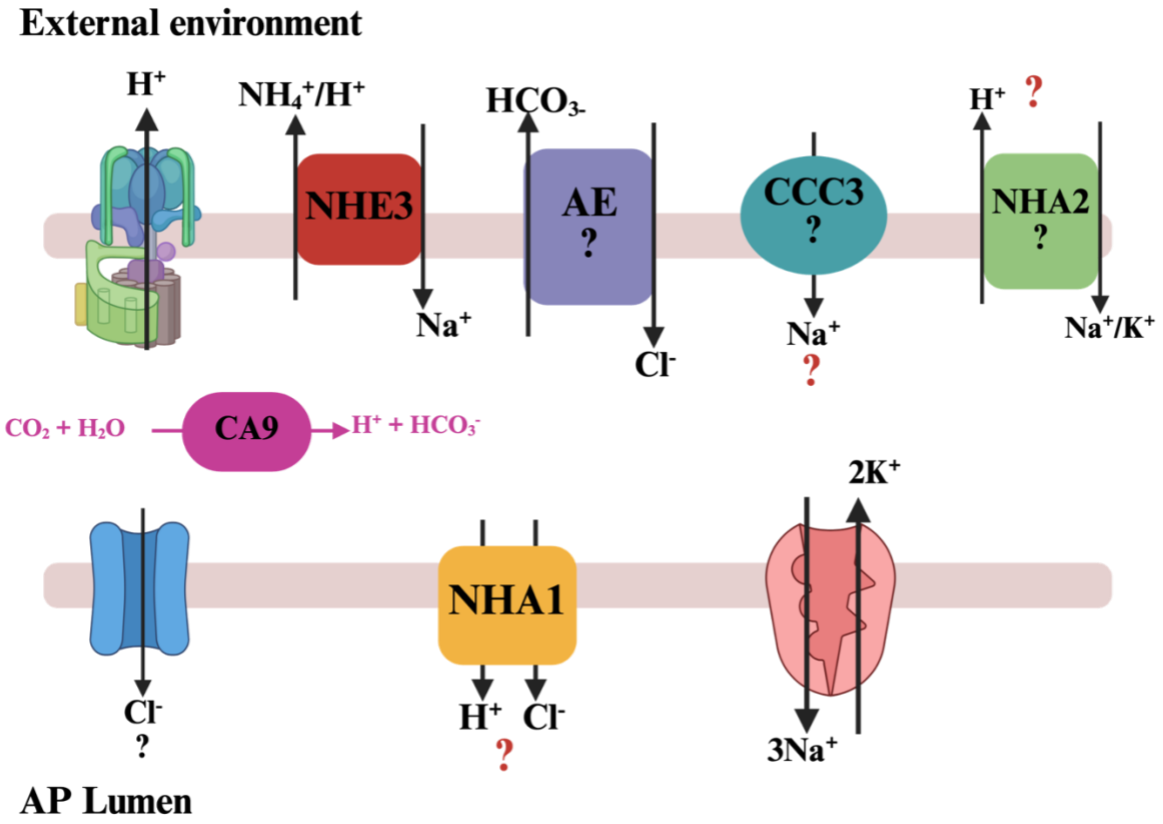

Figure 20. Updated proposed ion-transport model for the anal papillae (AP) in larval *Aedes aegypti*. This figure represents an updated AP larval ion-transport model for *A. aegypti* surrounded based on the expression findings reported in this present study. This includes the proposed localization/function of AeCCC3, AeNHA2 and proposed function of AeNHA1. Any black '?' associated with ion-transporters suggests the localization hasn't been evaluated and a red '?' associated with ion routes indicate the proposed function of these transporters (see main text). This figure was made using BioRender (biorender.com).

4.3. Expression of AeNHA1, AeNHA2, AeCA9 and AeCCC3 in *A. aegypti larvae* acutely exposed to salinity

4.3.1. Midgut

Acute salinity exposure resulted in a significant decrease of *ccc3* transcript abundance in the midgut but, had no effect on the other three genes that were examined. In addition, in the posterior midgut, AeNHA1 protein staining intensity and localization did not qualitatively change with salinity. It is plausible that the expression of Na^+/H^+ antiporters and CAs in the midgut is kept consistent despite changes in external salinity if their principal role is to maintain luminal pH and ion levels (Boudko et al. 2001a; Corena et al. 2002; Jagadeshwaran et al. 2010; Okech et al. 2008a). At the anterior midgut H^+ removal maintains alkalinization, and at the posterior midgut replenishing luminal ions like Na^+ where Na^+ is needed for hemolymph amino acid uptake would be a priority (Carpenter et al. 2012; Jagadeshwaran et al. 2010; Okech et al. 2008b). Indeed, in the midgut of mosquitoes a number of ion coupled amino acid transporters are expressed (Carpenter et al. 2012; Okech et al. 2008b). Collectively, AeNHA1, AeNHA2 and AeCA9 in the midgut could primarily serve this important function.

On the other hand, the decrease in *ccc3* transcript abundance may indicate that this transporter is important in maintaining ion and/or osmotic gradients across the midgut epithelia. These gradients may be passively maintained with the ingestion of BW (see D'Silva et al. 2017b). In the midgut, the gastric caeca is the recognized site that has ion regulatory functions where previous studies illustrated that raising *A. aegypti* larvae in BW reduces ion-transport and NKA/VA activities and this was proposed to reflect a reduced need to hyperregulate in salinity since ions are ingested from the surrounding media which maintains the transepithelial potential of ions within the caecal lumen (D'Silva et al. 2017b). Since CCCs are often associated with NKA (Katoh et al. 2008; Shirangi et al. 2017) it is tempting to cautiously propose that AeCCC3 may be

expressed in the gastric caeca and the decrease in transcript abundance of this transporter reflects its ion regulatory function.

4.3.2. Malpighian tubules

No changes in the transcript abundance of *nha1*, *nha2*, *ca9* and *ccc3* were detected in the MTs of larval *A. aegypti* exposed to BW. Furthermore, no qualitative differences in AeNHA1 protein expression were seen with BW. A few studies have characterized the functional implications of salinity exposure on the MTs of aquatic larval insects. In *A. aegypti* rearing larvae in BW resulted in no changes in fluid secretion rates or in $[Na^+]$ in secreted fluid of MTs compared to freshwater controls (Donini et al. 2006; Jonusaite et al. 2016). In the MTs of the midge, *Chironomus riparius* which has similar osmoregulatory motives to *A. aegypti*, no functional changes occur in the tubules when larvae are raised in BW compared to FW (Zadeh-Tahmasebi et al. 2016). These studies show that when larvae are faced with salinity the function of the MTs is generally unchanged, at least in terms of ion and overall fluid transport. This is likely to reflect the important function of the MTs in primary urine formation and elimination of metabolic wastes essential for survival and independent of external salinity. Therefore, the results of this study may not be surprising since the transporters that were assessed are likely to participate in the ion transport functions of the MTs which are essential for fluid secretion and waste elimination (see section 4.2 above).

4.3.3. Hindgut

No changes in the transcript abundance of *nha1*, *nha2*, *ca9* and *ccc3* were detected in the hindgut of larval *A. aegypti* exposed to salinity. Furthermore, the degree of AeNHA1 protein staining and its localization was unchanged with salinity. Since salinity has been previously found to cause increases in hemolymph ion levels in larval *A. aegypti* (Donini et al. 2006; Farrell et al.

2024; Jonusaite et al. 2016) it was expected that these ion-regulatory genes would be down-regulated in the hindgut to reduce ion-absorption. This assumption is based on findings from previous studies on aquatic insect larvae such as the midge *Chironomus riparius*, where it was shown that exposure to BW results in reduced total K^+ absorption by the hindgut and is is linked to reductions in NKA and VA activities (Jonusaite et al. 2013). How the transport capacity of the hindgut responds to BW in larval *A. aegypti* has not been studied making it difficult to interpret the expression results presented here.

4.3.4. Anal papillae

In the anal papillae, BW exposure resulted in a decrease in the transcript abundance of *nha1* and no statistically significant effects on the other genes examined. Qualitatively, there didn't appear to be any difference in the intensity of the immunohistochemical staining of AeNHA1 in the papillae of salinity exposed larvae compared with freshwater larvae and this was consistent with a quantitative assessment of the putative dimer of AeNHA1 using western blotting. In general, the findings on transcript abundance support the previous RNA-sequencing study from Durant et al. 2021, where transcripts for *nha1* and *ca9* are lower in the papillae of BW exposed larvae. Furthermore, the transcriptome study showed significantly higher transcript levels of *nha2* with BW (Durant et al. 2021). For *ca9* the present results are generally consistent with the transcriptome study since there appears to be a reduction in *ca9* transcript abundance with BW ($p=0.06$). However, for *nha2* there is an apparent opposite trend where *nha2* transcript levels appear lower in BW ($p=0.06$).

Considering the transcript abundance results and assuming that the apparent differences seen for *ca9* and *nha2* translate to differences in expression, the observed changes are linked to functional changes that occur in the anal papillae with BW exposure. The papillae of *A. aegypti*

reduce NaCl uptake when larvae are transferred to BW to limit the accumulation of salts in the hemolymph (Donini et al. 2007). The apparent reduction in expression of *ca9* and *nha2*, along with the significant reduction in *nha1* transcript abundance with BW exposure supports the reduction in NaCl uptake if these transporters are mediating NaCl uptake (see section 4.2 above). The discrepancy between *nha1* transcript levels and protein abundance found in this study may be explained by the time at which samples were collected. After a 24-hour exposure to BW the anal papillae may exhibit a reduction in transcript levels of ion transporters that are related to ion uptake; however, protein levels may require more time to manifest a reduction in expression. In general, mRNA and protein levels should not be assumed to be uniform, as in many cases they are not always correlated, which may be attributed to changes in translation efficiency and the degradation rates of both mRNA and protein (Fournier et al. 2010; Jonusaite et al. 2016, Jounsaite et al. 2017b). The transcript abundance of *ccc3* is unchanged with BW exposure, a result consistent with the transcriptome study (Durant et al. 2021). In the midge, *Chironomus riparius*, the papillae were shown to secrete Na^+ when exposed to 7g/L NaCl for 24-hours (Reinsborough and Donini 2025). Based on these findings, if *A. aegypti* papillae are capable of behaving in a similar fashion, this could suggest that AeCCC3 can partake in both ion uptake and ion secretion. To resolve the function of these transporters future studies should assess the effect of knocking down the expression of these ion-transporters on ion transport by the anal papillae of FW and BW exposed *A. aegypti* larvae. Although this was an objective of the current study the extensive efforts in achieving significant knockdown of these genes with dsRNA was unsuccessful.

4.4. Conclusions and Future directions

The FW mosquito *A. aegypti* is a well-studied disease vector, although understanding how the larvae ionoregulate within aquatic environments through the employment of different secondary ion-transporters in FW and BW environments remains an understudied area. This study was able to detect and illustrate the presence of several different ion-transporters such as AeNHA1, AeNHA2, AeCCC3 and the enzyme – AeCA9 throughout the osmoregulatory organs of the AFW larval *A. aegypti,* while also comparing how they differ in their expression when exposed to BW conditions. The detection of these transporters in FW throughout all the ion-regulatory organs suggest that they each serve as important mediators in maintaining osmotic homeostasis when in environments where the larvae are faced with passive water gain and ion loss. Furthermore, in some cases these transporters were observed to decrease or were unchanged as a function of salinity in the different organs assessed. Therefore, in most cases, this study was able to show that these ion-transporters are still expressed in BW in the different ion-regulatory organs, with only some observable changes. This provides foundational evidence to suggest that in some instances, these ion-transporters may be needed to mediate osmotic balance in salinated water. Furthermore, this study also detected the putative AeNHA1 protein in the MTs and AP through immunoblotting, and determined its localization throughout the gastric caeca, posterior midgut, MTs, hindgut and the anal papillae for the first time in *A. aegypti*. The consistent basal location for AeNHA1 in each organ studied suggests it aids in the ion-transport mechanisms of this membrane in each of the epithelia assessed.

Despite this study having detected and compared these ion-transporters in the different osmoregulatory organs, and how they adjust their abundance as a function of BW exposure, understanding the functional implications of each of these transporters has not yet been identified. To understand how these selected ion-transporters serve the osmoregulatory organs of larval *A.*

aegypti, future investigation should be considered. Specifically, the individual knockdown of each of the transporters (e.g., AeNHA1, AeNHA2, AeCA9 and AeCCC3) should be completed and confirmed throughout the midgut (gastric caeca, anterior and posterior midgut), MTs, hindgut and the anal papillae. Functional changes such as ion fluxes and fluid secretion (MTs) should be assessed in the face of knockdown to understand how each of these transporters serve the osmoregulatory organs or how they influence larval survival to understand different techniques to control *A. aegypti*. Nonetheless, the findings in this present study provide a foundation in understanding which secondary ion-transporters support the ion regulatory techniques of the alimentary canal and papillae organs of larval *A. aegypti* in their naturally adapted FW environments, and also when placed in BW to which they osmotically tolerate.

5.0. References

Abe FR, Coleone AC, Machado AA, Gonçalves Machado-Neto J. 2014. Ecotoxicity and Environmental Risk Assessment of Larvicides Used in the Control of *Aedes aegypti* to *Daphnia magna* (Crustacea, Cladocera). Journal of Toxicology and Environmental Health, Part A. 77(1–3):37–45. https://doi.org/10.1080/15287394.2014.865581

Akbari OS, Antoshechkin I, Amrhein H, Williams B, Diloreto R, Sandler J, Hay BA. 2013. The Developmental Transcriptome of the Mosquito *Aedes aegypti*, an Invasive Species and Major Arbovirus Vector. G3: Genes, Genomes, Genetics. 3(9):1493–1509. https://doi.org/10.1534/g3.113.006742

Arroyo JP, Kahle KT, Gamba G. 2013. The SLC12 family of electroneutral cation-coupled chloride cotransporters. Molecular Aspects of Medicine. 34(2–3):288–298. https://doi.org/10.1016/j.mam.2012.05.002

Barrera R, Amador M, Acevedo V, Caban B, Felix G, Mackay AJ. 2014. Use of the CDC Autocidal Gravid Ovitrap to Control and Prevent Outbreaks of *Aedes aegypti* (Diptera: Culicidae). Journal of Medical Entomology. 51(1):145–154. https://doi.org/10.1603/ME13096

Barrett ADT, Higgs S. 2007. Yellow Fever: A Disease that Has Yet to be Conquered. Annual Review of Entomology. 52(1):209–229. https://doi.org/10.1146/annurev.ento.52.110405.091454

Barroso IG, Ferreira C, Terra WR. 2025. Water Transport and Enzyme Recycling in *Tenebrio molitor* Midgut: Insights From Transcriptomics, Proteomics, and In Vivo Inhibition Assays. Archives of Insect Biochemistry and Physiology. 118(4). https://doi.org/10.1002/arch.70059

Beadle LC. 1939. Regulation of the Haemolymph in the Saline Water Mosquito Larva *Aedes Detritus* Edw. Journal of Experimental Biology. 16(3):346–362. https://doi.org/10.1242/jeb.16.3.346

Beyenbach KW, Piermarini PM. 2011. Transcellular and paracellular pathways of transepithelial fluid secretion in Malpighian (renal) tubules of the yellow fever mosquito *Aedes aegypti*. Acta Physiologica. 202(3):387–407. https://doi.org/10.1111/j.1748-1716.2010.02195.x

Beyenbach Klaus W, Skaer H, Dow JAT. 2010. The Developmental, Molecular, and Transport Biology of Malpighian Tubules. Annual Review of Entomology. 55(Volume 55, 2010):351–374. https://doi.org/https://doi.org/10.1146/annurev-ento-112408-085512

Beyenbach Klaus W., Skaer H, Dow JAT. 2010. The Developmental, Molecular, and Transport Biology of Malpighian Tubules. Annual Review of Entomology. 55(1):351–374. https://doi.org/10.1146/annurev-ento-112408-085512

Boudko DY, Moroz LL, Harvey WR, Linser PJ. 2001a. Alkalinization by chloride/bicarbonate pathway in larval mosquito midgut. Proceedings of the National Academy of Sciences. 98(26):15354–15359. https://doi.org/10.1073/pnas.261253998

Boudko DY, Moroz LL, Linser PJ, Trimarchi JR, Smith PJS, Harvey WR. 2001b. *In Situ* Analysis of pH Gradients in Mosquito Larvae Using Non-Invasive, Self-Referencing, pH-Sensitive Microelectrodes. Journal of Experimental Biology. 204(4):691–699. https://doi.org/10.1242/jeb.204.4.691

Bradley TJ. 1987. Physiology of Osmoregulation in Mosquitoes. Annual Review of Entomology. 32(1):439–462. https://doi.org/10.1146/annurev.en.32.010187.002255

Braga IA, Mello CB, Montella IR, Lima JBP, de Jesus Martins Júnior A, Medeiros PFV, Valle D. 2005. Effectiveness of Methoprene, an Insect Growth Regulator, Against Temephos-Resistant *Aedes aegypti* Populations from Different Brazilian Localities, Under Laboratory Conditions. Journal of Medical Entomology. 42(5):830–837. https://doi.org/10.1093/jmedent/42.5.830

Brett CL, Donowitz M, Rao R. 2005. Evolutionary origins of eukaryotic sodium/proton exchangers. American Journal of Physiology-Cell Physiology. 288(2):C223–C239. https://doi.org/10.1152/ajpcell.00360.2004

Carpenter VK, Drake LL, Aguirre SE, Price DP, Rodriguez SD, Hansen IA. 2012. SLC7 amino acid transporters of the yellow fever mosquito *Aedes aegypti* and their role in fat body TOR signaling and reproduction. Journal of Insect Physiology. 58(4):513–522. https://doi.org/10.1016/j.jinsphys.2012.01.005

Chasiotis H, Ionescu A, Misyura L, Bui P, Fazio K, Wang J, Patrick M, Weihrauch D, Donini A. 2016. An animal homolog of plant Mep/Amt transporters promotes ammonia excretion by the anal papillae of the disease vector mosquito, *Aedes aegypti*. Journal of Experimental Biology. https://doi.org/10.1242/jeb.134494

Chen C, Aldridge RL, Gibson S, Kline J, Aryaprema V, Qualls W, Xue R, Boardman L, Linthicum KJ, Hahn DA. 2023. Developing the radiation-based sterile insect technique (SIT) for controlling *Aedes aegypti*: identification of a sterilizing dose. Pest Management Science. 79(3):1175–1183. https://doi.org/10.1002/ps.7303

Chintapalli VR, Kato A, Henderson L, Hirata T, Woods DJ, Overend G, Davies SA, Romero MF, Dow JAT. 2015. Transport proteins NHA1 and NHA2 are essential for survival but have distinct transport modalities. Proceedings of the National Academy of Sciences. 112(37):11720–11725. https://doi.org/10.1073/pnas.1508031112

Clark TM, Bradley TJ. 1996. Stimulation of Malpighian tubules from larval *Aedes aegypti* by secretagogues. Journal of Insect Physiology. 42(6):593–602. https://doi.org/10.1016/0022-1910(95)00124-7

Clark TM, Koch A, Moffett DF. 2000. The Electrical Properties of the Anterior Stomach of the Larval Mosquito (*Aedes aegypti*). Journal of Experimental Biology. 203(6):1093–1101. https://doi.org/10.1242/jeb.203.6.1093

Clements AN. 1992. The biology of mosquitoes. Vol. I; Development, nutrition and reproduction. London: Elsevier

Dadd RH. 1975. Alkalinity within the midgut of mosquito larvae with alkaline-active digestive enzymes. Journal of Insect Physiology. 21(11):1847–1853. https://doi.org/10.1016/0022-1910(75)90252-8

Demaurex N, Orlowski J, Brisseau G, Woodside M, Grinstein S. 1995. The mammalian Na^+/H^+ antiporters NHE-1, NHE-2, and NHE-3 are electroneutral and voltage independent, but can couple to an H^+ conductance. The Journal of General Physiology. 106(1):85–111. https://doi.org/10.1085/jgp.106.1.85

Devine GJ, Vazquez-Prokopec GM, Bibiano-Marín W, Pavia-Ruz N, Che-Mendoza A, Medina-Barreiro A, Villegas J, Gonzalez-Olvera G, Dunbar MW, Ong O, Ritchie S, Churcher T, Kirstein O, Manrique-Saide P. 2021. The entomological impact of passive metofluthrin emanators against indoor *Aedes aegypti*: A randomized field trial. PLOS Neglected Tropical Diseases. 15(1):e0009036. https://doi.org/10.1371/journal.pntd.0009036

Dias CN, Moraes DFC. 2014. Essential oils and their compounds as *Aedes aegypti* L. (Diptera: Culicidae) larvicides: review. Parasitology Research. 113(2):565–592. https://doi.org/10.1007/s00436-013-3687-6

Dixon D, Van Ekeris L, Linser P. 2017. Characterization of carbonic anhydrase 9 in the alimentary canal of *Aedes aegypti* and its relationship to homologous mosquito carbonic anhydrases. International Journal of Environmental Research and Public Health. 14(2):213. https://doi.org/10.3390/ijerph14020213

Donini A, Gaidhu MP, Strasberg DR, O'Donnell MJ. 2007. Changing salinity induces alterations in hemolymph ion concentrations and Na and Cl transport kinetics of the anal papillae in the larval mosquito, *Aedes aegypti*. Journal of Experimental Biology. 210(6):983–992. https://doi.org/10.1242/jeb.02732

Donini A, O'Donnell MJ. 2005. Analysis of Na^+, Cl^-, K^+, H^+ and NH_4^+ concentration gradients adjacent to the surface of anal papillae of the mosquito *Aedes aegypti*: application of self-referencing ion-selective microelectrodes. Journal of Experimental Biology. 208(4):603–610. https://doi.org/10.1242/jeb.01422

Donini A, Patrick ML, Bijelic G, Christensen RJ, Ianowski JP, Rheault MR, O'Donnell MJ. 2006. Secretion of Water and Ions by Malpighian Tubules of Larval Mosquitoes: Effects of Diuretic Factors, Second Messengers, and Salinity. Physiological and Biochemical Zoology. 79(3):645–655. https://doi.org/10.1086/501059

D'Silva NM, Donini A, O'Donnell MJ. 2017a. The roles of V-type H^+-ATPase and Na^+/K^+-ATPase in energizing K^+ and H^+ transport in larval *Drosophila* gut epithelia. Journal of Insect Physiology. 98:284–290. https://doi.org/10.1016/j.jinsphys.2017.01.019

D'Silva NM, Patrick ML, O'Donnell MJ. 2017b. Effects of rearing salinity on expression and function of ion motive ATPases and ion transport across the gastric caecum of *Aedes aegypti* larvae. Journal of Experimental Biology. https://doi.org/10.1242/jeb.163170

Duca O del, Nasirian A, Galperin V, Donini A. 2011. Pharmacological characterisation of apical Na^+ and Cl^- transport mechanisms of the anal papillae in the larval mosquito *Aedes aegypti*. Journal of Experimental Biology. 214(23):3992–3999. https://doi.org/10.1242/jeb.063719

Duong PC, McCabe TC, Riley GF, Holmes HL, Piermarini PM, Romero MF, Gillen CM. 2022. Sequence analysis and function of mosquito aeCCC2 and Drosophila Ncc83 orthologs. Insect Biochemistry and Molecular Biology. 143:103729. https://doi.org/10.1016/j.ibmb.2022.103729

Durant AC, Donini A. 2018. Ammonia Excretion in an Osmoregulatory Syncytium Is Facilitated by AeAmt2, a Novel Ammonia Transporter in *Aedes aegypti* Larvae. Frontiers in Physiology. 9:339. https://doi.org/10.3389/fphys.2018.00339

Durant AC, Donini A. 2024. Ammonia transport in the excretory system of mosquito larvae (*Aedes aegypti*): Rh protein expression and the transcriptome of the rectum. Comparative Biochemistry and Physiology Part A: Molecular & Integrative Physiology. 294:111649. https://doi.org/10.1016/j.cbpa.2024.111649

Durant AC, Grieco Guardian E, Kolosov D, Donini A. 2021. The transcriptome of anal papillae of *Aedes aegypti* reveals their importance in xenobiotic detoxification and adds significant knowledge on ion, water and ammonia transport mechanisms. Journal of Insect Physiology. 132:104269. https://doi.org/https://doi.org/10.1016/j.jinsphys.2021.104269

Edwards HA. 1982. Ion Concentration and Activity in the Haemolymph of *Aedes Aegypti* Larvae. Journal of Experimental Biology. 101(1):143–151. https://doi.org/10.1242/jeb.101.1.143

Edwards HA, Harrison JB. 1983. An osmoregulatory syncytium and associated cells in a freshwater mosquito. Tissue and Cell. 15(2):271–280. https://doi.org/https://doi.org/10.1016/0040-8166(83)90022-8

Farrell S, Dates J, Ramirez N, Hausknecht-Buss H, Kolosov D. 2024. Voltage-gated ion channels are expressed in the Malpighian tubules and anal papillae of the yellow fever mosquito (*Aedes aegypti*) and may regulate ion transport during salt and water imbalance. Journal of Experimental Biology. 227(3). https://doi.org/10.1242/jeb.246486

Fay RW, Mccray EM Jr, Kilpatrick JW. 1963. Mass Production of Sterilized Male *Aedes aegypti*. 23(3):210–214.

Fernando HSD, Saavedra-Rodriguez K, Perera R, Black WC, de Silva BGDNK. 2020. Resistance to commonly used insecticides and underlying mechanisms of resistance in *Aedes aegypti* (L.) from Sri Lanka. Parasites & Vectors. 13(1):407. https://doi.org/10.1186/s13071-020-04284-y

Filippov V, Aimanova K, Gill SS. 2003. Expression of an *Aedes aegypti* cation-chloride cotransporter and its *Drosophila* homologues. Insect Molecular Biology. 12(4):319–331. https://doi.org/10.1046/j.1365-2583.2003.00415.x

Fournier ML, Paulson A, Pavelka N, Mosley AL, Gaudenz K, Bradford WD, Glynn E, Li H, Sardiu ME, Fleharty B, Seidel C, Florens L, Washburn M. 2010. Delayed Correlation of mRNA and Protein Expression in Rapamycin-treated Cells and a Role for Ggc1 in Cellular Sensitivity to Rapamycin. Molecular & Cellular Proteomics. 9(2):271–284. https://doi.org/10.1074/mcp.M900415-MCP200

Haas M, Forbush III B. 2000. The Na-K-Cl Cotransporter of Secretory Epithelia. Annual Review of Physiology. 62(1):515–534. https://doi.org/10.1146/annurev.physiol.62.1.515

Halstead SB. 2008. Dengue Virus–Mosquito Interactions. Annual Review of Entomology. 53(1):273–291. https://doi.org/10.1146/annurev.ento.53.103106.093326

Hansen IA, Boudko DY, Shiao S-H, Voronov DA, Meleshkevitch EA, Drake LL, Aguirre SE, Fox JM, Attardo GM, Raikhel AS. 2011. AaCAT1 of the yellow fever mosquito, *Aedes aegypti*: a novel histidine-specific amino acid transporter from the SLC7 family. The Journal of Biological Chemistry. 286(12):10803–13. https://doi.org/10.1074/jbc.M110.179739

Harold FM, Papineau D. 1972. Cation transport and electrogenesis by *Streptococcus faecalis*. The Journal of Membrane Biology. 8(1):45–62. https://doi.org/10.1007/BF01868094

Hartmann A-M, Tesch D, Nothwang HG, Bininda-Emonds ORP. 2014. Evolution of the Cation Chloride Cotransporter Family: Ancient Origins, Gene Losses, and Sub functionalization through Duplication. Molecular Biology and Evolution. 31(2):434–447. https://doi.org/10.1093/molbev/mst225

Hegarty JL, Zhang B, Pannabecker TL, Petzel DH, Baustian MD, Beyenbach KW. 1991. Dibutyryl cAMP activates bumetanide-sensitive electrolyte transport in Malpighian tubules. American Journal of Physiology-Cell Physiology. 261(3):C521–C529. https://doi.org/10.1152/ajpcell.1991.261.3.C521

Herz K, Rimon A, Jeschke G, Padan E. 2009. β-Sheet-dependent Dimerization Is Essential for the Stability of NhaA Na^+/H^+ Antiporter. Journal of Biological Chemistry. 284(10):6337–6347. https://doi.org/10.1074/jbc.M807720200

Hewett-Emmett D, Tashian RE. 1996. Functional Diversity, Conservation, and Convergence in the Evolution of the α-, β-, and γ-Carbonic Anhydrase Gene Families. Molecular Phylogenetics and Evolution. 5(1):50–77. https://doi.org/10.1006/mpev.1996.0006

Hossain Md Shakhawat, Raihan ME, Hossain Md Sakir, Syeed MMM, Rashid H, Reza MS. 2022. *Aedes* Larva Detection Using Ensemble Learning to Prevent Dengue Endemic. BioMedInformatics. 2(3):405–423. https://doi.org/10.3390/biomedinformatics2030026

Hwang PP, Lee TH, Lin LY. 2011. Ion regulation in fish gills: recent progress in the cellular and molecular mechanisms. American Journal of Physiology-Regulatory, Integrative and Comparative Physiology. 301(1):R28–R47. https://doi.org/10.1152/ajpregu.00047.2011

Jagadeshwaran U, Onken H, Hardy M, Moffett SB, Moffett DF. 2010. Cellular mechanisms of acid secretion in the posterior midgut of the larval mosquito (*Aedes aegypti*). Journal of Experimental Biology. 213(2):295–300. https://doi.org/10.1242/jeb.037549

Jones JC, Zeve VH. 1968. The fine structure of the gastric caeca of *Aedes aegypti* larvae. Journal of Insect Physiology. 14(11):1567–1575. https://doi.org/10.1016/0022-1910(68)90092-9

Jonusaite S, Donini A, Kelly SP. 2017a. Salinity alters snakeskin and mesh transcript abundance and permeability in midgut and Malpighian tubules of larval mosquito, *Aedes aegypti*. Comparative Biochemistry and Physiology Part A: Molecular & Integrative Physiology. 205:58–67. https://doi.org/https://doi.org/10.1016/j.cbpa.2016.12.015

Jonusaite S, Kelly SP, Donini A. 2013. Tissue specific ionomotive enzyme activity and K^+ reabsorption reveal the rectum as an important ionoregulatory organ in larval *Chironomous riparius* exposed to varying salinity. Journal of Experimental Biology. https://doi.org/10.1242/jeb.089219

Jonusaite S, Kelly SP, Donini A. 2016. The response of claudin-like transmembrane septate junction proteins to altered environmental ion levels in the larval mosquito *Aedes aegypti*. Journal of Comparative Physiology B. 186(5):589–602. https://doi.org/10.1007/s00360-016-0979-z

Jonusaite S, Kelly SP, Donini A. 2017b. Identification of the septate junction protein gliotactin in the mosquito, *Aedes aegypti*: evidence for a role in increased paracellular permeability in larvae. Journal of Experimental Biology. https://doi.org/10.1242/jeb.156125

Kalsi M, Gillen C, Piermarini PM. 2019. Heterologous Expression of Aedes aegypti Cation Chloride Cotransporter 2 (aeCCC2) in Xenopus laevis Oocytes Induces an Enigmatic Na^+/Li^+ Conductance. Insects. 10(3):71. https://doi.org/10.3390/insects10030071

Kang'ethe W, Aimanova KG, Pullikuth AK, Gill SS. 2007. NHE8 mediates amiloride-sensitive Na^+/H^+ exchange across mosquito Malpighian tubules and catalyzes Na^+ and K^+ transport in reconstituted proteoliposomes. American Journal of Physiology-Renal Physiology. 292(5):F1501–F1512. https://doi.org/10.1152/ajprenal.00487.2005

Katoh F, Cozzi RRF, Marshall WS, Goss GG. 2008. Distinct $Na^+/K^+/2Cl^-$ cotransporter localization in kidneys and gills of two euryhaline species, rainbow trout and killifish. Cell and Tissue Research. 334(2):265–281. https://doi.org/10.1007/s00441-008-0679-4

Kaushal SS, Likens GE, Pace ML, Reimer JE, Maas CM, Galella JG, Utz RM, Duan S, Kryger JR, Yaculak AM, Boger WL, Bailey NW, Haq S, Wood KL, Wessel BM, Park CE, Collison DC, Aisan BYI, Gedeon TM, Chaudhary SK, Widmer J, Blackwood CR, Bolster CM, Devilbiss ML, Garrison DL, Halevi S, Kese GQ, Quach EK, Rogelio CMP, Tan ML, Wald HJS, Woglo SW. 2021. Freshwater salinization syndrome: from emerging global problem to managing risks. Biogeochemistry. 154(2):255–292. https://doi.org/10.1007/s10533-021-00784-w

Kay BH, Ryan PA, Russell BM, Holt JS, Lyons SA, Foley PN. 2000. The Importance of Subterranean Mosquito Habitat to Arbovirus Vector Control Strategies in North Queensland, Australia. Journal of Medical Entomology. 37(6):846–853. https://doi.org/10.1603/0022-2585-37.6.846

Kirschner LB. 1983. Sodium chloride absorption across the body surface: frog skins and other epithelia. American Journal of Physiology-Regulatory, Integrative and Comparative Physiology. 244(4):R429–R443. https://doi.org/10.1152/ajpregu.1983.244.4.R429

Klein U. 1992. The insect V-ATPase, a plasma membrane proton pump energizing secondary active transport: immunological evidence for the occurrence of a V-ATPase in insect ion-transporting epithelia. Journal of Experimental Biology. 172(1):345–354. https://doi.org/10.1242/jeb.172.1.345

Koch HJ. 1938. The Absorption Of Chloride Ions By The Anal Papillae Of Diptera Larvae. Journal of Experimental Biology. 15(1):152–160. https://doi.org/10.1242/jeb.15.1.152

Kraemer MU, Sinka ME, Duda KA, Mylne AQ, Shearer FM, Barker CM, Moore CG, Carvalho RG, Coelho GE, van Bortel W, Hendrickx G, Schaffner F, Elyazar I, Teng H, Brady O, Messina J, Pigott D, Scott T, Smith D, Wint G, Golding N, Hay S. 2015. The global distribution of the arbovirus vectors *Aedes aegypti* and *Ae. albopictus*. eLife. 4. https://doi.org/10.7554/eLife.08347

Lee C, Kang HJ, von Ballmoos C, Newstead S, Uzdavinys P, Dotson DL, Iwata S, Beckstein O, Cameron AD, Drew D. 2013. A two-domain elevator mechanism for sodium/proton antiport. Nature. 501(7468):573–577. https://doi.org/10.1038/nature12484

Li Y, Piermarini PM, Esquivel CJ, Drumm HE, Schilkey FD, Hansen IA. 2017. RNA-Seq Comparison of Larval and Adult Malpighian Tubules of the Yellow Fever Mosquito *Aedes aegypti* Reveals Life Stage-Specific Changes in Renal Function. Frontiers in Physiology. 8. https://doi.org/10.3389/fphys.2017.00283

Ligon BL. 2006. Reemergence of an Unusual Disease: The Chikungunya Epidemic. Seminars in Pediatric Infectious Diseases. 17(2):99–104. https://doi.org/10.1053/j.spid.2006.04.009

Lindskog S. 1997. Structure and mechanism of carbonic anhydrase. Pharmacology & Therapeutics. 74(1):1–20. https://doi.org/10.1016/S0163-7258(96)00198-2

Linser PJ, Neira Oviedo M, Hirata T, Seron TJ, Smith KE, Piermarini PM, Romero MF. 2012. Slc4-like anion transporters of the larval mosquito alimentary canal. Journal of Insect Physiology. 58(4):551–562. https://doi.org/10.1016/j.jinsphys.2012.01.002

Linser PJ, Smith KE, Seron TJ, Neira Oviedo M. 2009. Carbonic anhydrases and anion transport in mosquito midgut pH regulation. Journal of Experimental Biology. 212(11):1662–1671. https://doi.org/10.1242/jeb.028084

Livak KJ, Schmittgen TD. 2001. Analysis of Relative Gene Expression Data Using Real-Time Quantitative PCR and the $2^{-\Delta\Delta CT}$ Method. Methods. 25(4):402–408. https://doi.org/10.1006/meth.2001.1262

Marusalin J, Matier BJ, Rheault MR, Donini A. 2012. Aquaporin homologs and water transport in the anal papillae of the larval mosquito, *Aedes aegypti*. Journal of Comparative Physiology B. 182(8):1047–1056. https://doi.org/10.1007/s00360-012-0679-2

Matsuoka R, Fudim R, Jung S, Zhang C, Bazzone A, Chatzikyriakidou Y, Robinson C v., Nomura N, Iwata S, Landreh M, Orellana L, Beckstein O, Drew D. 2022. Structure, mechanism and lipid-mediated remodeling of the mammalian Na^+/H^+ exchanger NHA2. Nature Structural & Molecular Biology. 29(2):108–120. https://doi.org/10.1038/s41594-022-00738-2

Matthews BJ, Dudchenko O, Kingan SB, Koren S, Antoshechkin I, Crawford JE, Glassford WJ, Herre M, Redmond SN, Rose NH et al. 2018. Improved reference genome of *Aedes aegypti* informs arbovirus vector control. Nature. 563(7732):501–507. https://doi.org/10.1038/s41586-018-0692-z

McNamara JC, Faria SC. 2012. Evolution of osmoregulatory patterns and gill ion transport mechanisms in the decapod Crustacea: a review. Journal of Comparative Physiology B. 182(8):997–1014. https://doi.org/10.1007/s00360-012-0665-8

McNaughton D, Miller ER, Tsourtos G. 2018. The Importance of Water Typologies in Lay Entomologies of *Aedes aegypti* Habitat, Breeding and Dengue Risk: A Study from Northern Australia. Tropical Medicine and Infectious Disease. 3(2). https://doi.org/10.3390/tropicalmed3020067

Meredith J, Phillips JE. 1973. Rectal ultrastructure in salt- and freshwater mosquito larvae in relation to physiological state. Zeitschrift fr Zellforschung und Mikroskopische Anatomie. 138(1):1–22. https://doi.org/10.1007/BF00307074

Misyura L, Grieco Guardian E, Durant AC, Donini A. 2020. A comparison of aquaporin expression in mosquito larvae (*Aedes aegypti*) that develop in hypo-osmotic freshwater and iso-osmotic brackish water. PLoS one. 15(8):e0234892-. https://doi.org/10.1371/journal.pone.0234892

Misyura L, Yerushalmi GY, Donini A. 2017. A mosquito entomoglyceroporin, *Aedes aegypti* AQP5 participates in water transport across the Malpighian tubules of larvae. Journal of Experimental Biology. https://doi.org/10.1242/jeb.158352

Noriega FG, Edgar KA, Bechet R, Wells MA. 2002. Midgut exopeptidase activities in *Aedes aegypti* are induced by blood feeding. Journal of Insect Physiology. 48(2):205–212. https://doi.org/10.1016/S0022-1910(01)00165-2

O'Connor KR, Beyenbach KW. 2001. Chloride Channels in Apical Membrane Patches of Stellate Cells of Malpighian Tubules of *Aedes Aegypti*. Journal of Experimental Biology. 204(2):367–378. https://doi.org/10.1242/jeb.204.2.367

Okech BA, Boudko DY, Linser PJ, Harvey WR. 2008a. Cationic pathway of pH regulation in larvae of *Anopheles gambiae*. Journal of Experimental Biology. 211(6):957–968. https://doi.org/10.1242/jeb.012021

Okech BA, Meleshkevitch EA, Miller MM, Popova LB, Harvey WR, Boudko DY. 2008b. Synergy and specificity of two Na^+–aromatic amino acid symporters in the model alimentary canal of mosquito larvae. Journal of Experimental Biology. 211(10):1594–1602. https://doi.org/10.1242/jeb.017244

Onken H, Moffett SB, Moffett DF. 2008. Alkalinization in the Isolated and Perfused Anterior Midgut of the Larval Mosquito, *Aedes aegypti*. Journal of Insect Science. 8(46):1–20. https://doi.org/10.1673/031.008.4601

Paluzzi JP, Vanderveken M. 2014. The Heterodimeric Glycoprotein Hormone, GPA2/GPB5, Regulates Ion Transport across the Hindgut of the Adult Mosquito, *Aedes aegypti*. PLoS one. 9(1):1–14. https://doi.org/10.1371/journal.pone.0086386

Patrick ML, Aimanova K, Sanders HR, Gill SS. 2006. P-type Na^+/K^+-ATPase and V-type H^+-ATPase expression patterns in the osmoregulatory organs of larval and adult mosquito *Aedes aegypti*. Journal of Experimental Biology. 209(Pt 23):4638–4651. https://doi.org/10.1242/jeb.0255

Patrick ML, Donini A, Zogby A, Morales C, O'Donnell MJ, Gill SS. 2024. Proton-driven sodium secretion in a saline water animal. Scientific Reports. 14(1):12738. https://doi.org/10.1038/s41598-024-62974-4

Phillips J. 1981. Comparative physiology of insect renal function. American Journal of Physiology-Regulatory, Integrative and Comparative Physiology. 241(5):R241–R257. https://doi.org/10.1152/ajpregu.1981.241.5.R241

Phillips JE, Hanrahan J, Chamberlin M, Thomson B. 1987. Mechanisms and Control of Reabsorption in Insect Hindgut. In: Evans PD, Wigglesworth VB, editors. Advances in Insect Physiology. Vol. 19: Academic Press; p. 329–422. https://doi.org/https://doi.org/10.1016/S0065-2806(08)60103-4

Picinic BN, Reinsborough A, Jonusaite S, Paluzzi JP, Donini A. 2026. Discovery of an aquaporin (CrAQP2) in the freshwater larval midge, *Chironomus riparius* and its role in response to road de-icers. Current Research in Insect Science. 9:100123. https://doi.org/10.1016/j.cris.2026.100123

Piermarini PM. 2016. Renal Excretory Processes in Mosquitoes. In; p. 393–433. https://doi.org/10.1016/bs.aiip.2016.04.003

Piermarini PM, Akuma DC, Crow JC, Jamil TL, Kerkhoff WG, Viel KCMF, Gillen CM. 2017. Differential expression of putative sodium-dependent cation-chloride cotransporters in *Aedes aegypti*. Comparative Biochemistry and Physiology Part A: Molecular & Integrative Physiology. 214:40–49. https://doi.org/https://doi.org/10.1016/j.cbpa.2017.09.007

Piermarini PM, Grogan LF, Lau K, Wang L, Beyenbach KW. 2010. A SLC4-like anion exchanger from renal tubules of the mosquito (*Aedes aegypti*): evidence for a novel role of stellate cells in diuretic fluid secretion. American Journal of Physiology-Regulatory, Integrative and Comparative Physiology. 298(3):R642–R660. https://doi.org/10.1152/ajpregu.00729.2009

Del Pilar Corena M, Seron TJ, Lehman HK, Ochrietor JD, Kohn A, Tu C, Linser PJ. 2002. Carbonic anhydrase in the midgut of larval *Aedes aegypti*: cloning, localization and inhibition. Journal of Experimental Biology. 205(5):591–602. https://doi.org/10.1242/jeb.205.5.591

Pullikuth AK, Aimanova K, Kang'ethe W, Sanders HR, Gill SS. 2006. Molecular characterization of sodium/proton exchanger 3 (NHE3) from the yellow fever vector, *Aedes aegypti*. Journal of Experimental Biology. 209(18):3529–3544. https://doi.org/10.1242/jeb.02419

Putney LK, Denker SP, Barber DL. 2002. The Changing Face of the Na^+/H^+ Exchanger, NHE1: Structure, Regulation, and Cellular Actions. Annual Review of Pharmacology and Toxicology. 42(1):527–552. https://doi.org/10.1146/annurev.pharmtox.42.092001.143801

Rahman RU, Cosme LV, Costa MM, Carrara L, Lima JBP, Martins AJ. 2021. Insecticide resistance and genetic structure of *Aedes aegypti* populations from Rio de Janeiro State, Brazil. PLoS Neglected Tropical Diseases. 15(2):e0008492. https://doi.org/10.1371/journal.pntd.0008492

Ramasamy R, Surendran SN. 2011. Possible impact of rising sea levels on vector-borne infectious diseases. BMC Infectious Diseases. 11(1):18. https://doi.org/10.1186/1471-2334-11-18

Ramasamy R, Surendran SN, Jude PJ, Dharshini S, Vinobaba M. 2011. Larval Development of *Aedes aegypti* and *Aedes albopictus* in Peri-Urban Brackish Water and Its Implications for Transmission of Arboviral Diseases. PLoS Neglected Tropical Diseases. 5(11):e1369. https://doi.org/10.1371/journal.pntd.0001369

Ramasamy R, Surendran SN, Jude PJ, Dharshini S, Vinobaba M. 2015. Adaptation of Mosquito Vectors to Salinity and Its Impact on Mosquito-Borne Disease Transmission in the South and Southeast Asian Tropics. In: Socio-Ecological Dimensions of Infectious Diseases in Southeast Asia. Singapore: Springer Singapore; p. 107–122. https://doi.org/10.1007/978-981-287-527-3_8

Ramsay JA. 1950. Osmotic Regulation in Mosquito Larvae. Journal of Experimental Biology. 27(2):145–157. https://doi.org/10.1242/jeb.27.2.145

Ramsay JA. 1953. Exchanges of Sodium and Potassium in Mosquito Larvae. Journal of Experimental Biology. 30(1):79–89. https://doi.org/10.1242/jeb.30.1.79

Reinsborough A, Donini A. 2025. Exposure to NaCl and beet juice brine de-icers alters the function of Malpighian tubules and anal papillae of chironomids (*Chironomus riparius*). Journal of Experimental Biology. 228(18). https://doi.org/10.1242/jeb.249920

Rheault MR, Okech BA, Keen SBW, Miller MM, Meleshkevitch EA, Linser PJ, Boudko DY, Harvey WR. 2007. Molecular cloning, phylogeny and localization of AgNHA1: the first Na^+/H^+ antiporter (NHA) from a metazoan, *Anopheles gambiae*. The Journal of Experimental Biology. 210(Pt 21):3848–61. https://doi.org/10.1242/jeb.007872

Richards AG, Meier TJ. 1974. The Osmolarity of the Blood of a Mosquito Larva (*Aedes aegypti* L.) Reared under Several Different Culture Conditions1. Annals of the Entomological Society of America. 67(3):424–426. https://doi.org/10.1093/aesa/67.3.424

Rimon A, Tzubery T, Padan E. 2007. Monomers of the NhaA Na+/H+ Antiporter of *Escherichia coli* are fully functional, yet dimers are beneficial under extreme stress conditions at alkaline pH in the presence of Na^+ or Li^+. Journal of Biological Chemistry. 282(37):26810–26821. https://doi.org/10.1074/jbc.M704469200

Rodan AR, Baum M, Huang CL. 2012. The *Drosophila* NKCC Ncc69 is required for normal renal tubule function. American Journal of Physiology-Cell Physiology. 303(8):C883–C894. https://doi.org/10.1152/ajpcell.00201.2012

Sáez AG, Lozano E, Zaldívar-Riverón A. 2009. Evolutionary history of Na,K-ATPases and their osmoregulatory role. Genetica. 136(3):479–490. https://doi.org/10.1007/s10709-009-9356-0

Sajadi F, Paluzzi JP. 2024. Molecular characterization, localization, and physiological roles of ITP and ITP-L in the mosquito, *Aedes aegypti*. Frontiers in Insect Science. 4. https://doi.org/10.3389/finsc.2024.1374325

Scott BN, Yu MJ, Lee LW, Beyenbach KW. 2004. Mechanisms of K^+ transport across basolateral membranes of principal cells in Malpighian tubules of the yellow fever mosquito, *Aedes aegypti*. Journal of Experimental Biology. 207(10):1655–1663. https://doi.org/10.1242/jeb.00932

Seron TJ, Hill J, Linser PJ. 2004. A GPI-linked carbonic anhydrase expressed in the larval mosquito midgut. Journal of Experimental Biology. 207(26):4559–4572. https://doi.org/10.1242/jeb.01287

Shirangi SA, Kalbassi MR, Khodabandeh S, Jafarian H, Lignot JH. 2017. Immunolocalization of Na^{+}/K^{+}-ATPase, $Na^{+}/K^{+}/2Cl^{-}$ co-transporter (NKCC) and mRNA expression of Na^{+}/K^{+}-ATPase α-subunit during short-term salinity transfer in the gills of Persian sturgeon (*Acipenser persicus*, Borodin, 1897) juveniles. Journal of Applied Ichthyology. 33(3):347–353. https://doi.org/10.1111/jai.13260

Skou JC. 1990. The energy coupled exchange of Na^{+} for K^{+} across the cell membrane. FEBS Letters. 268(2):314–324. https://doi.org/10.1016/0014-5793(90)81278-V

Smith KE, VanEkeris LA, Linser PJ. 2007. Cloning and characterization of AgCA9, a novel α-carbonic anhydrase from *Anopheles gambiae* Giles *sensu stricto* (Diptera: Culicidae) larvae. Journal of Experimental Biology. 210(22):3919–3930. https://doi.org/10.1242/jeb.008342

Smith KE, VanEkeris LA, Okech BA, Harvey WR, Linser PJ. 2008. Larval anopheline mosquito recta exhibit a dramatic change in localization patterns of ion transport proteins in response to shifting salinity: a comparison between anopheline and culicine larvae. Journal of Experimental Biology. 211(19):3067–3076. https://doi.org/10.1242/jeb.019299

Sohal RS, Copeland E. 1966. Ultrastructural variations in the anal papillae of *Aedes aegypti* (L.) at different environmental salinities. Journal of Insect Physiology. 12(4):429–434. https://doi.org/https://doi.org/10.1016/0022-1910(66)90006-0

Stobbart RH. 1959. Studies on the Exchange and Regulation of Sodium in the Larva of *Aedes aegypti* (L.): I. The Steady-State Exchange. Journal of Experimental Biology. 36(4):641–653. https://doi.org/10.1242/jeb.36.4.641

Stobbart RH. 1960. Studies on the Exchange and Regulation of Sodium in the Larva of *Aedes aegypti* (L.): II. The Net Transport and the Fluxes Associated with it. Journal of Experimental Biology. 37(3):594–608. https://doi.org/10.1242/jeb.37.3.594

Stobbart RH. 1965. The Effect of Some Anions and Cations Upon the Fluxes and Net Uptake of Sodium in the Larva of *Aedes aegypti* (L). Journal of Experimental Biology. 42(1):29–43. https://doi.org/10.1242/jeb.42.1.29

Stobbart RH. 1967. The Effect of Some Anions and Cations Upon the Fluxes and Net Uptake of Chloride in the Larva of *Aedes aegypti* (L.), and the Nature of the Uptake Mechanisms for Sodium and Chloride. Journal of Experimental Biology. 47(1):35–57. https://doi.org/10.1242/jeb.47.1.35

Surendran SN, Jude PJ, Thabothiny V, Raveendran S, Ramasamy R. 2012. Pre-imaginal development of *Aedes aegypti* in brackish and fresh water urban domestic wells in Sri Lanka. Journal of Vector Ecology. 37(2):471–473. https://doi.org/https://doi.org/10.1111/j.1948-7134.2012.00254.x

Taglicht D, Padan E, Schuldiner S. 1993. Proton-sodium stoichiometry of NhaA, an electrogenic antiporter from *Escherichia coli*. Journal of Biological Chemistry. 268(8):5382–5387. https://doi.org/10.1016/S0021-9258(18)53333-0

Terra WR. 1990. Evolution of Digestive Systems of Insects. Annual Review of Entomology. 35(1):181–200. https://doi.org/10.1146/annurev.en.35.010190.001145

Tikar SN, Mendki MJ, Chandel K, Parashar BD, Prakash S. 2008. Susceptibility of immature stages of *Aedes* (Stegomyia) *aegypti*; vector of dengue and chikungunya to insecticides from India. Parasitology Research. 102(5):907–913. https://doi.org/10.1007/s00436-007-0848-5

Uzdavinys P, Coinçon M, Nji E, Ndi M, Winkelmann I, von Ballmoos C, Drew D. 2017. Dissecting the proton transport pathway in electrogenic Na^+/H^+ antiporters. Proceedings of the National Academy of Sciences. 114(7). https://doi.org/10.1073/pnas.1614521114

Vieira Santos VS, Caixeta ES, Campos Júnior EO de, Pereira BB. 2017. Ecotoxicological effects of larvicide used in the control of *Aedes aegypti* on nontarget organisms: Redefining the use of pyriproxyfen. Journal of Toxicology and Environmental Health, Part A. 80(3):155–160. https://doi.org/10.1080/15287394.2016.1266721

Volkmann A, Peters W. 1989a. Investigations on the midgut caeca of mosquito larvae—I. Fine structure. Tissue and Cell. 21(2):243–251. https://doi.org/10.1016/0040-8166(89)90069-4

Volkmann A, Peters W. 1989b. Investigations on the midgut caeca of mosquito larvae—II. Functional aspects. Tissue and Cell. 21(2):253–261. https://doi.org/10.1016/0040-8166(89)90070-0

Wang X, Qian C, Zhang Chenxi, Hu S, Asad M, Yang C, Liao B, Guo X, Zhang Chen, Li Q, Li X, Huang Q, Si Y, Zhu B, Cao S, Ye J. 2025. Zika virus transmission in Aedes aegypti: A systematic study on the ability of mosquitoes to transmit the virus horizontally and vertically. Virologica Sinica. 40(2):192–205. https://doi.org/10.1016/j.virs.2025.02.001

Weihrauch D, O'Donnell MJ. 2015. Links between Osmoregulation and Nitrogen-Excretion in Insects and Crustaceans. Integrative and Comparative Biology. 55(5):816–829. https://doi.org/10.1093/icb/icv013

Weng X-H, Huss M, Wieczorek H, Beyenbach KW. 2003. The V-type H^+-ATPase in Malpighian tubules of *Aedes aegypti*: localization and activity. Journal of Experimental Biology. 206(13):2211–2219. https://doi.org/10.1242/jeb.00385

Wessing A, Zierold K, Bertram G. 1997. Carbonic anhydrase supports electrolyte transport in Drosophila Malpighian tubules. Evidence by X-ray microanalysis of cryosections. Journal of Insect Physiology. 43(1):17–28. https://doi.org/10.1016/S0022-1910(96)00078-9

Wieczorek H, Brown D, Grinstein S, Ehrenfeld J, Harvey WR. 1999. Animal plasma membrane energization by proton-motive V-ATPases. BioEssays: News and Reviews in Molecular, Cellular and Developmental Biology. 21(8):637–48. https://doi.org/10.1002/(SICI)1521-1878(199908)21:8<637::AID-BIES3>3.0.CO;2-W

Wigglesworth VB. 1938. The Regulation of Osmotic Pressure and Chloride Concentration in the Haemolymph of Mosquito Larvae. Journal of Experimental Biology.15(2):235–247. https://doi.org/10.1242/jeb.15.2.235

Wilke ABB, Vasquez C, Carvajal A, Ramirez M, Cardenas G, Petrie WD, Beier JC. 2021. Effectiveness of adulticide and larvicide in controlling high densities of *Aedes aegypti* in urban environments. PLoS one. 16(1):e0246046. https://doi.org/10.1371/journal.pone.0246046

Williams KA. 1999. Projection structure of NhaA, a secondary transporter from *Escherichia coli*, at 4.0 A resolution. The EMBO Journal. 18(13):3558–3563. https://doi.org/10.1093/emboj/18.13.3558

Xiang MA, Linser PJ, Price DA, Harvey WR. 2012. Localization of two Na^+- or K^+-H^+ antiporters, AgNHA1 and AgNHA2, in *Anopheles gambiae* larval Malpighian tubules and the functional expression of AgNHA2 in yeast. Journal of Insect Physiology. 58(4):570–579. https://doi.org/https://doi.org/10.1016/j.jinsphys.2011.12.009

Yadav M, Dahiya N, Sehrawat N. 2023. Mosquito gene targeted RNAi studies for vector control. Functional & Integrative Genomics. 23(2):180. https://doi.org/10.1007/s10142-023-01072-6

Zadeh-Tahmasebi M, Bui P, Donini A. 2016. Fluid and ion secretion by Malpighian tubules of larval chironomids, *Chironomus riparius*: Effects of rearing salinity, transport inhibitors, and serotonin Archives of Insect Biochemistry and Physiology. 93(2):67–85. https://doi.org/10.1002/arch.21342

Zhao Y, Schubert H, Blakely A, Forbush B, Smith MD, Rinehart J, Cao E. 2024. Structural bases for Na^+-Cl^- cotransporter inhibition by thiazide diuretic drugs and activation by kinases. Nature Communications. 15(1):7006. https://doi.org/10.1038/s41467-024-51381-y

Zhuang Z, Linser PJ, Harvey WR. 1999. Antibody to H^+ V-ATPase subunit E colocalizes with portasomes in alkaline larval midgut of a freshwater mosquito (*Aedes aegypti* L.). Journal of Experimental Biology. 202(18):2449–2460. https://doi.org/10.1242/jeb.202.18.2449

Appendix and Supplementary Data

Appendix A. Antibody controls for immunohistochemistry and western blotting

For immunohistochemistry, antibody controls were conducted for the secondary antibodies used for both VA and AeNHA1, and for the custom primary antibody used for AeNHA1. To ensure the secondary antibodies were specific, slides were processed that were not incubated with primary antibodies for both VA and AeNHA1. This was done using the same protocol of deparaffinization and re-hydration, heat induced isotope removal and a series of PBS washes, previously used to process the experimental slides (see Section 2.5). The slides were incubated overnight with ADB alone and no primary antibody was added. After the overnight incubation with ADB, the slides were washed again through a series of PBS washes as normal and were left to incubate with the secondary antibodies used for AeNHA1 (goat anti-rabbit AlexaFluor 594 - dilution 1:400 (Jackson Immunoresearch)) and VA (goat anti-guinea pig antibody AlexaFluor488 – dilution 1:500 (Jackson Immunoresearch)) for 1 hour and were subsequently washed and mounted with mounting media containing DAPI for nuclei staining. The specificity of the secondary antibodies was confirmed since no immunofluorescence was observed for VA or AeNHA1 in the absence of primary antibody (Figure A-1A). Since the primary antibody used for AeNHA1 was a new and custom-made antibody, the specificity was also tested through a peptide block on each of the osmoregulatory organs (e.g., midgut, Malpighian tubules, hindgut and anal papillae). This was done by diluting the primary antibody for AeNHA1 (1:25 rabbit polyclonal antibody against SHSEDGPVRRKSNLC, Genscript, NJ, USA) in ADB, also containing 5x the molar excess of AeNHA1 peptide used to construct this antibody, and the primary antibody for VA (Ab 353-2, 1: 5000 dilution, generously donated by Dr.H. Wieczorek, Osnabruck, Germany) as a membrane marker. At the same time, a regular preparation of AeNHA1 primary antibody with primary antibody for VA was also prepared in ADB. Both tubes were then left to mix for 2 hrs on a rotator

at room temperature. Once the slides were washed and processed, the primary antibody mixture containing the respective peptide was applied onto the slides and left to sit overnight in the fridge. The next day, after the slides were further processed through a washing series with PBS, the secondary antibodies used for AeNHA1 and VA were applied to the slides and left to incubate for 1 hour at room temperature, followed by a final series of washes before being mounted with mounting media containing DAPI. Blocking of the AeNHA1 antibody with the peptide was successful as no immunofluorescence was detected in each of the osmoregulatory organs assessed, indicating the specificity of the constructed antibody in targeting AeNHA1 (Figure A-1 B,C,D).

Specificity of the AeNHA1 primary antibody was also assessed through western blotting using protein from 24-hour treated AFW Malpighian tubule samples across three biological replicates (~75 larvae dissected for all 5 tubules = 1 replicate). This was done using the same western blotting protocol mentioned previously (see Section 2.6), but for the antibody incubation step, the primary antibody was omitted and instead, the blot was incubated with pre-immune serum (1:1000) that had been diluted in 5% skim milk. A blot with the same Malpighian tubule protein (n=3) was run alongside the control blot, but was given the custom AeNHA1 antibody overnight, prepared in 5% skim milk. The blots were then left rotating overnight at 4°C followed by secondary antibody incubation the next day (see Section 2.6). Upon imaging, no bands appeared on the pre-immune serum-treated blot relative to the experimental blot where two bands appeared at ~71 kDa and ~140 kDa, confirming the specificity of the AeNHA1 antibody for western blotting (Figure A-2).

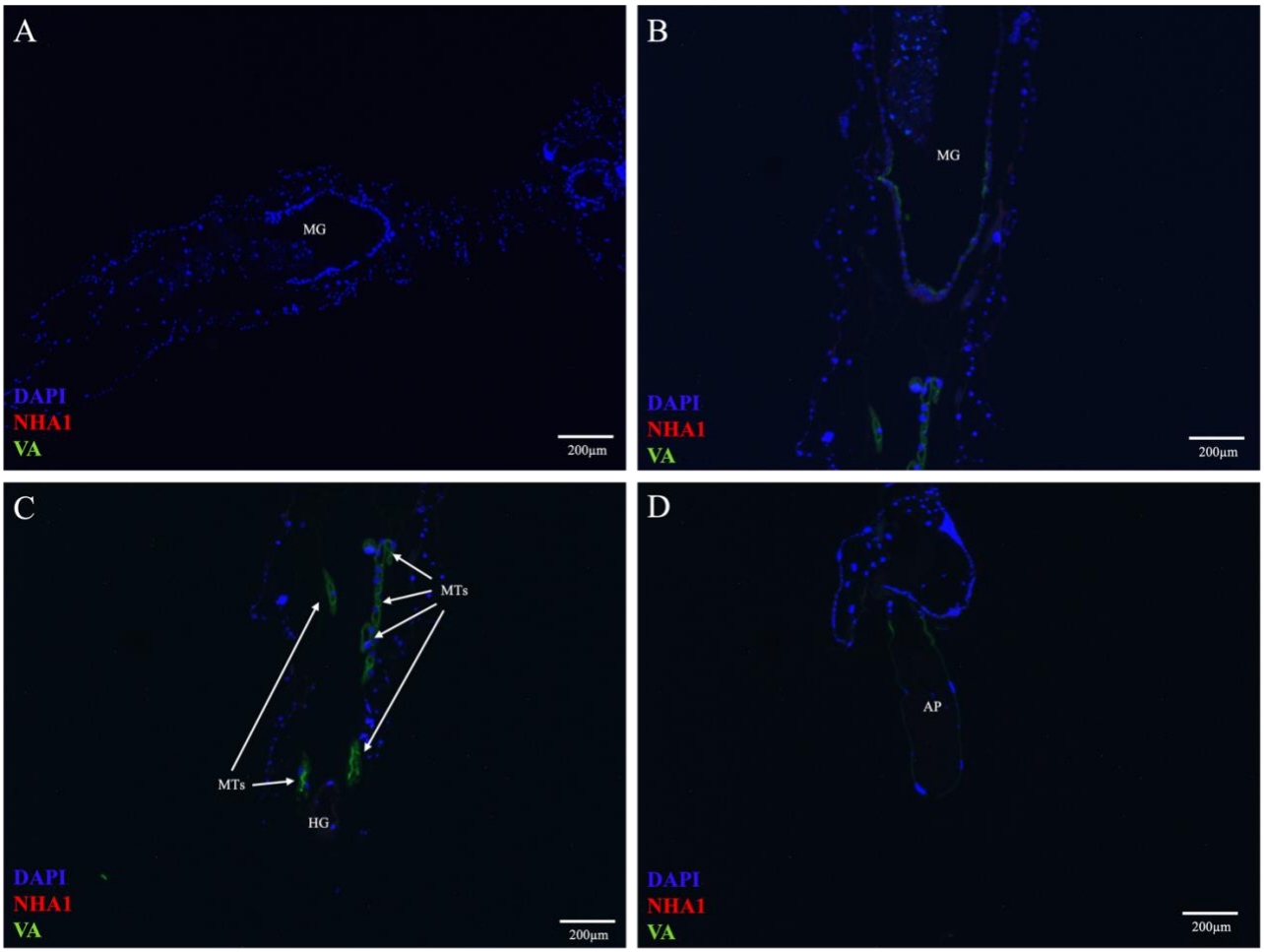

Figure A-21. Controls for secondary (VA & AeNHA1) and primary (AeNHA1) antibodies on tissue sections of *Aedes aegypti* larvae treated in artificial freshwater (AFW). (A) Shows the omission of the primary antibodies, but incubation with the secondary antibodies for AeNHA1 and VA on a whole-body tissue section, where blue (DAPI) staining indicates the presence of nuclei. A lack of red staining indicated no presence of NHA1 or VA immunofluorescence. (B,C,D) illustrate sections treated with the peptide block for AeNHA1 as well as the VA antibody for the midgut (MG) (B), Malpighian tubules (MTs), hindgut (HG) (C) and the anal papillae (AP) (D). AeNHA1 antibody specificity was confirmed with no AeNHA1 staining detected in tissue sections (red), where DAPI (blue) and VA (green) staining are shown.

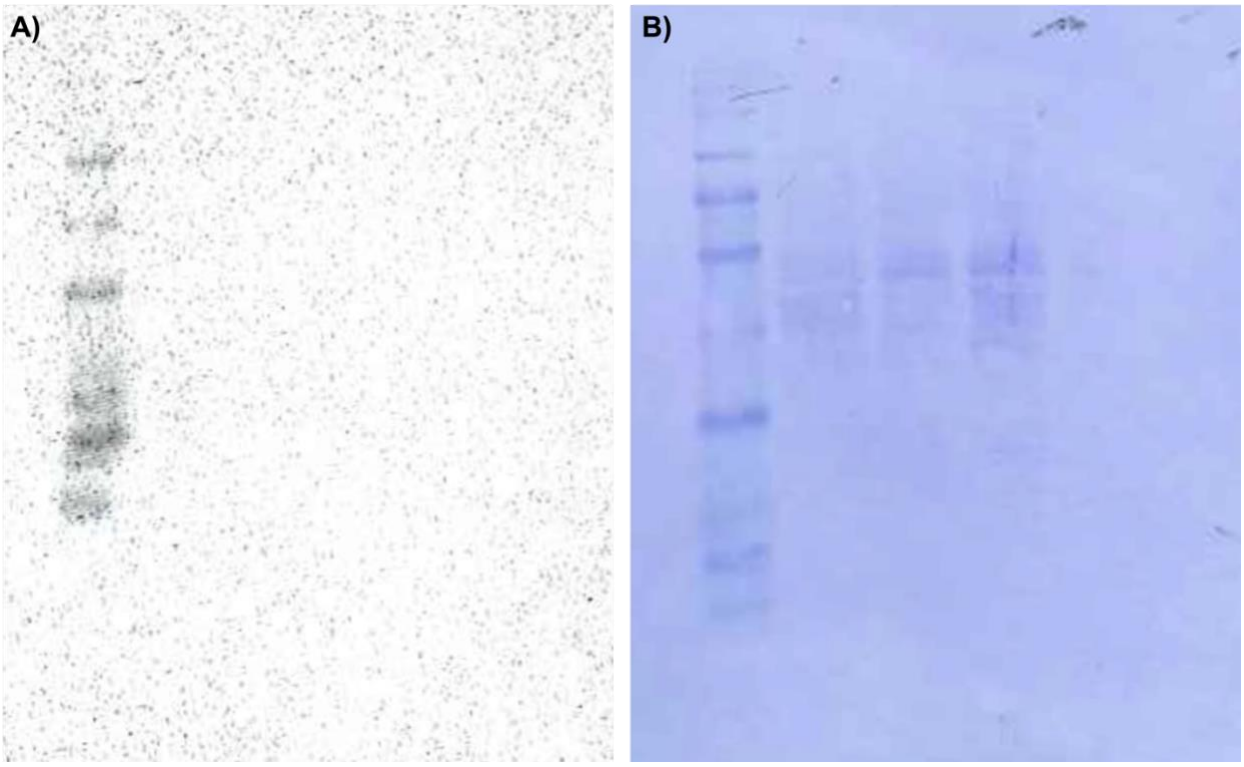

Figure A-22. Pre-immune serum-western blot (control) for AeNHA1 primary antibody. In (A), the western blot incubated with pre-immune serum instead of the AeNHA1 primary antibody is shown, where no bands were detected, indicating the specificity of this antibody. Protein samples from *A. aegypti* larval Malpighian Tubules (MTs) were collected and run on the blot for a total of three biological replicates. (B) the Coomassie staining for total protein loaded onto blot (A).